# High-Power Mode-Locked Semiconductor Lasers

by

Alan Mar

ECE Technical Report #94-25

Department of Electrical and Computer Engineering
University of California, Santa Barbara
October, 1994

University of California, Santa Barbara
Department of Electrical and Computer Engineering


**High Power Mode-Locked Semiconductor Lasers**


A Dissertation submitted in partial satisfaction
of the requirements for the degree of

Doctor of Philosophy

in

Electrical and Computer Engineering

by

**Alan Mar**

Faculty Committee

Professor John E. Bowers, Chair
Professor Larry A. Coldren
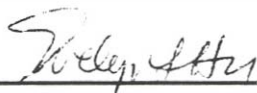Professor Evelyn L. Hu
Professor Mark J. Rodwell

October 1994

# High Power Mode-Locked Semiconductor Lasers

This dissertation by Alan Mar
is approved

_____

_____

_____

_____
Chairperson

October 1994

# Acknowledgements

I am greatly indebted to many people for their support over the years the work presented in this dissertation was conducted. First, I must thank my advisor, Professor John Bowers for his encouragement and continued support of this research, and especially for his assistance in developing relationships with researchers in laboratories outside UCSB. Much of the work in this dissertation was made possible through these collaborations, and supported by the Office of Naval Research and the National Science Foundation.

For their contribution in fabrication of multisegmented high-speed lasers, I am grateful to Daniel Renner, Rong-Ting Huang, Ching-Long Jiang, and Wood-Hi Cheng, formerly of Rockwell International (except for Rong-Ting Huang). The collaboration was very fruitful, resulting not only in excellent mode-locked laser devices, but also in high-speed lasers with record bandwidths. Also for fabricating excellent multi-segmented lasers, I thank Robert Thornton of Xerox Palo Alto Research Center. For fabricating high-power array laser devices at TRW Research Center, I thank Dan Botez (now at Univ. of Wisconsin, Madison) and Chuck Zmudzinski for their patience and expertise. I am also very grateful to Dave Welch and Dave Mehuys of Spectra Diode Laboratories for providing the excellent flared broad-area amplifiers used in this work.

I am fortunate to have been able to spend my years as a graduate student at UCSB Electrical and Computer Engineering, where I believe an exceptionally strong commitment to an environment of cooperation between research groups exists. I am grateful to Professors Larry Coldren, Evelyn Hu, and Mark Rodwell for their service and input as my faculty

# Vita

| | |
|---|---|
| **May 15, 1963** | Born, Los Angeles, California, United States of America |
| **June 1985** | A. B., Physics, Occidental College, Los Angeles |
| **June 1989** | M.S., Electrical Engineering, University of California, Santa Barbara |
| **1986 - 1988** | Research Assistant, Center For Robotic Systems in Microelectronics University of California, Santa Barbara |
| **1989 - Oct. 1994** | Research Assistant, Department of Electrical and Computer Engineering, University of California, Santa Barbara |

# Publications

1. "3-D Robotic Positioning Utilizing Holographic Interferometry," A. Mar, G. Beni, C.J. Landry, E. Hu, and S. Hackwood, Proceedings of the SPIE on Intelligent Robots and Computer Vision, 728, pp. 210-217, Cambridge, MA, October 26-31, 1986.

2. "Linewidth Measurement Using a Translating Phase Mask," A. Mar, Y. Xu, G. Wade, and E. Hu, Third IEEE/CHMT International Electronic Manufacturing Technology Symposium Proceedings 1987, pp.70-75, Anaheim, CA, October 1987.

3. "New Technique for Submicron Linewidth Measurement," Y. Xu, A. Mar, G. Wade, E. Hu, and C.J. Landry, Proceedings of SPIE on Advances in Intelligent Robotics Systems, Cambridge, MA, November 1987.

4. "Actively Mode Locked Semiconductor Lasers," J.E. Bowers, P.A. Morton, S. Corzine and A. Mar, J. Quantum Electronics, 25(6), 1426-1439, June (1989).

5. "Self Mode Locking of a Semiconductor Laser using Positive Feedback," D. J. Derickson, R. J. Helkey, A. Mar, P. A. Morton, and J. E. Bowers, Appl. Phys. Lett., 56, No. 1, 7-9 (1990).

6. "Residual and Absolute Timing Jitter in Actively Mode-Locked Semiconductor Lasers," D. J. Derickson, A. Mar, and J. E. Bowers, Electron. Lett., 26, 2026 (1990).

7.  "Optimum Facet Reflectivity for High Speed Lasers," A. Mar, P. A. Morton, and J. E. Bowers, Electron. Lett.,  26,17, 1382 (1990).

8.  "High Speed InGaAs/InP p-i-n Photodiodes Fabricated on a Semi-Insulating Substrate," D. L. Crawford, Y. G. Wey, A. Mar, J. E. Bowers, M. J. Hafich, and G. Y. Robinson,  Photonics Technology Lett., 2, 9, 647-649 (1990).

9.  "High-Speed and Low-Relative-Intensity Noise 1.3 μm InGaAsP Semi-Insulating Buried Crescent Lasers," W. H. Cheng, K. D. Buehring, A. Appelbaum, D. Renner, S. Shin, C. B. Su, A. Mar, and J. E. Bowers, J. of Quantum Electron., 27(6), 1642-1647, June (1991).

10. "Mode Locked Semiconductor Lasers," P. A. Morton, D. J. Derickson, R. J. Helkey, A. Mar, and J. E. Bowers, Laser Optics of Condensed Matter, Vol. 2, E. Garmire, A. A. Maradudin, and K. K. Rebane, eds., Plenum Press, New York, (1991).

11. "High-Speed, Low-Threshold InGaAsP Semi-Insulating Buried Crescent Lasers with 22 GHz Bandwidth," R. T. Huang, D. Wolf, W-H Cheng, C-L. Jiang, R. Agarwal, D. Renner, A. Mar, J. E. Bowers, Photon. Tech. Lett., 4(4), 293-295, April (1992).

12. "Mode-Locked Semiconductor Lasers, Short Pulse Small Package," D. J. Derickson, R. J. Helkey, A. Mar, J. B. Wasserbauer, W. B. Jiang, and J. E. Bowers, Optics and Photonics News, 3, 14-20, May (1992).

13. "Actively Mode-Locked External-Cavity Semiconductor Lasers With Transform-Limited Single Pulse Output," A. Mar, D. J. Derickson, R. Helkey, J. E. Bowers, R. T. Huang, and D. Wolf, Optics Lett., 17(12), 868-870, June (1992).

14. "Short Pulse Generation Using Multi-Segment Mode-Locked Lasers," D. J. Derickson, R. J. Helkey, A. Mar, J. R. Karin, J. G. Wasserbauer, and J. E. Bowers,  J. Quantum Electron., 28, 10, 2186-2202, Oct. (1992).

15. "Millimeter Wave Signal Generation Using Semiconductor Diode Lasers," R. J. Helkey, D. J. Derickson, A. Mar, J. G. Wasserbauer, J. E. Bowers, Microwave and Optical Technology Letters, 6(1), 1-5, January (1993).

16. "Repetition Frequency Stabilization of Passively Mode-Locked Semiconductor Lasers," R. J. Helkey, D. J. Derickson, A. Mar, J. Wasserbauer, J. E. Bowers, and R. L. Thornton, Electron. Lett., 28(20), 1920-1922, Sep. (1992).

17. "Resonantly Enhanced Semiconductor Lasers for Efficient Transmission of Millimeter Wave Modulated Light," R. Nagarajan, S. Levy, A. Mar, and J. E. Bowers, Photon. Tech. Lett., 5(1), 4-6, January (1993).

18. "Fiber-Optic PSK Subcarrier Transmission at 35 GHz Using a Resonantly Enhanced Semiconductor Laser," S. Levy, R. Nagarajan, A. Mar, P. Humphrey, and J. E. Bowers, Electron. Lett., 28(22), 2103, October (1992).

19. "Mode-Locked Semiconductor Lasers," D. Derickson, R. Helkey, A. Mar, J. Wasserbauer, and J. E. Bowers, Microwave Journal, November 1992.

20. "High-Speed 1.3 μm InGaAsP Fabry-Perot Lasers for Digital and Analog Applications," W. H. Cheng, A. Mar, J. E. Bowers, R. T. Huang, and C. B. Su, J. Quantum Electron., 29, 6, 1660-1667, June (1993).

21. "Colliding Pulse Effects in Mode-locked Semiconductor Lasers," R. J. Helkey, D. J. Derickson, J. R. Karin, A. Mar, J. G. Wasserbauer, and J. E. Bowers, submitted to J. of the Optical Society of America B, August (1992).

22. "Mode-Locked Multi-Segment Resonant-Optical-Waveguide Diode Laser Arrays," A. Mar, R. Helkey, T. Reynolds, J. Bowers, C. Zmudzinski, D. Botez, C. Tu, L. Mawst, Photonics Technology Letters, December (1993).

23. "Mode-Locked Operation of a Master Oscillator Power Amplifier" A. Mar, R. Helkey, J. Bowers, David Mehuys, David Welch, accepted to Photonics Technology Letters (1994).

24. "Modulation Frequency Dependence of Active Mode Locking of Semiconductor Lasers," J. E. Bowers, Y. G. Wey, A. Mar, P. A. Morton, and S. W. Corzine, Tenth IEEE International Conference on Semiconductor Lasers, Boston (1988).

25. "Phase Noise in Actively Mode Locked Semiconductor Lasers," J. E. Bowers, D. J. Derickson, A. Mar, P. A. Morton, and M. J. W. Rodwell, Seventh International Conference on Integrated Optics and Optical Fiber Communication, Kobe, Japan, July 18-21 (1989).

26. "Self Mode Locking of a Semiconductor Laser Using Positive Feedback," D. J. Derickson, R. J. Helkey, A. Mar, P. A. Morton, and J. E. Bowers, IEEE LEOS Annual Meeting paper, OE4.4, Orlando, (1989).

27. "High Speed Semiconductor Lasers and Applications in Subpicosecond Mode Locking," J. E. Bowers, P. A. Morton, R. Helkey, D. Derickson, and A. Mar, IEEE LEOS Annual Meeting, Invited Paper OE 7.1, Orlando, (1989).

28. "Monolithic Mode Locked Laser Arrays in Optical Computing," P. A. Morton, R. J. Helkey, A. Mar, D. J. Derickson, and J. E. Bowers, Invited Paper, SPIE Digital Optical Computing Meeting, Los Angeles, CA, Jan. (1990).

29. "Ultrafast Semiconductor Lasers," P. A. Morton, D. J. Derickson, R. J. Helkey, A. Mar, and J. E. Bowers, Fourth US-USSR Symposium on the "Physics of Optical Phenomena and their Use as Probes of Matter" Irvine, CA, Jan (1990).

30. "Absolute and Residual Timing Jitter In Actively Mode-Locked Semiconductor Lasers," D. J. Derickson, A. Mar, and J. E. Bowers, Int. Sem. Laser Conf., Davos, Switzerland, Sep. 9-14 (1990).

31. "Picosecond Dynamics in Semiconductor Lasers, " J. E. Bowers, D. J. Derickson, R. J. Helkey, J. R. Karin, A. Mar, P. A. Morton, and R. Nagarajan, Int. Sem. Laser Conference, paper A-3, Davos, Switzerland, Sep.,9-14 (1990).

32. "Reactively Sputtered Silicon Oxynitride for Anti-Reflection Optical Coatings," A. Mar, J. D. Dudley, E. L. Hu, and J. E. Bowers, Electronic Materials Conference, Santa Barbara, CA, Oct. (1990).

33. "Hybrid Integration of an InGaAs/InP PIN Photodiode with an Ultrafast Sampling Circuit," Y. G. Wey, M. Kamegawa, A. Mar, K. J. Williams, K. Giboney, D. L. Crawford, J. E. Bowers, and M. Rodwell, Optical Fiber Communication Conference, paper PD8-1, San Diego, CA, Feb. (1991).

34. "Graded Double Heterostructure Photodetectors," Y. G. Wey, D. Crawford, K. Giboney, A. Mar, and J. Bowers, Engineering Foundation Conference on High Speed Optoelectronics, Palm Coast, FL, Mar. (1991).

35. "1.4 Picosecond Pulses Directly Generated Using a Tandem-Contact Actively Mode-locked 1.3 μm Semiconductor Laser," A. Mar, D. Derickson, R. Helkey, J. Bowers, LEOS 1991 Annual Meeting, paper SDL14.1, San Jose, CA, Nov. (1991).

36. "Benefits of Intra-Waveguide Saturable Absorbers in External Cavity Mode-locked Semiconductor Lasers," D. Derickson, R. J. Helkey, A. Mar, R. L. Thornton, J. E. Bowers, OSA Annual Meeting, paper MG5, San Jose, CA, Nov. (1991).

37. "Comb and Signal Generation Above 100 GHz Using Optoelectronics," D. J. Derickson, R. J. Helkey, A. Mar, J. G. Wasserbauer, Y. G. Wey, J. E. Bowers, Photonic Systems for Antenna Applications Conference, Monterey, CA, Dec. (1991).

38. "A Comparison of Colliding Pulse and Self-Colliding Pulse Monolithic Cavity Mode Locked Semiconductor Lasers," D. J. Derickson, J. G. Wasserbauer, R. J. Helkey, A. Mar, J. E. Bowers, D. Coblentz, R. Logan, and T. Tanbun-Ek, Optical Fiber Communication Conference (OFC), paper ThB3, San Jose, CA, Feb. (1992).

39. "Design of Multi-Section Mode-Locked Semiconductor Lasers with Intra-Waveguide Saturable Absorbers," D. J. Derickson, R. J. Helkey, A. Mar, J. G. Wasserbauer, and J. E. Bowers, 1992 Integrated Photonics Research Topical Meeting, paper WC3, New Orleans, LA, Apr. (1992).

40. "High-Speed, Low-Threshold InGaAsP Semi-Insulating Buried Lasers," A. Mar, J. E. Bowers, R-T. Huang, D. Wolf, W-H. Cheng, C-L. Jiang, R. Agarwal, and D. Renner, InP and Related Materials Conference, paper THE3, Newport, RI, Apr. 21-24 (1992).

41. "Colliding Pulse Effects in Mode Locked Semiconductor Diode Lasers," R. J. Helkey, D. J. Derickson, A. Mar, J. G. Wasserbauer, and J. E. Bowers, Quantum Electronics and Laser Science Conference (CLEO), paper JThB2, Anaheim, CA, May 10-15 (1992).

42. "Microwave and Millimeter Wave Signal Generation Using Mode-Locked Semiconductor Lasers With Intra-Waveguide Saturable Absorbers," D. J. Derickson, R. J. Helkey, A. Mar, J. G. Wasserbauer, and J. E. Bowers, IEEE MTT International Microwave Symposium Digest, paper V-2, 753-756, Albuquerque, NM, June (1992).

43. "Integrated Optical Transmitters and Receivers Using Multi-Segment Laser Processes," J. G. Wasserbauer, D. J. Derickson, K. Giboney, R. J. Helkey, J. R. Karin, A. Mar, and J. E. Bowers, IEEE Lasers and Electro-optics Society Meeting on Integrated Optoelectronics, paper ThC1, Santa Barbara, CA, Aug., (1992).

44. "Mode-Locking of High-Power Resonant-Optical-Waveguide Diode Laser Arrays, ", A. Mar, D. J. Derickson, R. J. Helkey, J. E. Bowers, and D. Botez, 13th International Semiconductor Laser Conference, paper N-7, Takamatsu, Japan, Sep. (1992).

45. "Stabilization of Passively Mode-Locked Semiconductor Laser Repetition Frequency," R. J. Helkey, D. J. Derickson, A. Mar, J. G. Wasserbauer, J. E. Bowers, and R. L. Thornton, IEEE Lasers and Electro-optics Society Annual Meeting, paper DLTA4.2, Boston, MA, Nov. (1992).

46. "Subpicosecond Pulse Generation From Mode-locked Semiconductor Lasers," R. J. Helkey, A. Mar, W. X. Zou, D. B. Young, and J. E. Bowers, SPIE OE/LASE 1993 (INVITED PAPER), Los Angeles, CA, Jan. (1993).

47. "Resonant Enhancement of Semiconductor Laser Modulation Response for Efficient Analog Transmission at 35 GHz," S. Levy, R. Nagarajan, A. Mar, and J. E. Bowers, SPIE OE/LASE 1993, Los Angeles, CA, Jan. 18 - 20 (1993).

48. "Fiber Optic Transmission of 35 GHz Subcarrier BPSK Signal Using Resonant Enhancement of a Semiconductor Laser," S. Levy, R. Nagarajan, A. Mar, and J. E. Bowers, Optical Fiber Communication Conf./Int. Conf. on Integrated Optics and Optical Fiber Communication (OFC/IOOC), San Jose, CA, Feb. 21-26 (1993).

49. "Curved and Tapered Waveguide Mode-Locked InGaAs/AlGaAs Semiconductor Lasers Fabricated by Impurity Induced Disordering," R. Helkey, W. X. Zou, A. Mar, D. B. Young, and J. E. Bowers, Device Research Conference, Santa Barbara, June 21 - 23 (1993).

50. "Mode-Locked Multi-Segment Resonant-Optical-Waveguide Diode Laser Arrays," A. Mar, R. Helkey, T. Reynolds, J. Bowers, D. Botez, C. Zmudzinski, IEEE Lasers and Electro-optics Society Summer Topical Meeting on Optical Microwave Interactions, Postdeadline Paper, Santa Barbara, CA, July 19-21, 1993.

51. "Mode-Locked Operation of a Master Oscillator Power Amplifier," A. Mar, R. Helkey, J. Bowers, D. Mehuys, D. Welch, IEEE Lasers and Electro-optics Society Annual Meeting, paper MSFL4.2, San Jose, CA, November 15-18, 1993.

52. "High-Power Mode-Locked Semiconductor Lasers," A. Mar, J. Bowers, Optical Society of America Annual Meeting (INVITED PAPER), paper ThV1, Dallas, TX, October 2-17, 1994.

## Patents

1. "Method and Apparatus for Object Positioning," Gerardo Beni, Alan Mar, C. John Landry, U.S. Patent 4,871,252, October 30, 1989.

# Abstract

This dissertation addresses two major areas of deficiency regarding mode-locked semiconductor lasers. The first is the tendency for mode-locked external cavity lasers to emit multiple pulse bursts per repetition cycle. For most applications, the effective system impulse response from such an output is not to the stimulus of a single pulse, but rather to the long decay envelope of the multiple trailing pulses. The second issue investigated forms the greater part of the dissertation, namely that of improving on the relatively low output powers generated from diode lasers under mode-locked operation, typically a couple of milliwatts or less.

Multiple pulsing from mode-locked external cavity lasers is caused by the residual reflections from antireflection coatings used to couple laser diodes to external cavities. The approach taken in this work to overcome this problem is to incorporate longer device lengths and employ fast gain modulation such that the reflections are delayed sufficiently compared to the modulation waveform to result in their suppression. The use of diodes as long as 1000 µm has resulted in suppression of multiple pulses by a factor of 50, resulting in clean, single pulse output per repetition cycle.

Three main approaches to obtain higher mode-locked output powers are described in this work. Arrayed lasers were used to construct high power mode-locked lasers with high saturation energies due to the large mode cross section of the arrayed gain region.

Flared multisegment waveguide lasers and amplifiers were also investigated for generation of high power pulses. By flaring the waveguide to

be wider in the gain segment of the laser, improvements in both pulse energy and pulsewidth result. Output powers greater than 2W were obtained, which is the highest yet achieved with a single stripe laser.

Such a device was used as the injection source for a flared broad-area amplifier. Using this approach, record average and peak powers and pulse energies have been achieved, with pulses being generated of energies exceeding 100 pJ and peak powers of nearly 30W. The high average and peak powers make this a viable alternative to elaborate benchtop mode-locked laser systems, such as dye or solid-state lasers.

# Table of Contents

## Chapter 1

# Introduction

### 1.1. Short Pulse Generation From Semiconductor Lasers.

Because of their compactness, reliability, efficiency, and relatively low cost, semiconductor lasers are attractive as sources of short optical pulses. Such pulsed sources are of interest for use in physics measurements, for instrumentation systems, and for telecommunications applications. Other attractive features of pulsed semiconductor sources include the ability to operate at a wide range of repetition rates and the availability of devices over a wide range of wavelengths.

The two most important and practical techniques of producing short pulses from semiconductor lasers are gain switching and mode-locking. Of these two techniques, gain switching is simpler, involving only current modulation to the laser. The pulse duration from a gain switched laser is inversely proportional to the carrier density injected above threshold [1], and it is usually difficult to generate pulses of less than 10 ps duration. This is due to parasitic capacitance in the laser which degrades the transmission of electrical pulses to the active region, and the limit on maximum current in the laser before which failure occurs. Because no resonant cavity is involved, gain switching at varied repetition rates is easily achieved. However, gain switched pulses have relatively large amplitude noise and timing jitter due to the fact that the pulses arise from spontaneous emission noise [2]. The pulses from a

1

gain switched laser are usually highly chirped, due to the index changes induced by the modulation of carrier density. This phenomenon may be exploited to achieve pulse compression (using gratings or fibers, for example), although this partially negates the advantage of the simplicity of gain switched lasers.

Mode-locking is a technique for generating short pulses utilizing the resonant response of the laser cavity. The longitudinal resonance modes of a Fabry-Perot laser are separated in frequency by the inverse of the cavity round trip propagation time. By coupling these modes in phase, a train of short pulses is obtained. Mode-locked lasers have much less amplitude noise and timing jitter than gain switched lasers because the mode-locked pulses are seeded from pulses already circulating in the laser cavity, rather than from spontaneous emission noise. In contrast to gain switching, large signal high-speed modulation is not an inherent limitation, and shorter pulses are generally obtained from mode-locked lasers.

## 1.2. Focus of this Dissertation.

This dissertation addresses two major areas of deficiency regarding mode-locked semiconductor lasers. The first is the tendency for mode-locked external cavity lasers to emit multiple pulse bursts per repetition cycle. For most applications, the effective system impulse response from such an output is not the response to the stimulus of a single pulse, but rather to the long decay envelope of the multiple trailing pulses. The second

2

general issue investigated forms the greater part of the dissertation, namely that of improving on the relatively low power levels generated from diode lasers under mode-locked operation, typically a couple of milliwatts or less.

Multiple pulsing from mode-locked external cavity lasers is caused by the small residual reflections from antireflection coatings used to couple laser diodes to external cavities, which, when re-amplified in the laser amplifier, can become comparable in amplitude to the primary pulses. The approach taken in this work to overcome this problem is to incorporate longer device cleaved lengths and employ fast gain modulation such that the reflections are delayed sufficiently compared to the gain modulation waveform to result in their suppression. The use of diodes as long as 1000 $\mu$m has resulted in suppression of multiple pulses by a factor of 50, resulting in clean, single pulse output per repetition cycle.

Three main approaches to obtain higher mode-locked output powers are described in this work. Arrayed lasers were used to construct high power mode-locked lasers, with high saturation energies due to the large mode cross section of the arrayed gain region. The passively mode-locked pulse energy was 21.9 pJ, with peak powers of over 3 W. These characteristics of mode-locked array lasers indicate a strong potential for use in applications requiring high output powers.

Flared waveguide lasers and amplifiers were also investigated for generation of high power pulses. By flaring the waveguide to be wider in the gain segment of the laser than in the absorber region, improvements in both pulse energy and pulsewidth are obtained compared to the uniform

3

waveguide device and the device with the flared absorber. Output powers greater than 2W are obtained, which is the highest yet achieved with a single stripe laser.

Such a device was used as the injection source for a flared broad-area amplifier in the so-called master oscillator power amplifier (MOPA) configuration. Because the external power amplification occurs in a single pass, the amplifier may be operated in a more heavily saturated regime than in a mode-locked laser, where pulse evolution occurs over many round trips. This allows independent optimization of the mode-locked laser oscillator from the power amplification stage. Using the MOPA approach, record average and peak powers and pulse energies have been achieved, with pulses being generated of energies exceeding 100 pJ and peak powers of nearly 30W. The high peak powers available from the mode-locked MOPA make it an excellent candidate for nonlinear optics applications, especially with the further peak power improvements that would be obtained from pulse compression. The high average powers also make this a viable alternative to large benchtop mode-locked laser systems, such as dye or solid-state lasers.

### 1.3. Mode-Locking Techniques -Active and Passive Mode-locking.

Phase locking of the longitudinal modes of a laser may be effected by introducing a source of modulation in the laser cavity which is driven periodically at the cavity round trip propagation time, as shown in Figure 1.2a. This is commonly referred to as active mode-locking, as the modulation

4

## a.) Active mode-locking



high reflector

- pulses propagate through modulator when the transmission of the modulator is at maximum
- pulse shaping occurs because the peaks of pulses experience the most net gain

## b.) Passive mode-locking



- high peak intensity pulses propagate with least loss through the saturable absorber
- pulse sharpening occurs as the absorber attenuates the lower intensity pulse edges
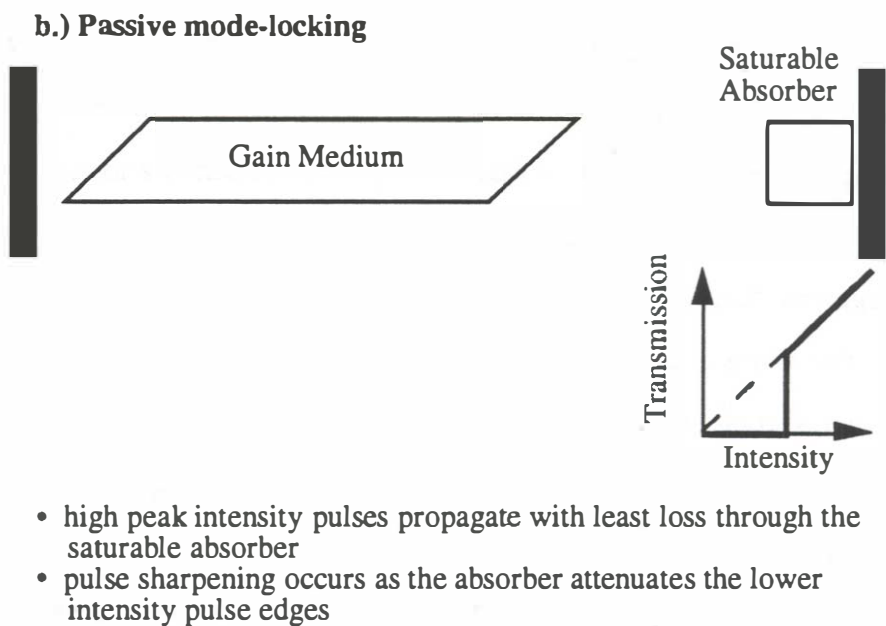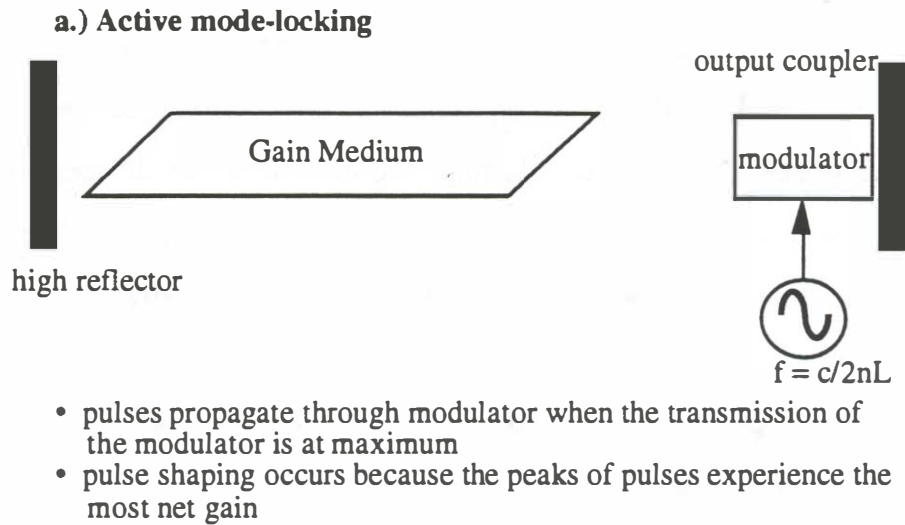
Figure 1.2 a. Active mode-locking using an intracavity modulator and
b. Passive mode-locking using a saturable absorber.

5

signal is applied from an external source. The modulation causes the formation of pulses that circulate in the cavity passing through the modulator on each round trip at the point of maximum transmission or gain. Pulse shortening occurs on each pass through the modulator, as the peak of the pulse experiences more net gain than the edges. This pulse shortening continues until balanced by some competing pulse broadening process. For example, the spectral width of the pulses necessarily becomes wider for shorter pulses, a process which may eventually become limited by the finite bandwidth of the gain medium.

Passive mode-locking refers to the use of a saturable absorber in the cavity to accomplish the gain modulation that causes mode-locking, as shown in Figure 1.2b. A saturable absorber has an optical transmission that is small at low input intensities, but whose absorption saturates and decreases at higher intensities. Short pulses of high peak power experience the least loss in propagation through the absorber, as the peak of a pulse undergoes less loss than the rising and falling edges. In practice, real saturable absorbers do not recover sufficiently fast to shape the trailing edge of a pulse, and pulse shortening occurs through the sharpening only of the rising edge, as shown in Figure 1.3.

This type of absorber is commonly referred to as a slow saturable absorber. For passive mode-locking to take place, however, the absorption recovery time must be at least as fast as the round trip propagation time in the laser so that absorption recovery occurs between the passage of pulses.

The pulse shaping mechanisms of active gain modulation and saturable

6
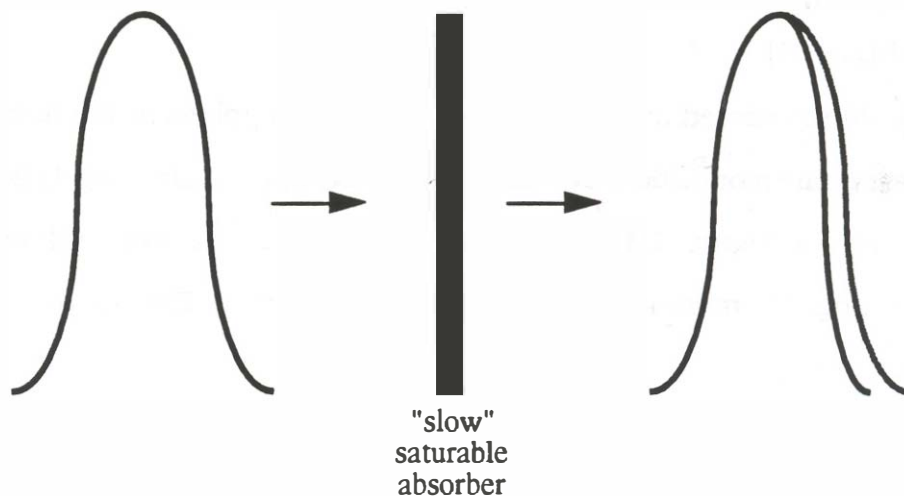
Figure 1.3. Pulse shaping resulting from passage through a "slow" saturable absorber. The leading edge of the pulse is steepened by the saturable absorption, but the absorption recovers too slowly to affect the trailing edge.

absorption may both be applied simultaneously in a mode-locked laser. This is frequently referred to as hybrid mode-locking, and allows some advantages over simpler purely active or passive techniques.

### 1.4. Implementation of Mode-locking With Semiconductor Lasers

Mode-locking of a semiconductor laser is most simply accomplished using passive mode-locking. Saturable absorption at a laser facet may be introduced by ion implantation [4]. This type of absorber may have fast recovery characteristics due to the reduced carrier recombination time caused by the implantation. The stability of this type of absorber is in question, however, and an alternative method is simply to segment the

7

electrical contact to the laser so that a short segment of the laser may be reverse-biased [5].

Multi-segmented diode lasers may be used to implement the functions of DC gain, gain modulation, and saturable absorption within a single device. As shown in Figure 1.4., this allows for active, passive and hybrid modelocking of monolithic semiconductor lasers. The mode-locked repetition rate,

$$f = \frac{c}{2 n L},$$

1.1.

is determined by the length L of the laser waveguide, where c is the speed of light, and n is the group velocity index in the laser. This repetition rate can therefore be quite high, and mode-locking frequencies as high as 350 GHz have been demonstrated [6]. Monolithic mode-locked lasers may also be useful as compact and efficient sources of millimeter-wave electrical signals by using fast photodetectors to detect the optical pulse stream, or perhaps more simply by using the current from absorber segment of the laser itself. Monolithic mode-locked lasers using ring structures have been demonstrated [7], which may be particularly useful for integration with electrical circuits because they do not require cleaving of the wafer or fabrication of DBR type structures. Some of the limitations of monolithic mode-locked lasers may be overcome by use of external cavity laser designs. As shown in Figure 1.5., this is done by anti-reflection coating the laser diode on one facet whose output is

8

**Active:**



$$f = \frac{C}{2nL}$$

**Passive:**



**Hybrid:**



$$f = \frac{C}{2nL}$$
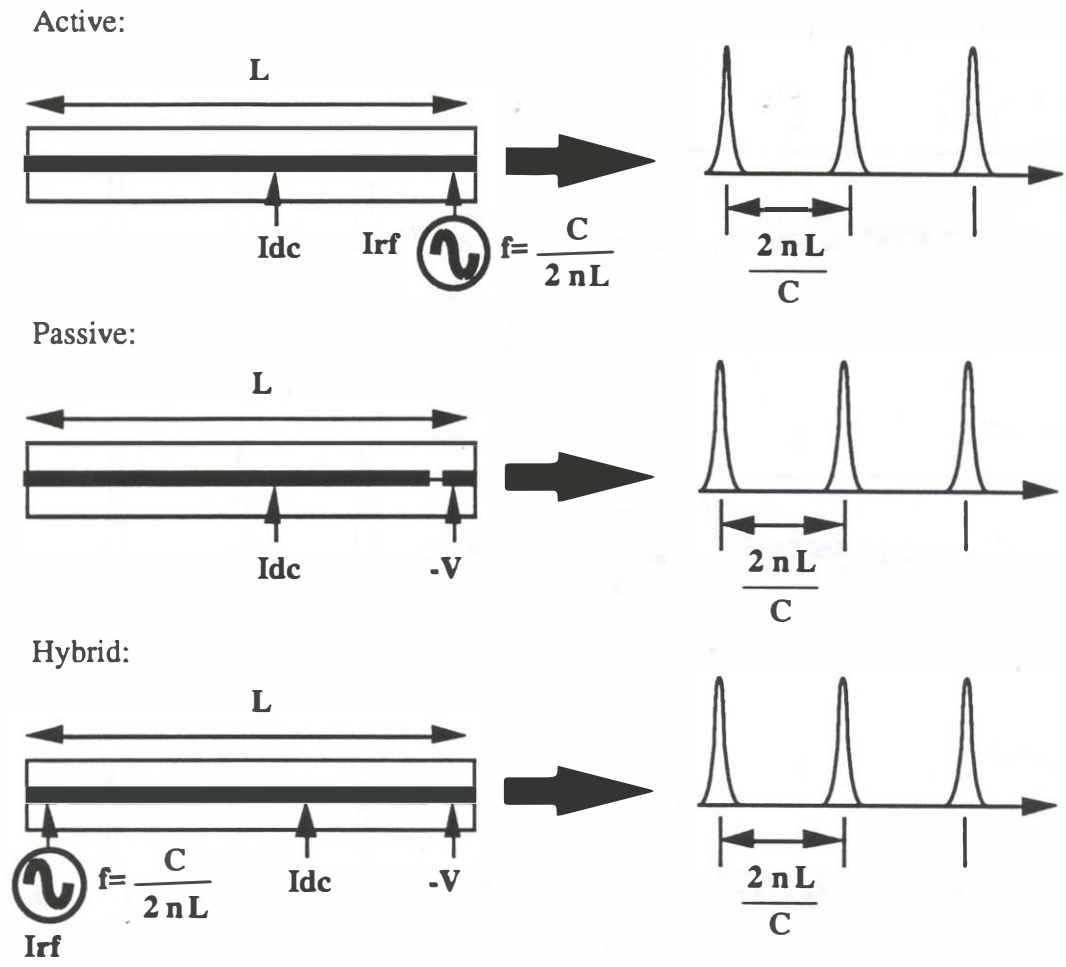
- segmented lasers can provide the functions of gain, modulation, and saturable absorption
- repetition period limited by laser diode cavity length

Figure 1.4. Monolithic mode-locked lasers using segmented contact devices.

9

**Active:**

L

mirror    AR coated    Vac

Idc    $f = \dfrac{C}{2L}$

$\dfrac{\sim 2L}{C}$

**Passive:**

L

mirror    AR coated

Idc    -V

$\dfrac{\sim 2L}{C}$

**Hybrid:**

L

mirror    AR coated    -V

Idc + IRF

$\dfrac{\sim 2L}{C}$
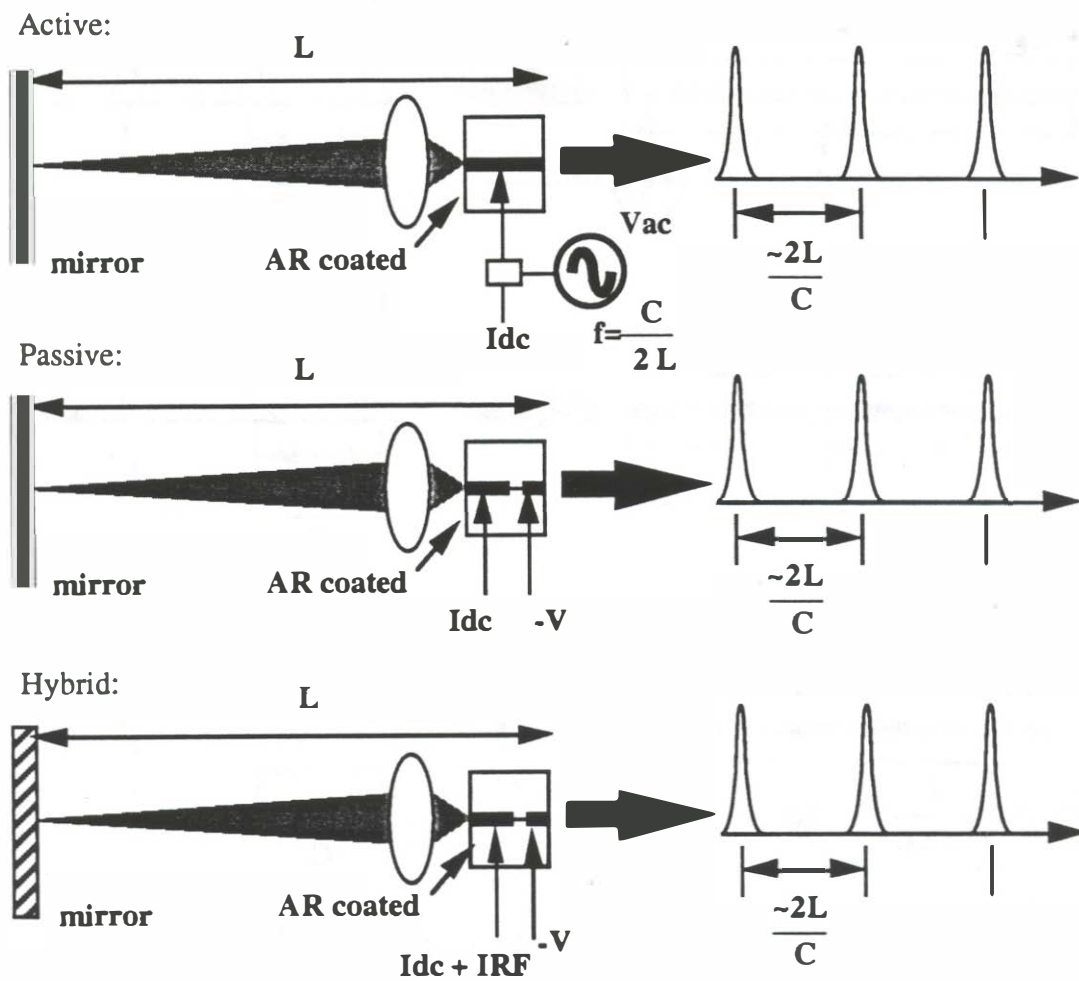
- requires use of anti-reflective diode facet coatings
- repetition period can be adjusted by external cavity length

Figure 1.5. External-cavity mode-locked lasers.

then coupled to an external cavity using bulk optics. The repetition rate of such a laser is determined by the length of the external cavity and thus may be adjusted mechanically. The earliest demonstrations of mode-locked semiconductor lasers were done using external cavities [8], so that the resulting mode-locking frequencies fall within the range of common microwave sources and instrumentation.

### 1.5. Advantages and Disadvantages of the Various Mode-Locking Techniques

<u>External Cavity vs. Monolithic.</u>

Of the aforementioned techniques for mode-locking diode lasers, the passively mode-locked monolithic laser is the simplest, requiring no external modulation sources or external cavity optics. The lower bound on the repetition rate of monolithic devices is set by the cleaved waveguide length, resulting repetition rates in hundreds of GHz for typical device lengths of a few hundred microns. Low repetition rate devices require long waveguides, which places severe requirements on materials growth and processing uniformity. Repetition rates as low as 2.2 GHz have been demonstrated from devices of 2 cm. length [9]. The external differential quantum efficiency,

$$\eta = \frac{\alpha_{mirror}}{\alpha_{mirror} + \alpha_{internal}} \text{,} \qquad \qquad \textbf{1.2}$$

is poor because of the relatively high internal loss in such long devices, and it

11

may be difficult to obtain very much output power from them. Long devices also require large amounts of space on a wafer, which makes them more costly to manufacture.

For these reasons, external cavity designs are in common use for mode-locking semiconductor lasers, and are the subject of much of the experimental work in this dissertation. As previously mentioned, the repetition rate of such a laser is determined by the length of the external cavity and thus may be adjusted mechanically. They also afford the advantage of flexibility in constructing lasers incorporating tuning elements, filters, dispersion compensation elements, etc. It is also easier to obtain high peak powers and high pulse energies at lower repetition rates, because of the resulting lower duty cycle of the pulses, mitigating issues such as thermal limits on device operation. External cavity lasers have the major disadvantage of requiring the alignment of bulk optics. Another important problem is their tendency to generate bursts of multiple pulses per round trip, which is an issue addressed in Chapter 2 of this dissertation.

## Active vs. Passive Mode-Locking

Actively mode-locked lasers are more complex than passively mode-locked lasers in that they require an electrical drive signal to effect gain modulation. It has been shown that fast electrical signals are required to provide sufficient pulse shaping to obtain pulsewidths on the order of one picosecond [10-12]. This necessitates the use of high frequency modulation or high-speed impulse generation circuits, as well as high-speed laser designs

12

with minimal parasitic capacitance, and high-speed packaging. For these reasons, it has generally been easier to obtain short pulses with saturable absorption as the dominant pulse shaping mechanism, as is the case with passively and hybridly mode-locked lasers.

For many applications of mode-locked lasers, the pulse to pulse timing jitter is of critical importance. Particularly in applications where data is obtained over many pulses, with the exception of pump-probe type configurations, the effective system temporal impulse response is limited by the combined effects of pulsewidth and jitter, and there is little advantage to having pulsewidths that are shorter than the rms timing jitter.

Active mode-locking produces the least pulse-to-pulse timing jitter [13]. The jitter in the optical pulses is often very close to that of the electrical source used to drive the mode-locking, and may be well under 0.5 ps. Passive mode-locking produces very large amounts of timing jitter, bounded only by the measurement interval which sets a lower limit on the frequency range over which the phase noise is integrated. This may typically result in hundreds of ps timing jitter over a one second measurement [14]. The high level of timing jitter in passively mode-locked lasers is due to the fact that there is no driving signal for timing stabilization, which leaves the free-running laser susceptible to noise sources, such as spontaneous emission.

At frequencies greater than about 20 GHz, it becomes difficult to directly modulate the laser efficiently, so active mode-locking may not be a practical technique for pulse timing synchronization at millimeter-wave frequencies. However, techniques for phase-locking passively mode-locked

13

lasers to lower frequency sources have been demonstrated [15, 16]. These techniques involve applying timing correction by varying the DC bias to the absorber segment of the laser, which can result in stabilization of mode-locking frequencies well beyond the electrical parasitic-limited cutoff frequency for direct modulation.

For certain applications it is essential to have the optical pulse output synchronized with external signals, which is a fundamental characteristic of actively mode-locked lasers. However, active gain modulation tends to weaken as a pulse shaping process as the optical pulses become short compared to the gain modulation speed. In passively mode-locked lasers, pulse shaping in saturable absorbers is more independent of the pulsewidth, and, as previously mentioned, it is generally therefore easier to generate short pulses with this technique. Hybrid mode-locking therefore offers the advantages of both the pulse shaping characteristics of using saturable absorbers and of synchronized pulse output due to active gain modulation.

## 1.6. Power Output of Mode-Locked Semiconductor Lasers

Typically, semiconductor lasers output much less average power under mode-locked operation than they do under cw conditions. This is fundamentally due to pulse broadening effects in semiconductor amplifiers [17], particularly when the pulse energies approach the saturation energy,

$$E_{sat} = \frac{h\nu\,A}{\Gamma\,dg/dn} \qquad\qquad 1.3.$$

14

where A is the active region cross section, $h\nu$ the photon energy, $\Gamma$ the confinement factor, and $dg/dn$ the differential gain. In passively mode-locked lasers, as one attempts to operate the laser at higher pulse energies, this pulse broadening overwhelms the pulse shaping process in the saturable absorber, which results in the cessation of mode-locking at pulse energies approaching $E_{sat}$. In actively mode-locked lasers, operation in this regime results in poor quality pulses, with broad pulsewidths and excess optical bandwidths. This pulse energy limit is typically about 2 pJ for a single-mode laser, which, depending on the repetition rate, results in mode-locked average powers far below the laser's cw power capability. For example, at a repetition rate of 1 GHz, this results in an internal average power of 2 mW within in the laser, which may represent less than 1 mW output power after the losses due to output coupling.

In this dissertation, three approaches for improving the pulse energy limitation of mode-locked semiconductor lasers are explored. The first approach involves the use of arrayed laser structures to increase the active region cross section A, and thereby increase the pulse energy. Multi-section devices were fabricated and tested to demonstrate active, passive and hybrid mode-locking of arrayed devices. Another approach is to use a flared waveguide laser, where the active region in the gain segment is widened beyond the limit for single mode operation. Fundamental mode selectivity in these devices is provided in other segments that have single-mode waveguides. The last approach is that of the MOPA (Master Oscillator Power

15

Amplifier) configuration, where the output of a conventional mode-locked laser is amplified using a flared high-gain single-pass external semiconductor amplifier.

## 1.7. Organization of the Dissertation

This introductory chapter has served to introduce some of the topics to be addressed in the following chapters of this dissertation. There are four such chapters, and three appendices that discuss technological issues related to semiconductor laser mode-locking.

Chapter two addresses the problem of multiple pulse formation in external cavity lasers. This phenomenon originates from the finite residual reflection from the antireflection coating that is used to couple the laser diode to the external cavity. The multiple pulse phenomenon exists even for very low values of reflectivity from this coating, and it is not a practical approach to attempt to eliminate multiple pulsing by further reductions in the coating reflectivity. It is shown that multiple pulsing may be eliminated by careful selection of device lengths and cavity geometries, taking into consideration the dynamics of gain modulation and absorption recovery in the device being employed.

In Chapter three, arrayed laser structures are used to improve the pulse energy performance from semiconductor lasers. Anti-guide array structure devices are used because of their excellent far-field characteristics, and it is shown that such devices couple well to external cavities with careful

optical design, with coupling efficiencies comparable to those obtained using conventional single-element lasers. Active, passive, and hybrid mode-locking configurations are demonstrated using multi-segment devices. Pulse energy performance is improved, scaling with the number of array elements in the laser structure.

Chapter four reports the use of flared waveguide devices to improve pulse energy performance in single-stripe lasers and amplifiers. Comparisons are made between uniform waveguide devices and devices with waveguide flaring both in the absorber and in the gain segments. By flaring the waveguide to be wider in the gain segment of the laser than in the absorber region, improvements in both pulse energy and pulsewidth are obtained compared to the uniform waveguide device and the device with the flared absorber. A flared Master Oscillator Power Amplifier (MOPA) configuration is also demonstrated, independently optimizing the mode-locked laser oscillator from the power amplification stage. Using this approach, record average and peak powers and pulse energies have been achieved, with pulse energies exceeding 100 pJ and peak powers of nearly 30 W being generated.

17

# References

1. P. M. Downey, J. E. Bowers, R. S. Tucker, and E. O. Göbel, "Picosecond dynamics of a gain-switched InGaAsP laser", IEEE J. Quantum Electron. QE-23, p. 1039, 1987.

2. Y. Arakawa, T. Sogawa, M. Nishioka, M. Tanaka, and H. Sakaki, "Picosecond pulse generation (<1.8 ps) in a quantum well laser by a gain switching method," Appl. Phys. Lett., vol. 51, pp. 1295-1297, 1987.

3. A. E. Siegman, Lasers, University Science Books, Mill Valley, CA.

4. J. P. Van Der Ziel, R. A. Logan, and R. M. Mikulyak, "Generation of subpicosecond pulses from an actively mode-locked GaAs laser in an external ring active cavity", Applied Physics Letters, 39, pp.867-869, 1981.

5. C. Harder, J. S. Smith, K. L. Lau, and A. Yariv, "Passive mode-locking of buried heterostructure lasers with non-uniform current injection," Appl. Phys. Lett., vol. 42, pp. 772-774, 1983.

6. Y. K. Chen, M. C. Wu, T. Tanbun-Ek, R. A. Logan, and M. A. Chin, "Subpicosecond monolithic colliding pulse mode-locked multiple quantum well lasers," Appl. Phys. Lett., vol. 58, pp. 1253-1255, 1991.

7.  Hohimer, J. P., Vawter, G. A., "Passive Mode Locking Of Monolithic Semiconductor Ring Lasers At 86 GHz," Applied Physics Letters, Sept. 20, V63 N12:1598 1600, 1993.

8.  P. T. Ho, "Coherent pulse generation with a GaAlAs laser by active mode locking," Electron. Lett., vol. 5, pp. 526-527, 1979.

9.  P. B. Hansen, G. Raybon, and U. Koren, "5.5 mm long InGaAs monolithic extended cavity laser with an integrated Bragg-reflector for active mode-locking," IEEE Photonics Tech. Lett., vol. 4, March, 1992.

10. S. W. Corzine, J. E. Bowers, G. Przybylek, U. Koren, B. I. Miller, C. E. Soccolich, "Active mode locked GaInAsP laser with sub-picosecond output," Appl. Phys. Lett., vol. 52, p. 348, 1988.

11. M. Schell, A. Weber, E. Schol, D. Bimberg, "Fundamental limits of sub-picosecond pulse generation by active mode-locking of semiconductor lasers: the spectral gain width and the facet reflectivities", IEEE Journal of Quantum Electronics, QE-27, 1661, 1991.

12. A. Mar, D. J. Derickson, R. J. Helkey, J. E. Bowers, R. T. Huang, D. Wolf, "Actively Mode-Locked External-Cavity Semiconductor Lasers with Transform-Limited Single Pulse Output", Optics Letters, 17, p. 868-870, June 1992.

13. D. J. Derickson, A. Mar, and J. E. Bowers,"Residual and absolute timing jitter in actively mode-locked semiconductor lasers," Electronics Letters, vol. 26, pp. 2026-2027, 1990.

14. R. J. Helkey, Ph.D Dissertation, University of California at Santa Barbara, Science and Engineering Library, 1993.

15. R. J. Helkey, D. J. Derickson, A. Mar, J. E. Bowers, R. L. Thornton, "Repetition frequency stabilization of passively mode-locked semiconductor lasers", Electronics Letters, **28**, 1920-1922, Sept. (1992).

16. J. B. Georges, L. Buckman, D. Vassilovski, J. Park, K. Y. Lau, "Stable Picosecond Pulse Generation At 46 GHz By Modelocking Of A Semiconductor Laser Operating In An Optoelectronic Phaselocked Loop," Electronics Letters, 1994 Jan 6, V30 N1:69-71.

17. G. P. Agrawal, "Effect of gain dispersion on ultrashort pulse propagation in semiconductor laser amplifiers," IEEE J. Quantum Electronics, QE-27, pp. 1843-1849, 1991.

**Chapter 2**

# Suppression of Multiple Pulsing in External Cavity Mode-Locked Lasers

## 2.1. Observations Of Multiple Pulse Bursts From Mode-locked Lasers.

Ideally, a mode-locked laser emits a single pulse per repetition cycle, the period of which is set by the overall roundtrip propagation time in the laser cavity. However, there are many reports of mode-locking where the output consists of multiple pulse bursts per repetition cycle [1-5]. Such output typically consists of a series of decaying pulses separated by the roundtrip propagation delay in the laser diode itself, as shown in Figure 2.1.
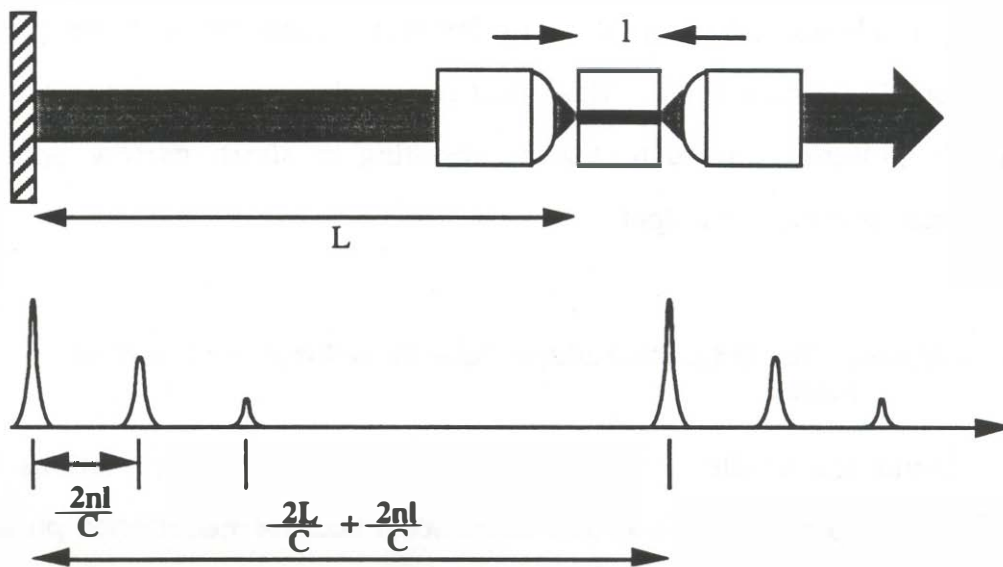
Figure 2.1. Multiple pulse output from a mode-locked semiconductor laser.

21

The trailing pulses can be quite large in amplitude, and have been prevalent in nearly all external cavity mode-locked lasers that emit pulses about as short as one picosecond or less, examples of which are shown in Figure 2.2. Diode lasers actively mode-locked in an external cavity have produced such multiple pulse bursts with individual pulses as short as 0.58 ps [1] at a 16 GHz repetition rate, but this behavior is unsuitable for most applications. Multiple pulsations in an external cavity mode-locked laser result from weak reflections from the antireflection (AR) coated laser facet that is used for coupling to an external cavity. The use of monolithic structures for mode-locking eliminates the source of multiple reflections and short, single-pulse outputs have been demonstrated [6,7]. Saturable absorbers have also been employed to suppress multiple pulse output in passively mode-locked external cavity lasers [8]. In this chapter, the design of actively mode-locked external cavity lasers to suppress multiple pulse behavior will be considered. This effort has resulted in the suppression of multiple pulsations in such devices, resulting in short, narrow optical bandwidth, single-pulse output.

## 2.2. Analysis Of The Origin Of Multiple Pulse Behavior In Mode-locked Lasers.

Numerical studies have revealed that large multiple pulsations in external cavity actively mode-locked lasers occur because the reflected pulses from the imperfect AR coating experience a large gain as the RF current pulse used to drive the mode-locking continues after emission of the main pulse [1].
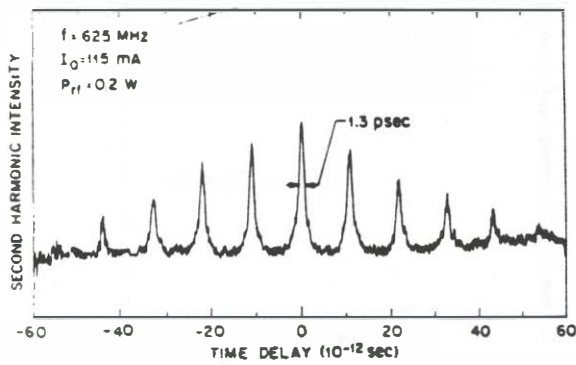
**Passively Mode-Locked:**
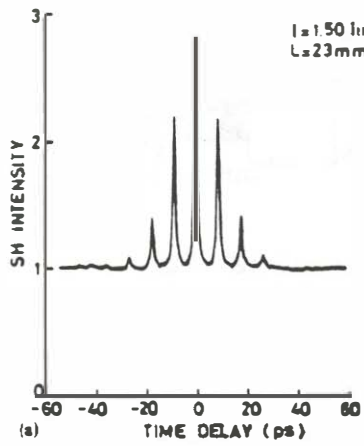

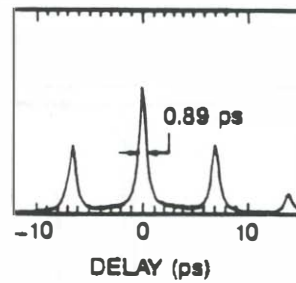
Yokoyama et al., 1981
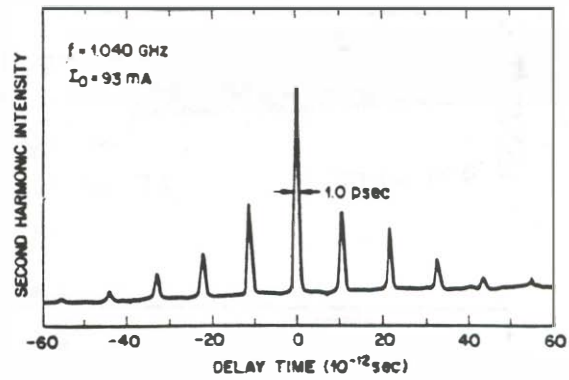


van der Ziel et al., 1981

**Actively Mode-Locked:**



van der Ziel et al., 1981



Corzine et al., 1987

Figure 2.2. Published examples of multiple pulsing behavior from mode-locked external cavity lasers.
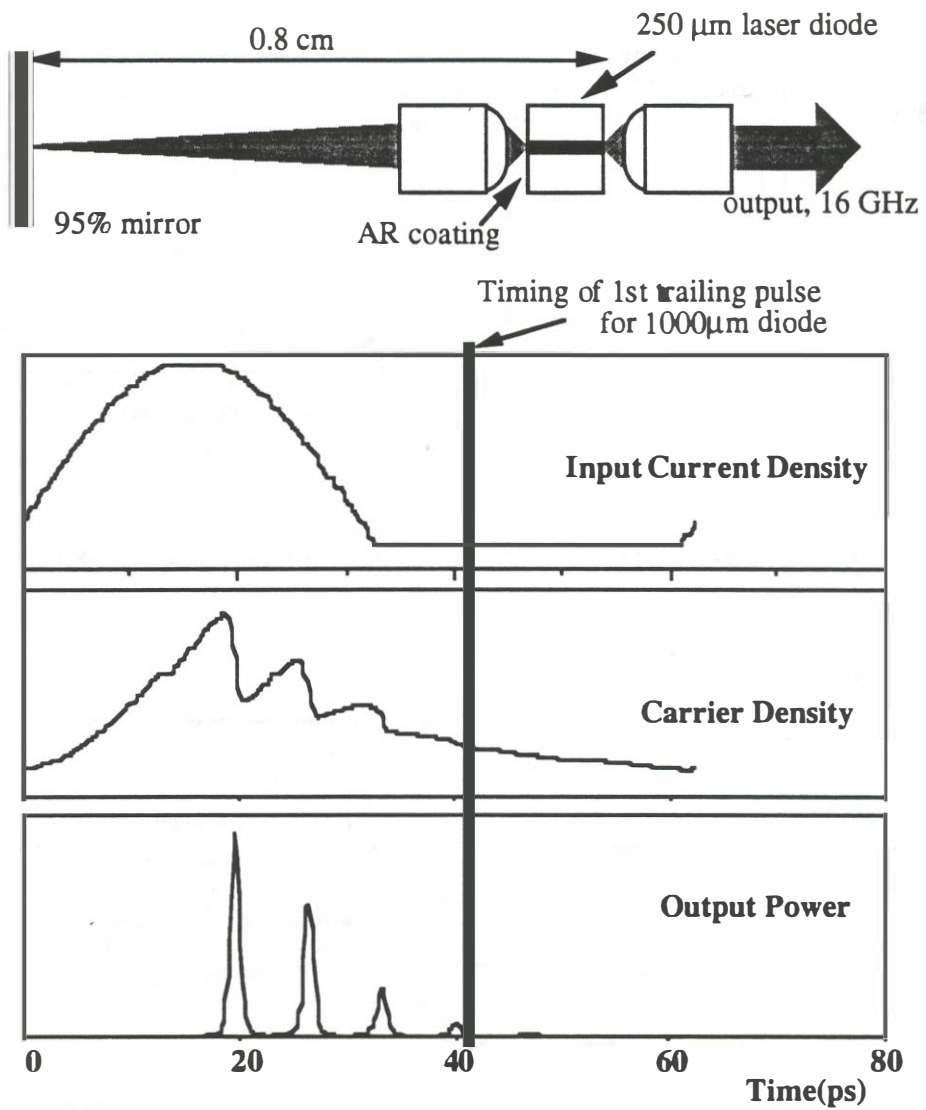
23

Figure 2.3. Analysis of multiple pulse formation in an actively mode-locked external cavity laser.

As shown in Figure 2.3, the primary pulse only partially depletes the carriers through stimulated emission and the pump current injects additional carriers causing the gain to rise after passage of this first pulse. This causes the carrier density in the laser to remain above transparency as the pulse is partially reflected back into the laser diode. This small reflected pulse thus experiences gain and grows over many round trips in the laser until a steady-state condition is reached due to gain saturation. This first trailing pulse may seed a further pulsation if the pump current and subsequent gain recovery continues after its passage. Depending on the duration of the electrical pump pulses, gain may exist long enough for several reflections to be amplified. Even though they are seeded by small reflections, the trailing pulses may grow to be comparable in amplitude to the main pulse, their growth over many round trips being limited by the gain recovery and saturation processes. Schell et al. have done a similar analysis which verifies this origin of large multiple pulsations [9]. In addition, they show that strong multiple pulsing occurs even for very low AR coating reflectivities, shown in Figure 2.4. Antireflection-coated facet reflectivities as low as $R = 10^{-5}$ may be necessary to eliminate the AR coating as the source of multiple pulsations. This is a very difficult value to achieve experimentally, so it is impractical to pursue this approach to eliminate multiple pulses. The analysis of Schell et al. also shows the influence of the injection current falltime on the amplification of trailing pulses, also shown in Figure 2.4. This illustrates the importance of reducing the falltime of the injection current to the laser compared to the roundtrip delay between pulse reflections. The experiments and calculations presented

25
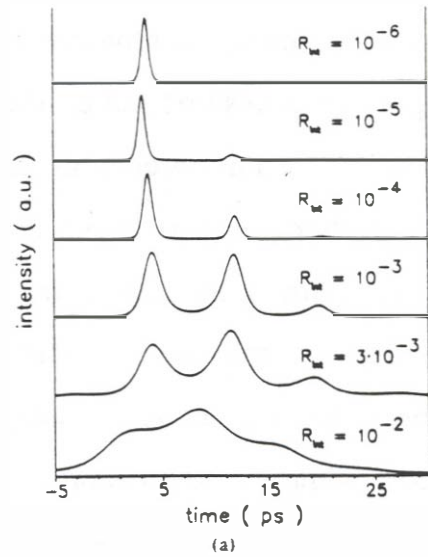
**Optical output for different internal facet reflectivities Rint: Temporal Pulse Shape**
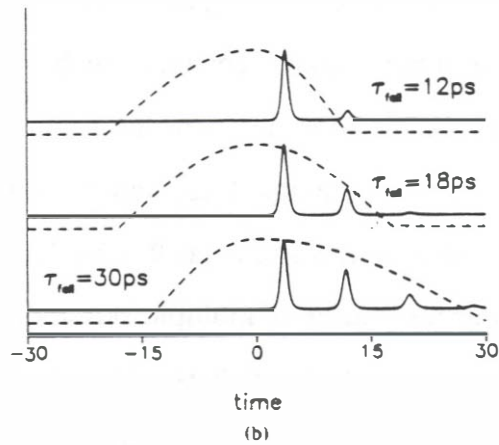


**Influence of the injection current.
Variation of the injection current fall time.**

Figure 2.4.  Results of Schell et al. [9], analyzing the case of different AR coating reflectivities and modulation current falltimes.

from References 1 and 9 are based on a laser diode cleaved length of 250 μm, pumped by a 16 GHz sinusoid, resulting a reflected pulse spacing of 7 ps and a pump current duration of roughly 20 ps FWHM. These parameters fall well within the regime where multiple pulses are expected. **This analysis suggests that multiple pulse behavior will be suppressed if the time delay between reflected pulses is made larger than the drive pulse falltime.** This may be implemented by the use of fast electrical pulses to drive the mode-locking and also by **using longer laser diodes in the laser cavity.** A further refinement is the use of multi-section lasers to optimize bias conditions and enhance the falltime of the gain in the modulated section. This is the approach that is investigated in the experiments described in this chapter.

## 2.3. Multi-segment laser designs for improved mode-locking characteristics.

Multiple section lasers allow for the separation and independent optimization of the functions of DC gain and gain modulation in a single device, as shown in Figure 2.5. The devices were fabricated by etching the top contacts of high-speed bulk active region semi-insulating buried heterostructure InP lasers into two sections: a 20-40 μm section for RF modulation, and a longer dc biased section. Because high-speed electrical modulation was desired, device structures were employed with attention to low parasitic capacitance. Fe-doped InP current blocking layers were used for current confinement without incurring the capacitance that reverse-biased junction blocking layers add. In addition, polyimide filling was used under bondpad metal to reduce the capacitance from the p-side contacts
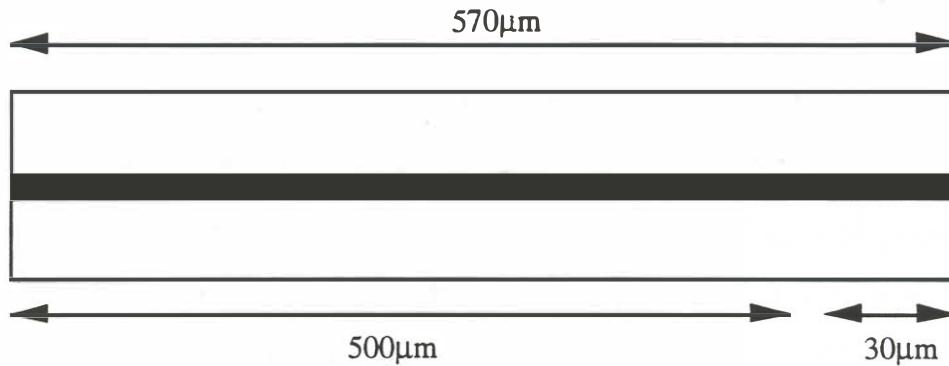
27

Figure 2.5. A typical segmented laser used in the external cavity mode-locking experiments.

[10]. Electrical isolation between sections of typically hundreds of ohms was achieved by etching away the p+ contact layer between breaks in the ohmic contact, which were made 10 $\mu$m wide.

There are many advantages to the segmented contact laser design for mode-locked lasers. The longer DC gain segment of the laser is used to provide the gain required to reach lasing threshold. Because the short modulator section is not relied upon to supply DC gain it may be left at zero bias or even reversed biased, resulting in very high modulation depth in this section of the laser. The modulation index that is achieved in such a segment for a given amplitude electrical modulation is thus much greater than in a conventional laser in which the entire device must be modulated with a superimposed forward DC bias. The efficiency of gain modulation in a short zero or reverse-biased segment is also enhanced because of the differential

28

gain (or loss) is greater at low carrier densities. To be discussed further in Chapter 4, this effect also makes it possible for such an absorbing section to function as a saturable absorber that has a lower saturation energy than in the gain segment, fulfilling the requirements for stable passive mode-locking [11]. The high gain modulation index in the modulator segment is very beneficial for generating short pulses with 100% modulation.

Reverse biasing of the laser modulator segment also has other advantages. Such a segment behaves essentially as a waveguide photodetector, with the reverse bias serving to create electric field in the active region which aids the removal of carriers. The absorption recovery in such a segment can be very fast, less than 10 ps, as measured by Karin et al. [12], using pump-probe techniques with a femtosecond laser. In an actively mode-locked laser, this characteristic of fast field-aided recovery allows the gain modulation to fall quickly, presuming the use of a current modulation waveform with a fast falltime. This effect is of great importance for suppression of the multiple pulse phenomenon.

## 2.4. Demonstration of multiple pulse suppression by increased device lengths.

Figure 2.6 shows the configuration used for these experiments. Two segment lasers are coupled to an external cavity, with the laser diode oriented such that the DC gain segment faces the external cavity. The facet is antireflection coated, and a GRINROD lens is used to collect the output into a 5 cm external cavity. This arrangement maximizes the delay of the pulses
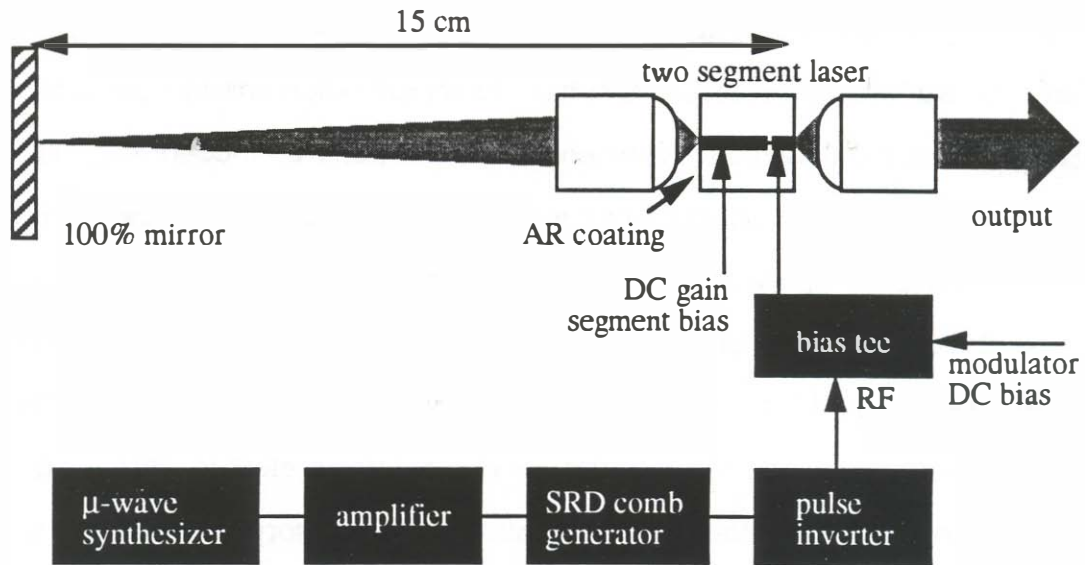
29

Figure 2.6. Diagram of actively mode-locked two segment external cavity laser experiment.

reflected from the AR coating arriving to the modulator segment. Experiments were performed using both an 830 lines/mm grating and a 100% bias -lower intracavity beam onto the external cavity mirror, as this allows for a greater degree of angular misalignment of this mirror and therefore a cavity that has greater stability against mechanical fluctuations.

It was found in [1] that short pulses were obtained only for high modulation rates because short RF pulses are necessary in shaping short optical pulses. To achieve a similar effect at lower repetition rates, a step recovery diode (SRD) comb generator is used. Pulses of 29 ps duration and 7 V amplitude from the comb generator were measured using a 40 GHz

30
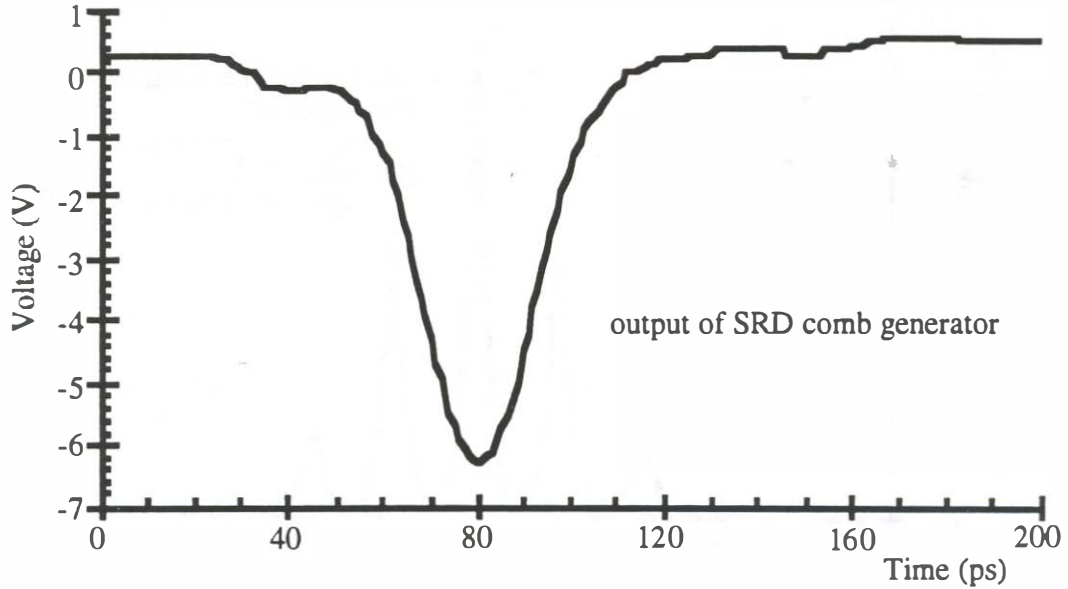
Figure 2.7. Output of the SRD comb generator used to gain modulated the laser experiments.

sampling oscilloscope, as shown in Figure 2.7. As the SRD module generates negative-polarity pulses, a coaxial pulse inverter was used which broadened the pulses to 33 ps.

To study the effect of cleaved device lengths on multiple pulse suppression, the broadband dielectric mirror was placed in the cavity. Lasers of 430 and 990 $\mu$m lengths were cleaved from the same section of processed material, and AR coated in consecutive coating sessions. Spectral analysis of the amplified spontaneous emission (ASE) from these devices indicate that the coatings have reflectivities of between $5x10^{-4}$ and $1x10^{-3}$, which has been shown [1,9] to be more than sufficient to cause multiple pulsation effects.

31

Figure 2.8. Comparison of pulse output from devices of 450 μm and 900 μm cleaved lengths.
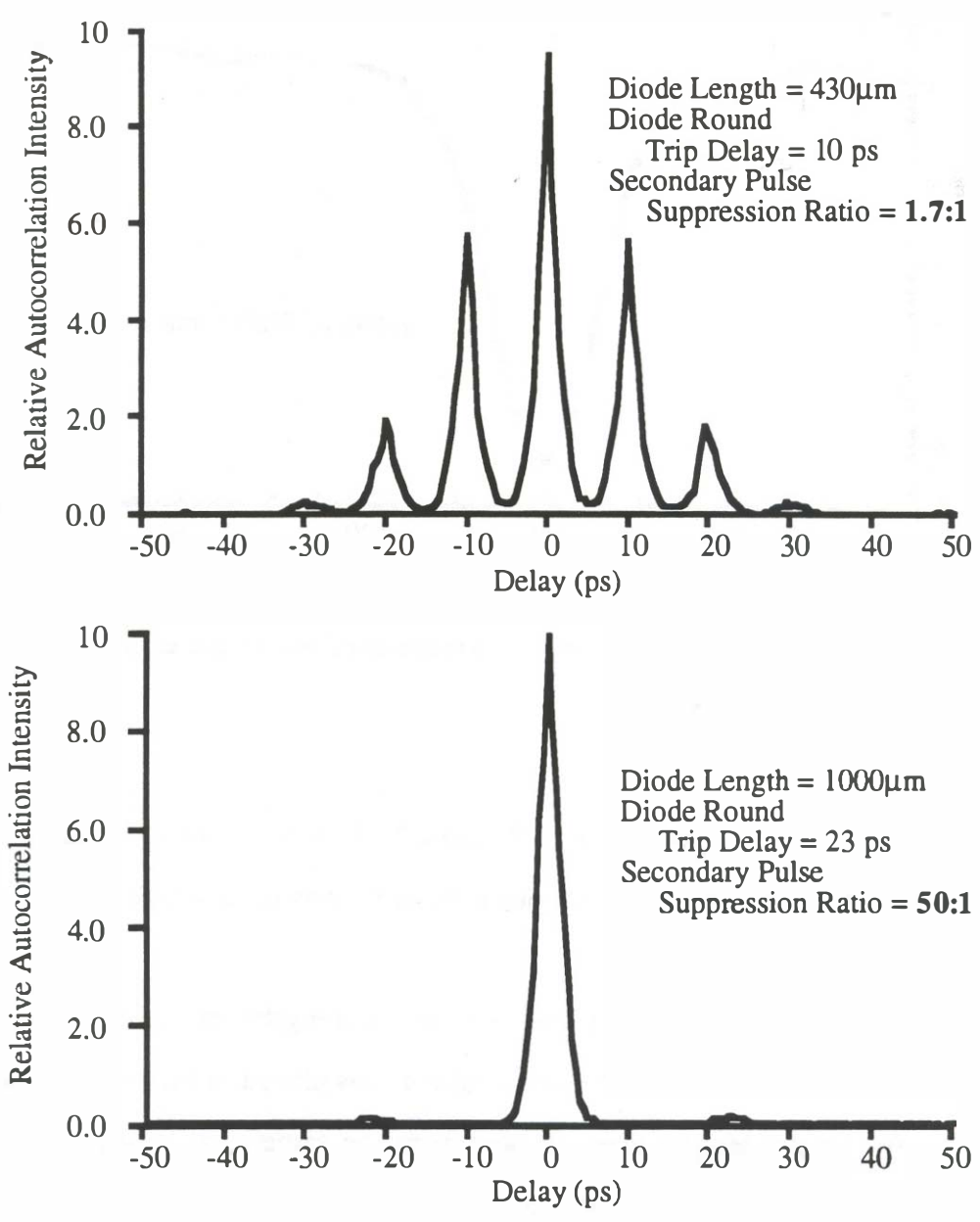
The autocorrelations of the pulse output of these two lasers are shown in Figure 2.8. The 430 μm diode, operated with a DC current of 40 mA and RF electrode reverse bias of 1.0 V and modulation from the SRD, exhibits severe multiple pulsation effects as the round trip delay in this device is only 10 ps. The amplitude of the primary pulse is only 1.7 times the amplitude of the first trailing pulse. Two more trailing pulses are also distinctly visible. In contrast, the 990 μm diode, with a round trip delay of 22 ps, exhibits almost no trailing pulsations at all. A reflected pulse at this delay is just barely discernible, being 50 times smaller than the primary pulse. The bias conditions in this case were 70 mA DC current and 1.6 V reverse bias on the RF electrode.

These results show very dramatically the effectiveness of using laser diodes of sufficient length such that the AR facet-reflected pulses are delayed in arriving to the modulator segment until the gain modulation has been shut off. Multiple pulsing observed from a device of 430 μm length is nearly completely suppressed in an otherwise similar device by more than doubling the length to 990 μm, changing the delay of reflected pulses from 10 ps to 22 ps. The pulsewidths in both cases were nearly identical, about 2.0 ps, assuming hyperbolic secant squared pulseshapes.

### 2.5. Effect of reverse bias tuning of the laser gain modulator.

Another effect of the reverse bias on the RF modulated section of the laser is the shortening of the current pulses to the laser, as shown in Figure 2.9. As the reverse bias is increased, only the peak of the RF signal forward
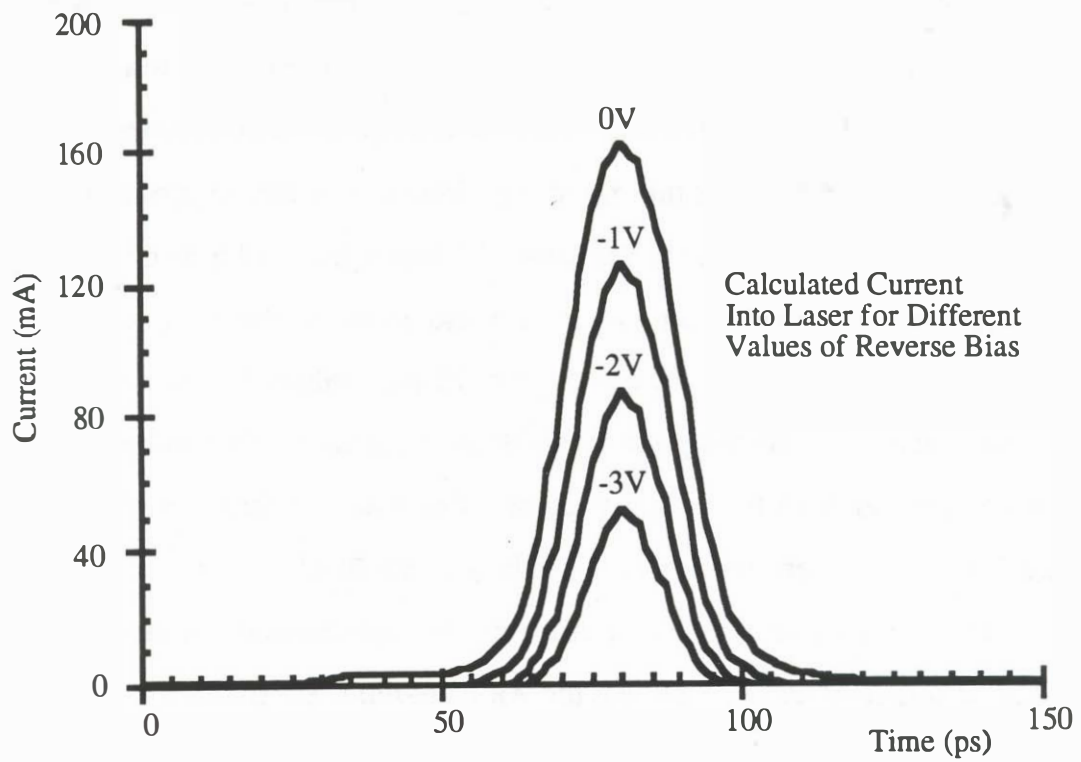
Figure 2.9. Dependence of modulation current waveforms on reverse bias to the gain modulator.
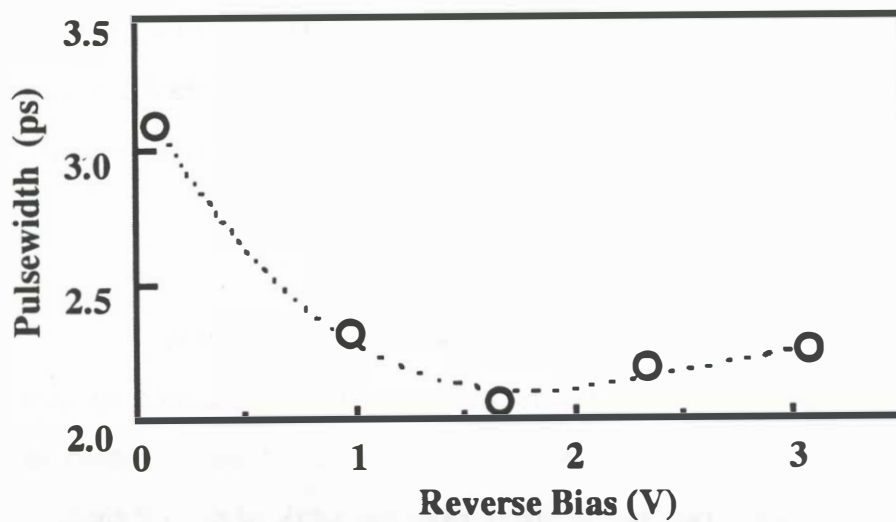


Figure 2.10. Pulsewidth dependence on modulated electrode DC reverse bias.

34

biases the laser, resulting in a shorter but lower amplitude current pulse. Thus, the laser pulsewidth will be shortest for a particular value of reverse bias -lower values resulting in longer current pulses, and higher values resulting in too little peak current for good pulse shaping characteristics. This characteristic is shown for one particular device in Figure 2.10.

By optimizing the RF electrode reverse bias and external cavity length tuning, pulses as short as 2.1 ps autocorrelation width were obtained without multiple pulsations, shown in Figure 2.11. These results were obtained on a device of 600 $\mu$m cleaved length, operated with 70 mA DC bias current and 1.0 V reverse bias on the modulated electrode. The autocorrelation shape is in reasonable agreement with that of hyperbolic secant squared pulses, which corresponds to 1.4 ps pulsewidth. The optical spectral width measured was be 1.9 nm, resulting in a time-bandwidth product of 0.47, indicating that the pulses have very little chirp. The average power was about 1 mW, corresponding to peak powers of over 200 mW.
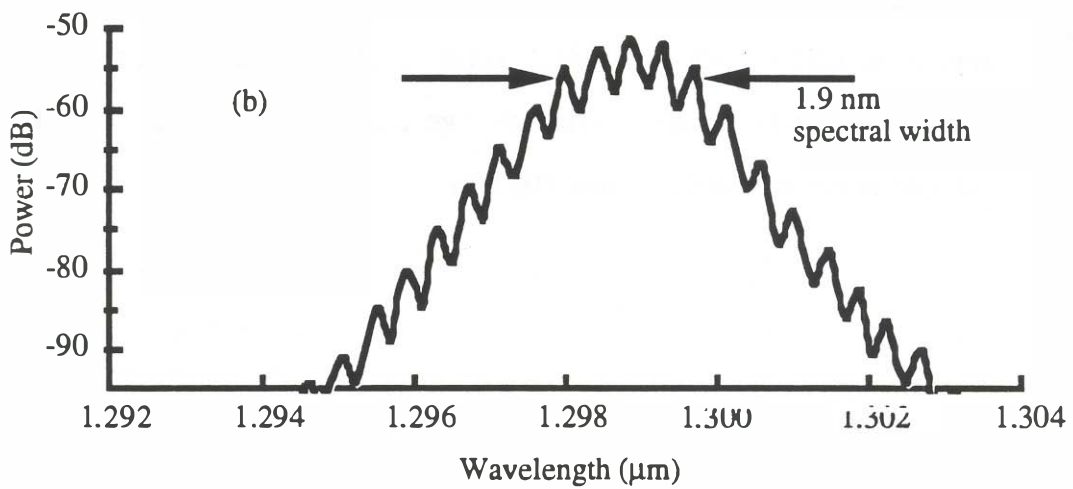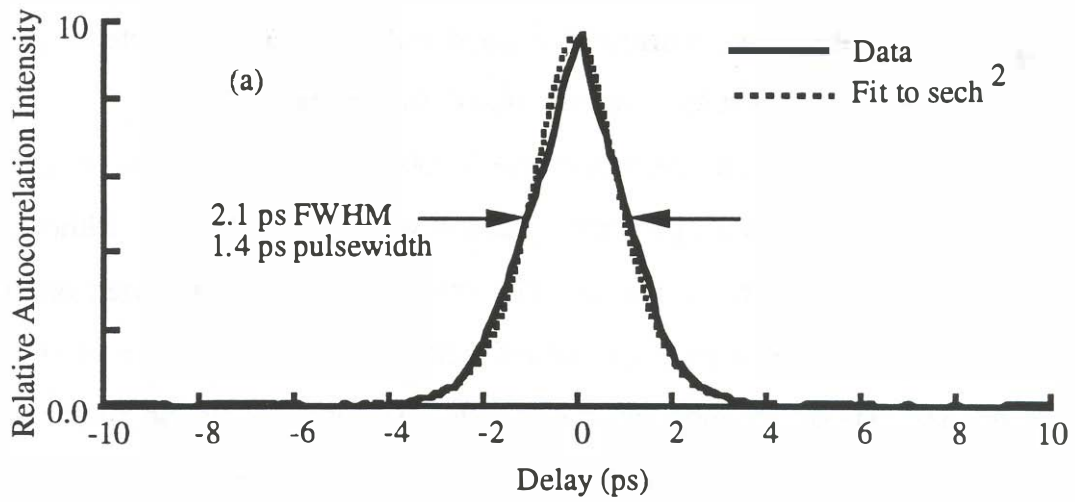
Figure 2.11. Autocorrelation (a) and optical spectra (b) of shortest pulses observed.

## 2.5. Generation of transform-limited pulses using an external cavity grating.

The use of external cavity feedback allows the use of a diffraction grating reflector as a bandwidth tuning and filtering element. The bandwidth of the grating feedback to the laser decreases as the illuminated spot size on the grating is increased, which may be done by the selection of the intracavity lens. The GRINROD lens used in the cavity (NSG PCH type), when adjusted for a collimated (not converging nor diverging) beam, illuminates a spot on the grating of approximately 2 mm diameter. With the grating installed in the external cavity in place of the dielectric mirror, pulses of 11.5 ps duration were obtained for a bias level of 120 mA in the DC gain section and -2.5 V reverse bias on the modulated section, with over 1 mW of average output power. The autocorrelation and optical spectrum of these pulses is shown in Figure 2.12. The optical bandwidth of these pulses is only 0.22 nm, resulting in a time-bandwidth product (TBP) of 0.30. The pulse shape is a excellent fit to a hyperbolic secant squared pulseshape which has a theoretical TBP of 0.31, showing that the pulses are TBP-limited. In this case, the pulsewidth is entirely limited by the grating bandwidth. Such a source employing a 1.55 $\mu$m- emitting laser would be an excellent soliton source, which requires unchirped hyperbolic secant squared pulses.
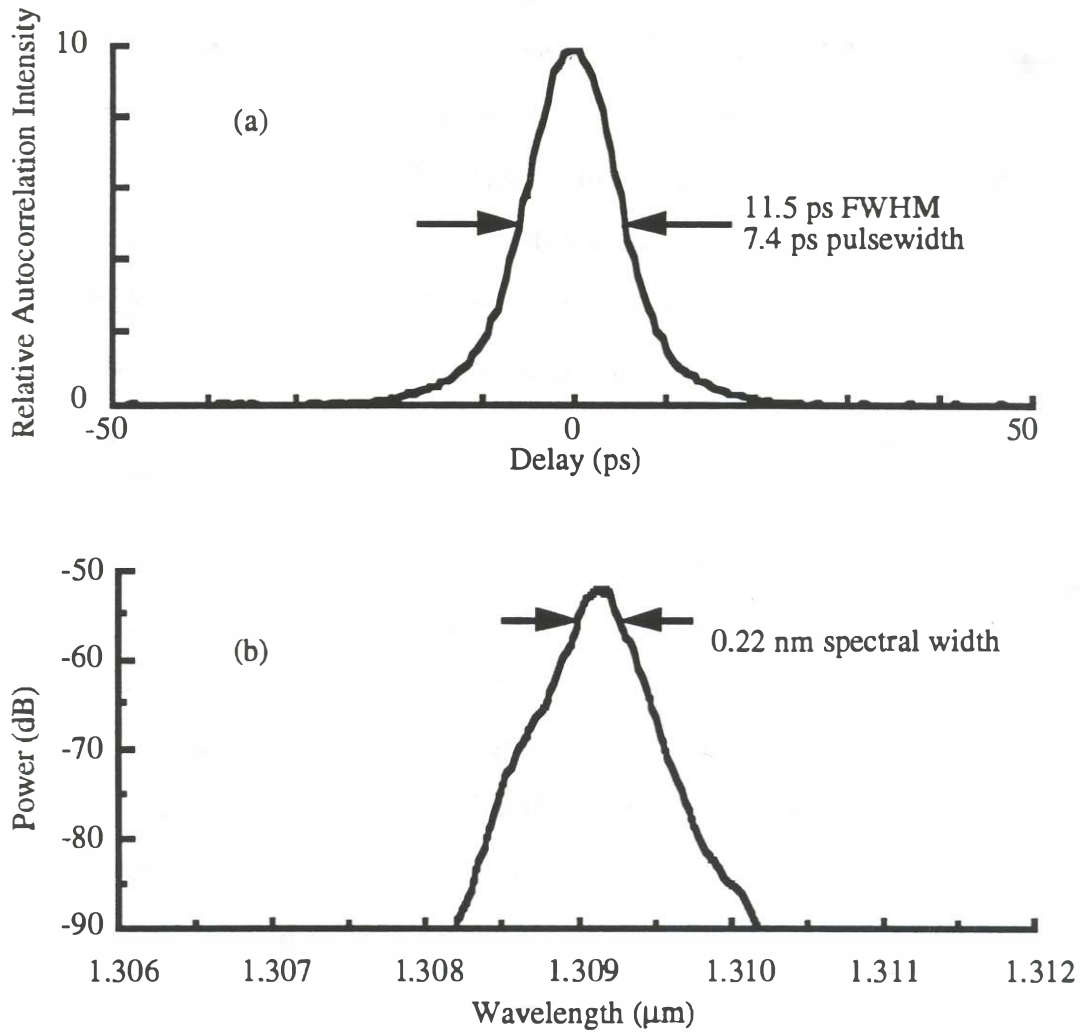
37

Figure 2.12. Autocorrelation and optical spectrum of transform-limited pulses generated using external grating feedback.

## 2.6. Timing Jitter Of The Two Section External Cavity Actively Mode-locked Laser.

For many applications, pulse-to-pulse timing fluctuations are as important as the pulsewidth itself for good time resolution. It is therefore important to determine whether the designs leading to multiple pulse suppression in actively mode-locked external cavity lasers also result in a degradation of timing jitter performance. Single-section actively mode-locked external cavity lasers have been measured to have rms timing jitter as low as 170 fs, dominated by the jitter in the electrical oscillator driving the mode-locking [13].

Timing jitter was measured using a high-speed p-i-n photodetector and a microwave spectrum analyzer (HP71400). The mode-locked pulse stream is displayed in the frequency domain and is visible as a series of spectral peaks at the repetition rate frequency and its harmonics. The purpose of this measurement is to determine L(f), the noise sideband level as a function of offset frequency from the carrier or its harmonics, normalized to a 1 Hz bandwidth. L(f) contains information about both amplitude and phase fluctuations in the pulse stream. However, the phase noise contribution to L(f) in dB rises as 20 log n (where n is the harmonic number), while amplitude noise rises as 10 log n. Therefore, noise sidebands at high harmonics are mostly phase noise in nature. The phase noise may be isolated by taking the measurement of L(f) at a sufficiently high harmonic number so that the phase noise contribution is dominant over that from the amplitude noise.

L(f) is integrated to obtain the overall rms timing jitter. This value of

39

timing jitter accounts only for noise contributions within the frequency limits of integration. The integration to be performed is [14]:

$$\sigma_{rms} = \frac{1}{2\pi \, n \, f_{mod}} \sqrt{\int_{f_{low}}^{f_{high}} L(f) \, df}$$

2.1

where $\sigma_{rms}$ is the rms timing jitter, n the harmonic number, $f_{mod}$ the pulse repetition rate, and $f_{low}$ and $f_{high}$ are the offset frequency limits of integration over which the noise is accounted.

For the measurements to be as accurate as possible, the local oscillator of the spectrum analyzer was used as the frequency reference for the synthesizer (HP 8340) used to drive the laser. Because the noise figure of the spectrum analyzer is relatively poor (>20 dB), a low noise preamplifier is used to amplify the signal from the photodetector before it is connected to the input of the spectrum analyzer.

Figure 2.13. shows the measurement of L(f) from the laser used to obtain the output shown in Figure 2.8. When the noise is due to phase fluctuations, the noise level between the fundamental and the 4th harmonic will rise by 12 dB and an additional 3.5 dB at the 6th harmonic, close to what is observed in the measurement. Integrating at the 6th harmonic, the rms jitter is 410 fs (150 Hz -500 MHz). This is excellent performance compared to other types of mode-locked lasers, and has a significant contribution from the jitter of the synthesizer itself, which was measured to be 132 fs rms (5

40

GHz, 150 Hz -5 MHz).

## 2.7. Summary.

Multiple pulsation effects in external cavity mode-locked lasers are due to imperfections in the AR coating used in coupling laser diodes to external cavities. Reflections from this coating can result in multiple pulse bursts if the gain modulation falltime is longer than the delay between reflections. It is demonstrated that this is very effectively suppressed by designing the laser so that the time delay between such reflected pulses is made longer than the drive pulse falltime. This is done by using longer cleaved device lengths, fast electrical drive pulses, and multi-segmented lasers with reverse-biased modulators.

At the date this work was published, these were the shortest single pulses directly generated from an actively mode-locked external cavity semiconductor laser. With the incorporation of a grating filter in the external cavity, time-bandwidth limited pulses are obtained, fulfilling the requirements for a soliton source. Because actively mode-locked external cavity lasers offer the advantages of widely tunable repetition rates, synchronization with external timing signals, and low levels of pulse-to-pulse timing jitter, such devices are an attractive source for many applications that require fast optical pulses.
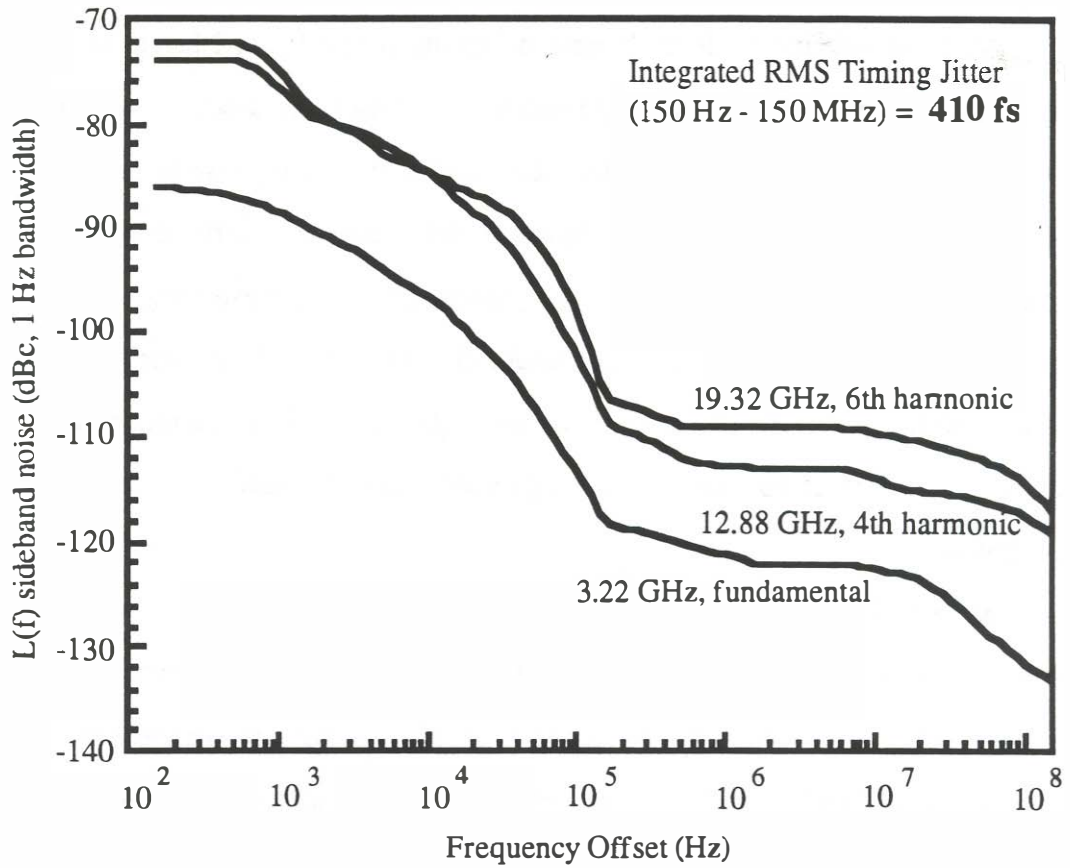
41

Figure 2.13. Sideband noise measured from single-pulse external cavity mode-locked laser, taken at several different harmonics.

# References

1. S. W. Corzine, J. E. Bowers, G. Przybylek, U. Koren, B. I. Miller, C. E. Soccolich, "Active mode locked GaInAsP laser with sub-picosecond output," Appl. Phys. Lett., vol. 52, p. 348, 1988.

2. A. Mar, D. J. Derickson, R. J. Helkey, J. E. Bowers, R. T. Huang, D. Wolf, "Actively Mode-Locked External-Cavity Semiconductor Lasers with Transform-Limited Single Pulse Output", Optics Letters, 17, p. 868-870, June 1992.

3. Yokoyama et al., 1981

4. J. P. Van Der Ziel, R. A. Logan, and R. M. Mikulyak, "Generation of subpicosecond pulses from an actively mode-locked GaAs laser in an external ring active cavity", Applied Physics Letters, 39, pp.867-869, 1981.

5. J. P. Van Der Ziel, W. T. Tsang, R. A. Logan, R. M. Mikulyak, and W. M. Augustyniak, "Subpicosecond pulses from passively mode-locked GaAs buried optical guide semiconductor lasers," Applied Phys. Lett., vol. 39, pp. 525, 1981.

6. P. A. Morton, J. E. Bowers, L. A. Koszi, M. Soler, J. Lopata, and D. P. Wilt, " Monolithic hybrid mode-locked 1.3 μm semiconductor lasers", Appl. Phys. Lett., 56, pp. 111-113, 1990.

7.  R. S. Tucker, U. Koren, G. Raybon, C. A. Burrus, B. I. Miller, T. L. Koch, and G. Eisenstein, "40 GHz active mode-locking in a monolithic long cavity laser," Electronics Letters, **25**, 621, 1989.

8.  D. J. Derickson, R. J. Helkey, A. Mar, J. E. Bowers, and R. L. Thornton, "Suppression of multiple pulse formation in external cavity mode-locked semiconductor lasers using intra-waveguide saturable absorbers," IEEE Photonics Tech. Lett., **4**, pp. 333-335, 1992.

9.  M. Schell et al.,"Fundamental limits of sub-picosecond pulse generation by active mode-locking of semiconductor lasers: the spectral gain width and the facet reflectivities" IEEE J. Quantum Electron., QE-25, 1426-1439.

10. R. T. Huang, D. Wolf, W-H Cheng, C-L. Jiang, R. Agarwal, D. Renner, A. Mar, J. E. Bowers, "High-Speed, Low-Threshold InGaAsP Semi-Insulating Buried Crescent Lasers with 22 GHz Bandwidth," Photon. Tech. Lett., 4(4), 293-295, April 1992.

11. H. A. Haus, "Parameter ranges for CW passive mode-locking", IEEE J. Quantum Electron., **QE-12**, pp. 169-176, 1976.

12. J. R. Karin, D. J. Derickson, R. J. Helkey, J. E. Bowers, and R. L. Thornton "Field-enhanced GaAs/AlGaAs waveguide saturable absorbers," submitted to the 1992 Ultrafast Phenomena VIII conference, Antibes Juan-les-Pins, France, 1992.

13. D. J. Derickson, A. Mar, and J. E. Bowers,"Residual and absolute timing jitter in actively mode-locked semiconductor lasers," Electronics Letters, vol. 26, pp. 2026-2027, 1990.

14. M. J. W. Rodwell, D. M. Bloom, and K. J. Weingarten, "Sub-picosecond laser timing stabilization", IEEE J. Quantum Electron., **QE-25**, pp. 817-828, 1989.

## Chapter 3

# Mode-Locked Diode Laser Arrays

### 3.1. Arrayed Diode Lasers For High-Power Applications

Much research has been devoted towards arraying diode lasers to emit high output powers into a diffraction-limited beam. Such a source would be attractive for applications such as free space communication, laser radars, and optical harmonic generation. Some initial attempts at developing such a source involved fabrication of multiple fundamental mode waveguides in close proximity on the wafer [1,2]. This approach relies on evanescent fields for coupling between adjacent waveguides. Diffraction-limited output results when this coupling results in coherence between all the emitters. An unfortunate feature of these designs is the strong tendency to lase in the so-called "out-of-phase" mode at higher powers, a condition where each array element is 180° phase shifted with respect to its neighbors. This results in a multi-lobed emission pattern, as shown in the analysis of Butler et al. [3], shown in Figure 3.1. The out-of-phase mode tendency exists because it results in nulls in the near-field between the emitters, which minimizes the loss in these regions. Figure 3.2. shows two experimental examples [4,5] of far-field emission patterns from laser arrays that exhibit the out-of-phase mode signature.

The poorly-behaved emission patterns characteristic of evanescently
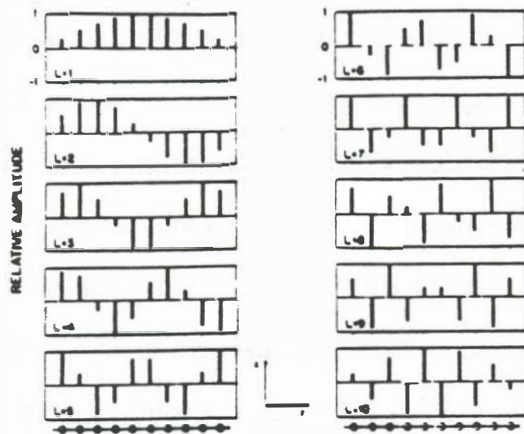
FIG. 1. Normalized amplitudes of the allowed modes of a ten-element array. The open circles show the position of the emitters.
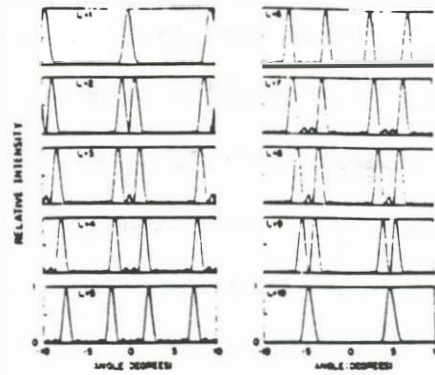
FIG. 2. Normalized far-field intensity distribution for a ten-element array with the emitters on 5-μm centers.

Figure 3.1. Coupled mode analysis of Butler et al., calculating lateral modes and far-field patterns from an array laser.
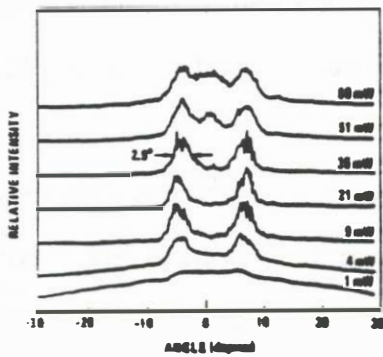


Ackley, 1983

Scifres et al., 1982

Figure 3.2. Published examples of far-field patterns characteristic of the out-of-phase array mode.

47

coupled arrays have impeded efforts to mode-lock such devices. Fiber nonlinearities were employed to produce bursts of multiple subpicosecond pulses from such an array [6]. The complex radiation patterns make it difficult to couple the arrays to external cavities with high efficiency. This is evident in the measurements of L-I curves with and without external cavity feedback, where the weak feedback causes only a marginal fractional reduction of lasing threshold. Figur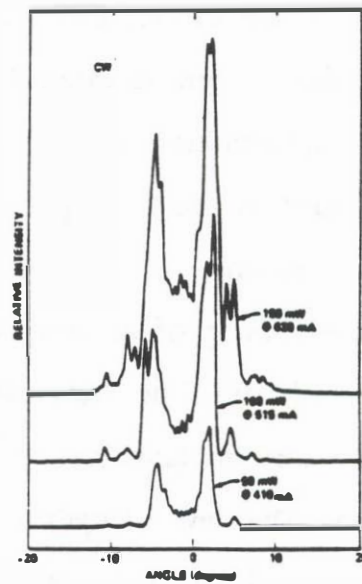e 3.3. shows some published examples of such L-I curves [7-9]. Reference 9 describes one of the more exotic external cavity designs which involves the use of a phase conjugate mirror (PCM), which in theory should cause ideal reciprocal imaging of the optical field in the external cavity back into the array. Unfortunately, the PCM provides a power reflectivity of only about 15%, and its use therefore provided only a marginal improvement in external cavity feedback. This is in contrast to the case of single-emitter external cavity lasers, where, with AR coatings, threshold shifts on the order of a factor of two due to external cavity coupling are not uncommon.

Mode-locking of an array without an external cavity has also been demonstrated [10]. The array used in Reference 10 was passively mode-locked by ion implantation of a facet, forming a center of saturable absorption. The device length was 1000 $\mu$m, resulting in a pulse repetition rate of 40 GHz. High average (400 mW) and peak power (2W) was generated from this device. However, most applications will require lower repetition rates and single-lobed beam emission patterns.

More recently, antiguide array designs have demonstrated in-phase

48
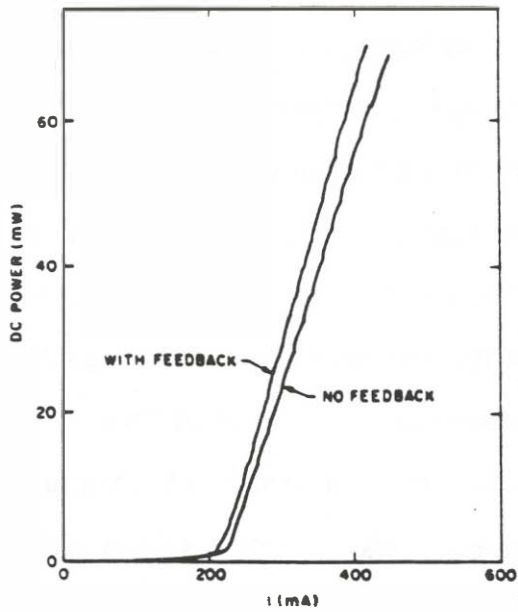
van der Ziel et al., 1984

Masuda et al., 1989

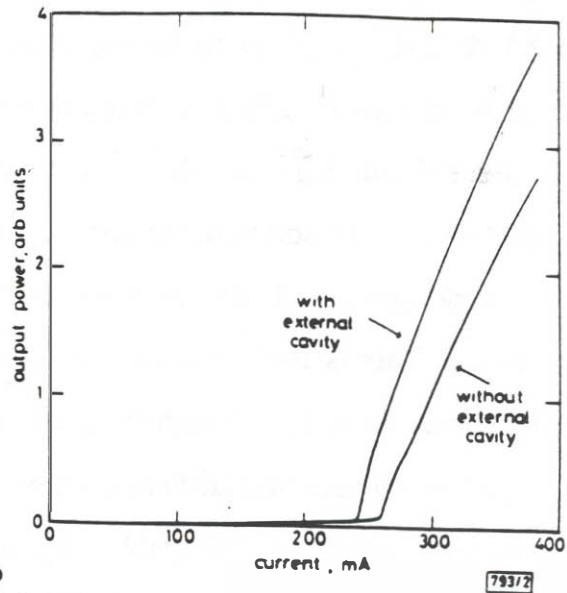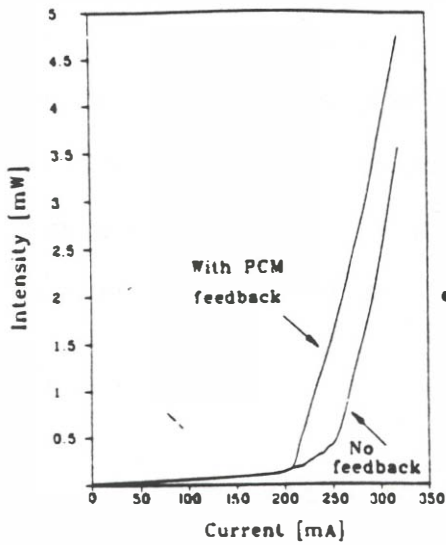**Fig. 2** *I/L characteristics*

Segev et al., 1990

- **Multi-lobed radiation patterns cause external cavity coupling efficiencies to be low compared with cavities using single-element lasers**

Figure 3.3. Light vs. current characteristics from evanescently-coupled array lasers in external cavities.

(single main-lobed) diffraction-limited operation at total output powers of up to 2.1 W [11]. Contrary to conventional laser waveguide designs, antiguide arrays have a lower refractive index in the regions of optical gain relative to the interelement regions. This causes very strong optical coupling between array elements. In addition, the interelement spacing and lateral index profile may be designed such that, at the lasing wavelength, this lateral coupling is resonant. This is the basis of the so-called Resonant Optical Waveguide (ROW) array laser, first investigated extensively by Botez et al. at TRW [11]. The light vs. current and far-field pattern characteristics of such a ROW array are shown in Figure 3.4. The stable, single-lobed emission patterns from such devices make them good candidates for high power semiconductor laser mode-locking in external cavities. Therefore, a collaboration was arranged with Botez et al. at TRW to investigate mode-locking of ROW arrays. In this chapter, the first mode-locked operation of such devices is described, with external cavity coupling efficiencies comparable to that typically obtained using single-element lasers. Mode-locking without multiple pulsations using multi-segment structures is achieved with increased output power proportional to the number of array elements.

## 3.2. Pulse energy output power limitation of mode-locked lasers.

A single-mode semiconductor laser is typically able to deliver CW output powers of about 50 mW or more before catastrophic damage occurs. In AlGaAs lasers, this may be due to facet destruction at high photon

50
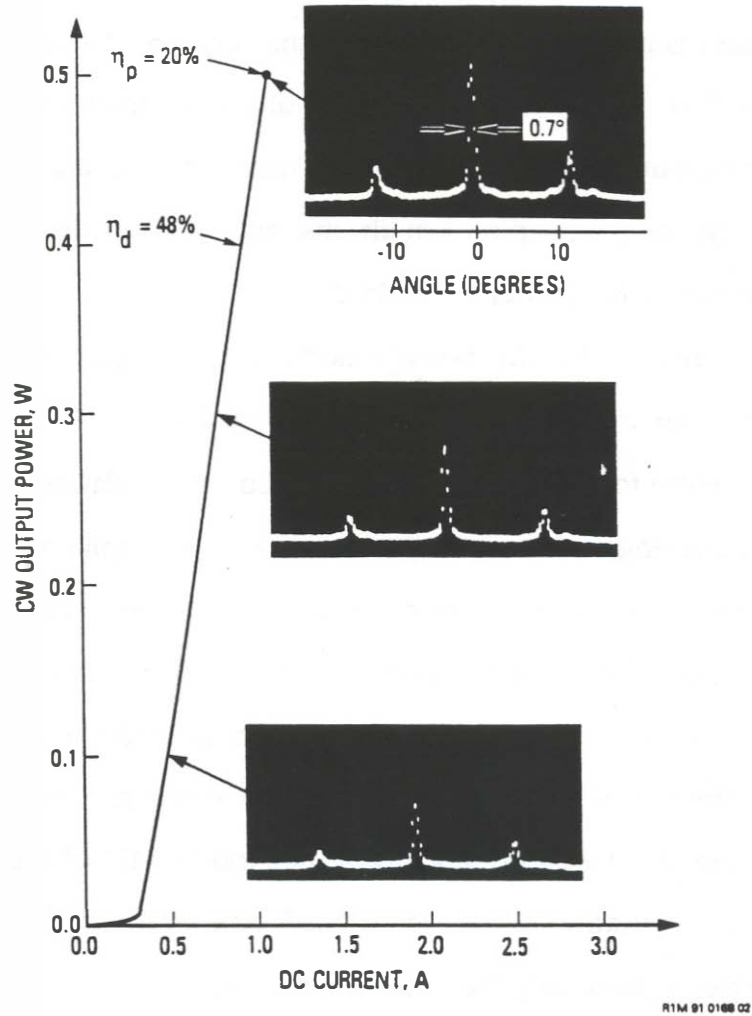
Figure 3.4.  The light vs. current and far-field pattern characteristics of a ROW array laser.

densities due to surface recombination, subsequently leading to a runaway process of absorption, heating, bandgap shrinkage, and increased absorption [12]. The threshold power density for such damage in InGaAsP lasers is approximately an order of magnitude higher [13]. The maximum operating power of a laser is also limited by heating, the turn-on of parasitic leakage paths, or the failure of other types of current-blocking structures. However, the maximum output power that is obtained under mode-locked conditions is even lower, typically a couple of milliwatts, which is a problem for many applications where higher power is required.

The main reason that the average mode-locked output power from a semiconductor laser is so much lower than the cw limit is the limitation on pulse energy. Pulse formation in a mode-locked laser balances competing pulsewidth broadening and shortening processes. The amplification of large pulses induces changes in carrier density and gain saturation pulse broadening, which also leads to self-phase modulation (SPM) due to the coupling between carrier density and refractive index in the semiconductor. SPM broadens the optical bandwidth of the pulses, which results in additional pulse broadening due to group velocity dispersion (GVD) of the amplifier gain [14]. Gain saturation and SPM-induced pulse broadening increases rapidly at energies approaching the saturation energy,

$$E_{sat} = \frac{h\nu\, A}{\Gamma\, dg/dn}, \qquad\qquad\qquad 3.1.$$

where hv is the photon energy, A the active region cross-sectional area, $\Gamma$ the confinement factor, and dg/dn is the differential gain. The broadening overwhelms the pulse shortening that is provided by the saturable absorber, and prevents mode-locked operation at higher pulse energies. This process is illustrated in Figure 3.5. which shows the calculated pulse shaping contributions in propagation through a gain-saturable absorber cascade. (Details regarding the calculation itself are given in Chapter 4.) Mode-locking is feasible only in the regime where there is net pulsewidth shaping < 1. For a
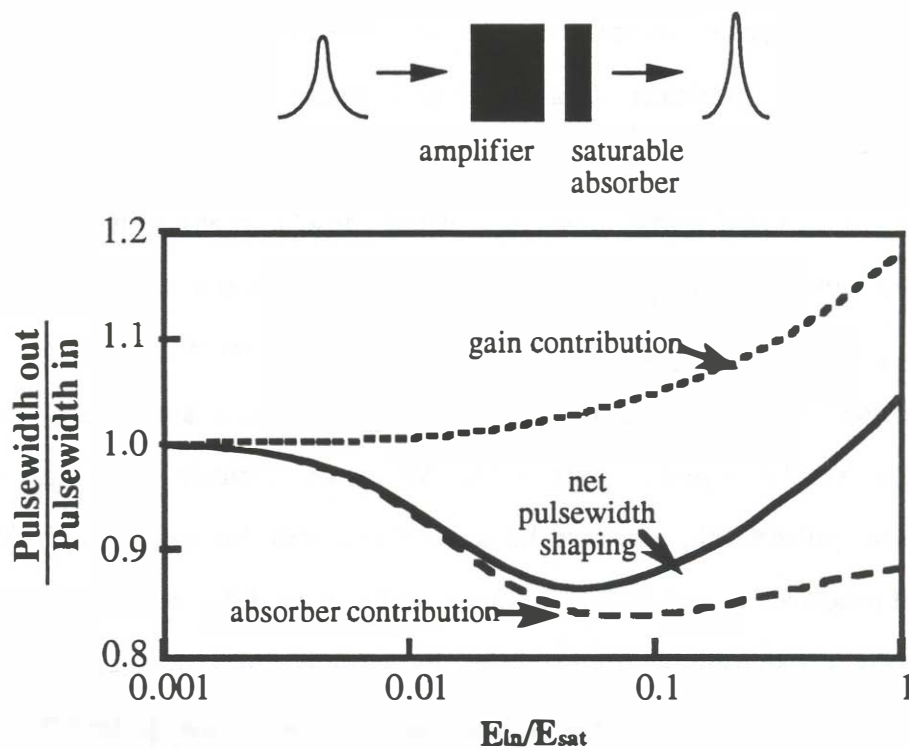


Figure 3.5. Pulse shaping in single pass propagation through gain and saturable absorber cascade.

53

single stripe laser with a mode cross-section of $6 \cdot 10^{-13}$ m$^2$ and dg/dn of $4 \cdot 10^{-20}$ m$^2$, $E_{sat}$ is about 4 pJ, which, assuming output coupling of 0.3, a repetition rate of 1 GHz and a lens collection efficiency of 0.6, results in an average output power of only 0.7 mW. Arrays have the advantage of increased pulse energies because the saturation energy, being proportional to A, can be made relatively large for an arrayed gain region. If an array of 20 such emitters is used, the saturation energy would scale by this factor, resulting in an $E_{sat}$ of approximately 80 pJ.

The saturation energy limits the pulse energies that can be generated from a passively mode-locked laser. Actively mode-locked lasers rely on gain modulation for pulse formation and thus are not as subject to the same saturation energy limitation. In addition to potentially higher pulse energies, actively mode-locked lasers also provide the advantage of synchronizing the output to an external signal. Gain modulation functions as a pulse formation mechanism even at high pulse energies with severe gain saturation and SPM induced pulse broadening. However, it is more difficult to generate very short pulses using this technique because the pulse shortening factor decreases as the optical pulsewidth becomes shorter than the gain modulation pulsewidth, and also because it requires the use of high-speed electrical modulation and laser structures with minimized electrical parasitics. The pulsewidth shaping factor provided by saturable absorption is relatively independent of pulsewidth and remains effective when the pulses become very short. For this reason, in hybridly mode-locked lasers, the dominant

54

pulse shaping element is often the saturable absorber. The saturation energy therefore also limits the energies of the short pulses generated from hybridly mode-locked lasers, but such lasers offer the advantages of both the pulsewidth performance provided by saturable absorption and of synchronized pulse output due to active gain modulation.

### 3.3. Segmented ROW Array Devices

As described in Chapter 2, the use of segmented lasers for external cavity mode-locking has been demonstrated to result in improved performance and operational flexibility. Multi-segment lasers allow for the separation of the functions of DC gain, gain modulation, and saturable absorption within a single device. This results in shorter pulses and suppression of the secondary pulsations seeded by reflections from the AR coated facet at the interface between the laser and the external cavity. To apply these principles with arrayed lasers, 2-segment ROW devices were fabricated by etching the p-contact layer and metallization to result in lasers with electrically isolated absorbing sections of 25 and 50 µm lengths at the output facet, with the balance of the device used as a DC gain segment. The lasers were 1000 µm long overall, and the electrical isolation between segments was typically 70 $\Omega$. To allow separate contacting of the device segments in the p-side down mounting configuration, an electrically insulating diamond heat spreader is used between the laser and the copper heatsink, as shown in Figure 3.6. This 1000 µm square diamond heat spreader has a patterned solder metallization to match the device's segmented contact

55

ROW Laser Chip (p-side down)

Au bondwires

Copper Heat Sink

Diamond Heat Spreader w/ Patterned Metallization

50 Ω Transmission Lines

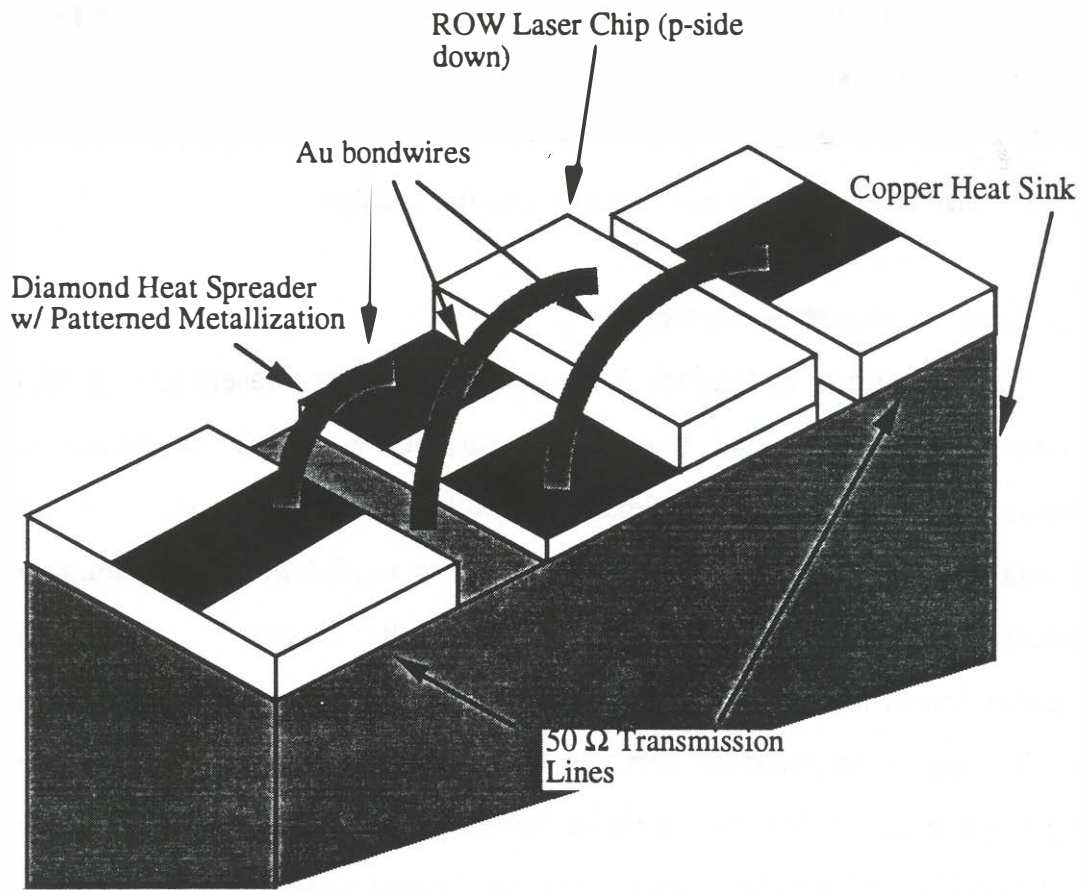Figure 3.6. Packaging of a multisegment ROW laser array mounted p-side down on a patterned diamond heatsink.

design, and allows for sufficient overhang for bondwire attachment to adjacent transmission lines. The diamond heatsinks were fabricated by evaporating a chrome adhesion layer under 5 μm of indium, and patterning using photoresist as an etch mask. This pattern is carefully designed to allow

56

for some misalignment tolerance in mating with the laser die so that the segments are not shorted together. The backside of the diamond heatsink is also evaporated with indium solder, with care taken not to deposit onto the side edges of the diamond so as to preserve electrical isolation between the front and backsides. The package is assembled by first attaching the transmission lines using a AuSn solder (with a higher melting point than indium), and then attaching the diamond and laser die in a separate reflow step. Gold ribbon wires are attached to the indium solder using a heated bondwiring tool (heated above the indium melting point), and thermocompression bonded to the adjacent transmission lines. Wires are also used to electrically connect the backside metal of the laser die to the heatsink.

### 3.4 External Cavity Performance

The experiments employed 20-element arrays with a lasing wavelength of 850 nm. Half-wave $Al_2O_3$ coatings were evaporated onto both diode facets to increase the catastrophic facet damage output power limit. The facet used to couple to the external cavity was then additionally antireflection coated with a reactively sputtered anti-reflective quarter-wave $SiN_xO_y$ layer (index~1.83). Such coatings reproducibly reduce laser facet reflectivities to less than 0.1% [15].

The ROW arrays are coupled to an external air cavity using three intra-cavity lenses, as shown in Figure 3.7. An AR-coated GRINROD lens is used at the laser facet because of its high numerical aperture and collection

57
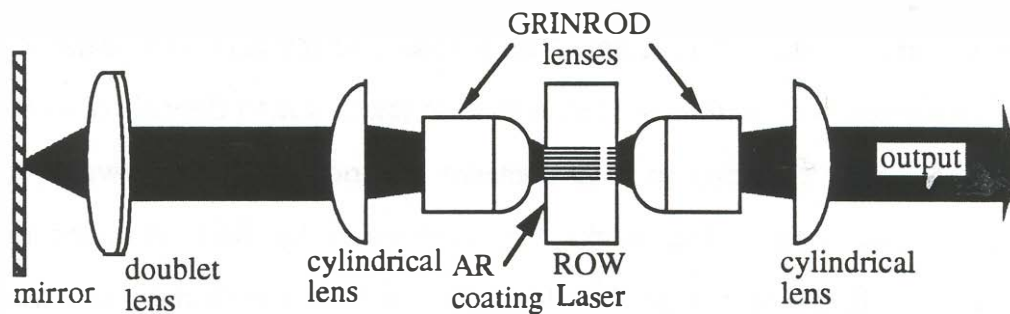
Figure 3.7. Schematic of the ROW array external cavity mode-locked laser.

efficiency. The cylindrical lens is used to compensate for astigmatism that was present in the laser emission. The beam is focused onto the external cavity mirror using an achromatic doublet. This doublet is beneficial because the non-circular beam profile fills most of the lens and would be subject to the off-axis aberrations characteristic of a singlet lens, which are compensated in an achromatic lens.

Figure 3.8. shows the light vs. current dependence of an array laser with and without feedback from the external cavity. The external cavity coupling reduces the threshold current from 570 to 330 mA, which is about the same as the threshold before AR-coating. This means that the cavity coupling efficiency is approximately 30%. The output beam is collimated by a GRINROD and cylindrical lens. The ROW array's external cavity coupling compares well with what is typically achieved using single element lasers [16]. This illustrates that the well-behaved emission pattern from the ROW array

58
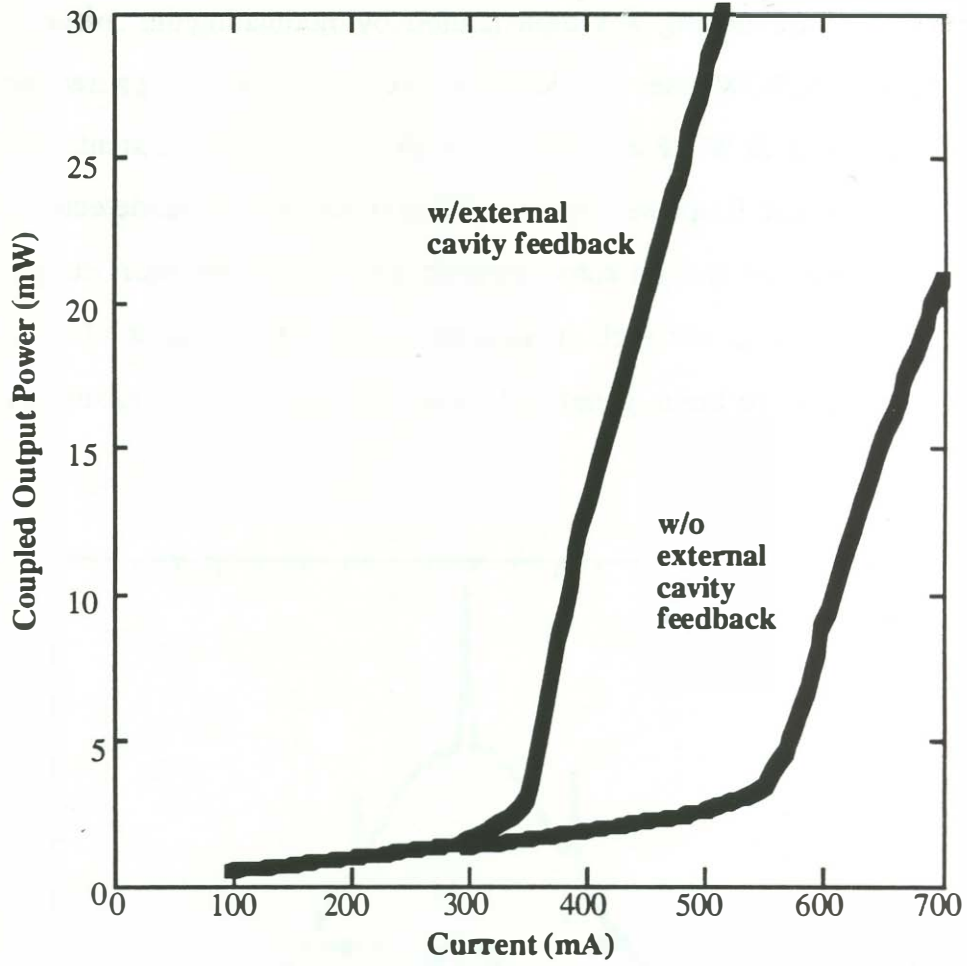
Figure 3.8. ROW array external cavity laser light vs. current characteristics.

design lends itself well to incorporation of arrayed lasers in external cavities.

## 3.5. Active Mode Locking

Active mode-locking was implemented by modulating the current at 1 GHz to a 500 μm ROW laser coupled to a 15 cm cavity to using a frequency synthesizer and a 20 W RF amplifier through an impedance-matching stub tuner. A high-speed (impulse response~22 ps) GaAs PIN photodetector and 40 GHz oscilloscope and an autocorrelator are used to monitor the pulse output. Figure 3.9. shows such an autocorrelation measurement. Pulses as short as 23 ps have been generated, with slightly broader pulses being
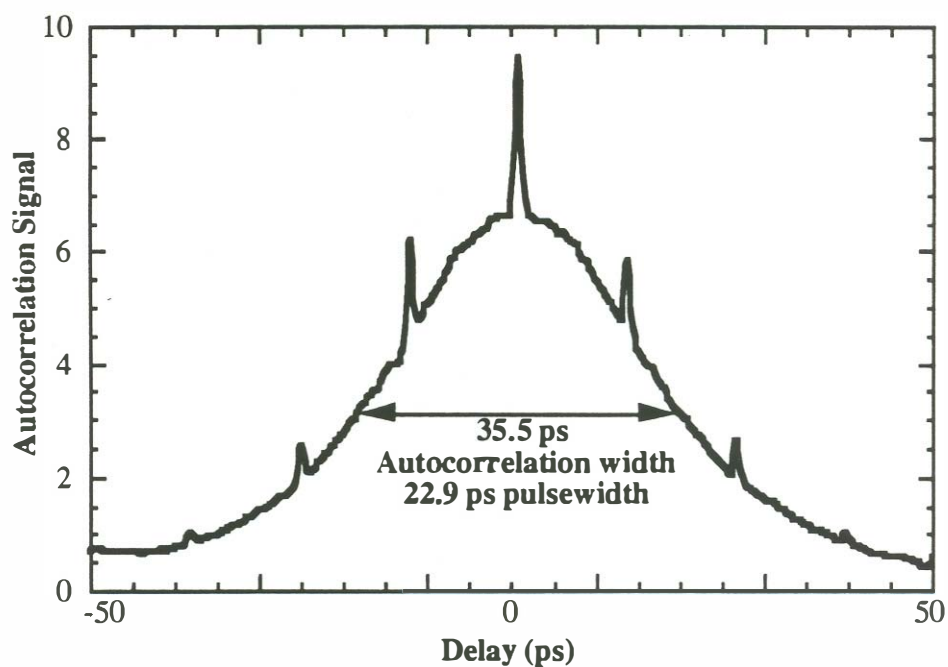
Figure 3.9. Autocorrelation of pulses from actively mode-locked ROW array laser.

obtained at higher output powers. The maximum power of 51 mW was limited due to the current capacity of the bias tee used. Taking into account the external coupling of 30% and a lens collection efficiency of approximately 70%, this corresponds to a 242 pJ internal pulse energy within in the laser itself, demonstrating that pulses of energy larger than $E_{sat}$ can be generated using active gain modulation. Because this laser structure is not optimized for high-speed modulation and also because of the effects of gain saturation and SPM at these large pulse energies, the pulses are relatively long in duration. To generate shorter pulses using this structure, it is necessary to employ a saturable absorber to provide stronger pulse shaping.

### 3.6. Passive Mode-Locking

The multi-segment devices were coupled to an external cavity similar to that described above of approximately 19 cm length, corresponding to a repetition rate of 775 MHz. Passive mode-locking was initiated by reverse-biasing (typically -0.5 to -1.0V) the short laser section and forward-biasing the gain section above threshold. Measurements on single-stripe devices have shown that such short reverse-biased sections act as intra-waveguide saturable absorbers with fast (~15 ps) recovery times and lower saturation energies than the forward-biased gain segments due to the sublinearity of the differential gain vs. carrier density characteristic [17]. Essentially functioning as a waveguide photodetector, such an absorber also provides a useful source of electrical signals that are synchronized with the pulse output of the

61
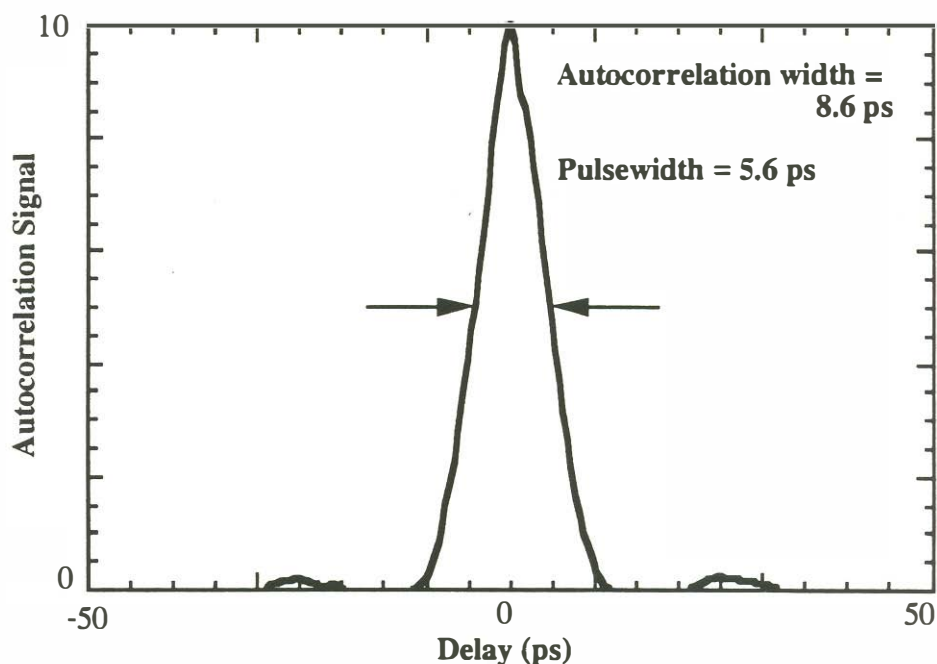
Figure 3.10. Autocorrelation of pulses from passively mode-locked ROW array laser.

passively mode-locked laser. The absorber electrical output was amplified and used to trigger the time base of the sampling oscilloscope, providing a low-jitter measurement as in the actively mode-locked case where the modulation source itself was used as the trigger signal. Such a measurement results in pulsewidths of 23 ps, which is the impulse response of the measurement system. Autocorrelation measurements show that the pulses generated are of 9-10 ps autocorrelation width, corresponding to pulsewidths of 6-7 ps using a deconvolution factor of 1.55 (appropriate for hyperbolic secant squared pulses). Figure 3.10. shows the autocorrelation of the shortest pulses measured, with an autocorrelation width of 8.6 ps corresponding to a

pulsewidth of 5.6 ps. These pulses were obtained at an average power of 13.4 mW, corresponding to peak powers of over 3 W. The measurement also shows good suppression of the trailing pulses that occur from reflections from the AR coated laser facet. A maximum pulse energy of 21.9 pJ is obtained at 800 mA gain bias current. This corresponds to a 104 pJ pulse energy in the laser itself, in reasonable agreement with the calculated value of saturation energy. This demonstrates the effectiveness of increasing the saturation energy of the laser by increasing the mode cross-sectional area in an arrayed structure.

### 3.7. Hybrid Mode-Locking

For certain applications it is necessary to synchronize the optical pulse output with an external electrical signal. Hybrid mode-locking was therefore investigated as a technique to combine the strong pulse-shortening effect of the saturable absorber with external gain modulation. Electrical pulses were injected into the gain segment of the laser along with the DC forward bias, with the short absorber section reverse-biased as in the passively mode-locked case. When the modulation frequency was tuned to match the round trip time of the laser, short pulses with characteristics similar to that of the passively mode-locked case were generated, with pulsewidths less than 6.5 ps as measured by autocorrelation. This is due to the fact that the saturable absorption is the dominant pulse-shaping mechanism in this configuration. Figure 3.11. shows the connection of the sampling oscilloscope for the

63
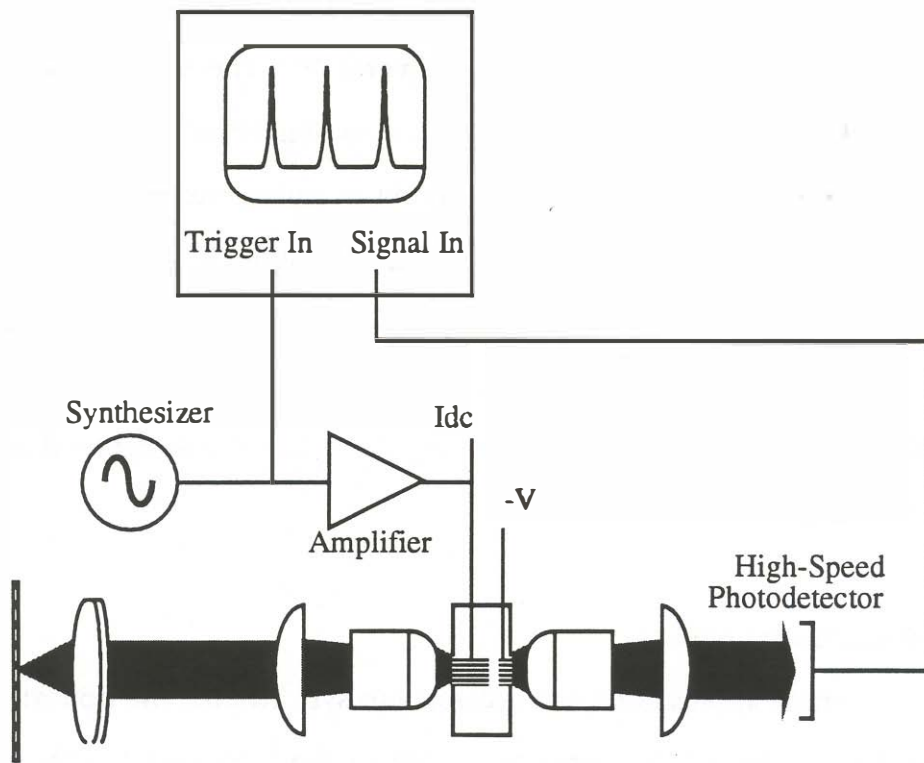
Figure 3.11. Oscilloscope connection for measurement of hybridly mode-locked ROW array laser.

measurement of pulses generated in this manner, with the time base triggered by the rf modulation source. With this connection of the time base, timing jitter in the optical pulse stream will broaden the pulsewidths in the sampling oscilloscope measurement. As shown in Figure 3.12, the oscilloscope displays the pulsewidth to be 23 ps which again is the impulse response limit of the oscilloscope and photodetector, indicating that the pulses are short and have very low timing jitter with respect to the drive signal.
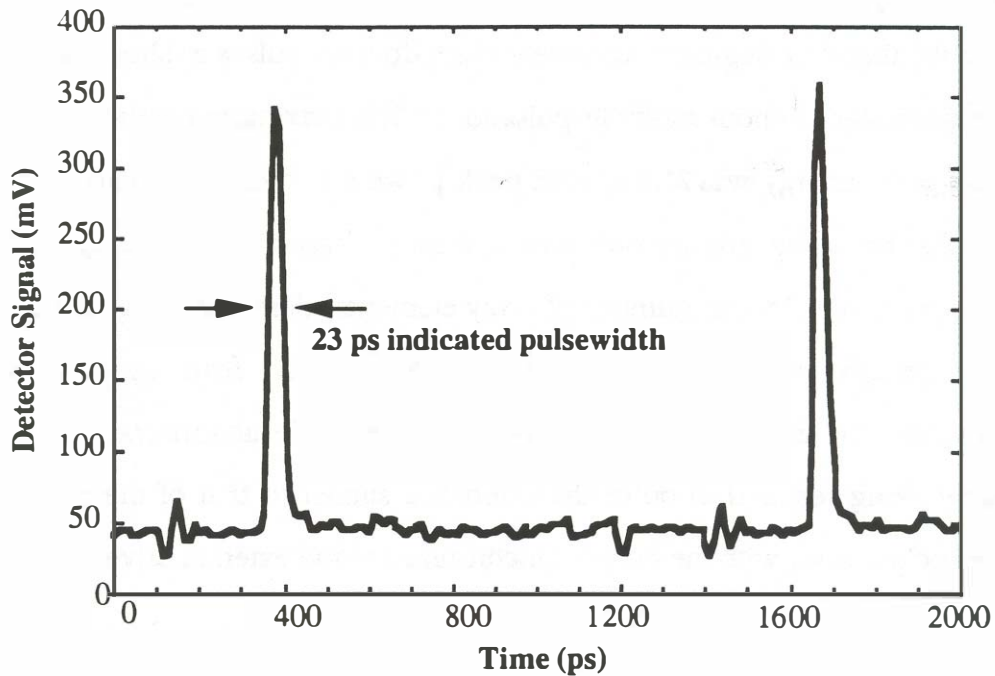
Figure 3.12. Sampling oscilloscope of pulses from hybridly mode-locked ROW array laser.

## 3.8. Summary

The first active, passive, and hybrid mode-locking of ROW laser arrays has been demonstrated. The in-phase operation of such arrays results in well-behaved emission patterns that allow for coupling into external cavities with high efficiencies comparable to those of single-stripe laser designs. Active mode-locking of such lasers resulted in >50 pJ pulse energies that are not limited by the gain saturation energy, but were relatively long in duration (22 ps), because of gain saturation pulse broadening and because high-speed gain

modulation was not feasible. By utilizing multi-segment devices with a short saturable absorber segment, passively mode-locked pulses as short as 5.6 ps were generated without multiple pulsations. The maximum passively mode-locked pulse energy was 21.9 pJ with peak powers of over 3 W. This is about the value of pulse energy one would expect, based on a scaling of the saturation energy by the number of array elements, demonstrating that ROW arrays are effective for increasing the output powers from mode-locked semiconductor lasers with intra-waveguide saturable absorbers. Hybrid mode-locking resulted in pulse characteristics similar to that of the passively mode-locked case, with the output synchronized to the external drive signal.

## References

1.  S. Mukai, C. Lindsey, J. Katz, E. Kapon, Z. Rav-Noy, S. Margalit, A. Yariv, "Fundamental mode oscillation of a buried ridge waveguide laser array," Appl. Phys. Lett., vol. 45, pp. 834-835, 1984.

2.  E. Kapon, Z. Rav-Noy, S. Margalit, A. Yariv, "Phase-locked arrays of buried-ridge InP/InGaAsP diode lasers," J. Lightwave Technol., vol. LT-4, pp. 919-925, 1986.

3.  J. K. Butler, D. E. Ackley, D. Botez, "Coupled-mode analysis of phase-locked injection laser arrays," Appl. Phys. Lett. 44 (3), 1 February 1984.

4.  D. E. Ackley, "Single longitudinal mode operation of high power multiple-stripe injection lasers," Appl. Phys. Lett. 42(2), 15 January 1983.

5.  D. R. Scifres, R. D. Burnham, W. Streifer, "High power coupled multiple stripe quantum well injection lasers," Appl. Phys. Lett. 41 (2), 15 July.1982.

6.  L. Y. Pang, J. G. Fujimoto, E. S. Kintzer, "Ultrashort-pulse Generation From High-power Diode Arrays By Using Intracavity Optical Nonlinearities," Optics Letters, V17 N22:1599-1601, Nov 15, 1992.

7.  J. P. Van Der Ziel, H. Temkin, R. D. Dupuis, R. M. Mikulyak, "Mode-locked picosecond pulse generation from high power phase-locked GaAs laser arrays", Applied Physics Letters, 44, pp.357, 1984.

8. H. Masuda, A. Takada, "Picosecond Optical Pulse Generation from Mode-locked Phased Laser Diode Array," Electronics Letters, 25 Aug. 1989.

9. M. Segev, Y. Ophir, B. Fischer, G. Eisenstein, "Mode locking and frequency tuning of a laser diode array in an extended cavity with a photorefractive phase conjugate mirror," Appl. Phys. Letts., vol. 57, 24, 10 December 1990.

10. J. H. Zarrabi, E. L. Portnoi, A. V. Chelnokov, Passive mode locking of a multistripe quantum well GaAs laser diode with an intracavity saturable absorber," Appl. Phys. Lett. 59 (13), 23 September 1991.

11. L. J. Mawst, D. Botez, C. Zmudzinski, M. Jansen, C. Tu, T. J. Roth, and J. Yun, "Resonant Self-aligned-stripe Antiguided Diode Laser Array," Appl. Phys. Lett. 60 (6), 10 February 1992.

12. Wakao, K. W., Takagi, N. Shima, K., Hanamitsu, K., Hori, K., and Takusagawa, M., "Catastrophic Degradation Level of Visible and Infrared GaAlAs Lasers," Applied Physics Letters, 41, 1113-1115, 1982.

13. H. Temkin, A. Mahajan, M. A. DiGiuseppe, A. G. Dentai, Applied Physics Letters, 40, pp. 562, 1982.

14. G. P. Agrawal and N. A. Olsson, "Self-phase modulation and spectral broadening of optical pulses in semiconductor laser amplifiers," IEEE J. Quantum Electronics, vol. QE-25, pp. 2297-2306, 1989.

15. A. Mar, J. D. Dudley, E. L. Hu, and J. E. Bowers, "Reactively Sputtered Silicon Oxynitride for Anti-Reflection Optical Coatings," Electronic Materials Conference, Santa Barbara, CA, Oct. (1990).

16. J. E. Bowers, P.A. Morton, S. Corzine and A. Mar, "Actively Mode Locked Semiconductor Lasers," J. Quantum Electronics, 25(6), 1426-1439, June 1989.

17. D. J. Derickson, R. J. Helkey, A. Mar, J. R. Karin, J. G. Wasserbauer, and J. E. Bowers, "Short Pulse Generation Using Multi-Segment Mode-Locked Lasers," J. Quantum Electron., 28, 10, 2186-2202, Oct. 1992.

# Chapter 4

# High-Power Mode-Locked
# Flared Lasers and Amplifiers

## 4.1. Flared Waveguide Lasers and Amplifiers For High-Power Applications.

Another approach to achieving high output powers in a diffraction-limited beam is the use of broad-area semiconductor devices. Simple broad-area lasers typically lase in higher-order lateral modes, with unstable emission patterns far in excess of diffraction-limited performance. Techniques to maintain a single lateral mode with broad-area structures include antiguide arrays [1,2], unstable resonators [3,4], and external injection of broad-area amplifiers [5]. In the latter approach, commonly referred to as a Master Oscillator Power Amplifier (MOPA) configuration, control of the lateral mode is determined by the profile of the injected beam. This approach requires sufficient power from the input laser to saturate the amplifier and suppress amplified spontaneous emission (ASE), on the order of 100's of mW [5], which is beyond the normal capabilities of single-mode diode lasers. The desire to use a diode laser input source has led to the development of flared amplifier structures [6,7]. Flared amplifiers operate with high small-signal gain because of minimized parasitic gain depletion from ASE noise, particularly at the narrow input end of the amplifier. By expanding the gain cross-section area along the length of the amplifier, as the amplified power grows, a more uniform power density and degree of gain saturation is maintained

70

throughout the amplifier [8].

Flared amplifiers have also been used to construct high power diffraction limited lasers with as much as 4.2 W output power [4]. The flared waveguide expands the optical mode from a narrow region which ensures fundamental lateral optical mode operation, to a wide multimode region for higher power at the output facet. However, the advantage of the MOPA configuration over this simpler approach is that single frequency and/or high modulation bandwidth sources may be used for injection and amplification, characteristics that are probably not so easily achieved in a flared broad-area laser itself.

Flared broad-area amplifiers operate with sufficient gain to enable the use of diode lasers as input sources. 2W CW output power has been demonstrated using diode laser injection in both discrete element [9] and monolithically integrated [10] MOPA configurations. A small-signal gain of 1000 was measured from the discrete amplifier in Reference 6, with 25 mW injection power used to saturate the amplifier at the highest output powers obtained. Because of the possibility of saturating such amplifiers using injection sources of relatively modest power, it becomes feasible to construct a MOPA using a mode-locked laser as the master oscillator. In collaboration with Spectra Diode Laboratories (SDL), where much of the work on flared broad-area amplifiers has been done, such experiments have been conducted here at UCSB using amplifiers fabricated at SDL. To achieve the injection powers necessary to saturate the amplifier, a flared waveguide device design is employed also in the mode-locked master oscillator used in

71

these experiments. This has resulted in the first mode-locked operation of a flared amplifier MOPA, resulting in record high average powers and pulse energies from an all-semiconductor source. In this chapter, the mode-locked pulsed characteristics of both flared amplifiers and flared lasers are presented along with an analysis of these structures, using an extension of the numerical model developed by Helkey et al. [11] to study pulse propagation in laser amplifiers, which has been modified for application to flared waveguide device designs.

## 4.2. Modeling of Pulse Propagation in Laser Amplifiers.

Because the optical pulses generated in mode-locked lasers are typically short compared to the transit time through the devices, the usual spatially-averaged rate equations for the carrier and photon populations are inappropriate for this problem. The usual method for dealing with this analysis is to model the device as many short segments, also accounting separately for the forward and reverse propagating photon densities [12]. The spatial and temporal resolution of the variation in photon and carrier densities is determined by the length and transit time in the segments used for the calculation. Helkey et al. [11] greatly improved the computational efficiency of the calculation by using an exponential basis function to model the gain in each segment, as opposed to the linear relation that had been previously used. Because this models the gain in each device segment much more accurately, and also because the spatial variation of the carrier density is slow compared to that of the photon density, an amplifier may be modeled

72

with fewer gain segments, each separated by free space segments which do not require computation. A fine segment spacing is used as necessary for resolution of the spatial variation in the optical field, but computation of the carrier density is done only in the few gain segments.

Agrawal and Olsson [13] have derived parametrized rate equations that are particularly useful for the analysis of semiconductor laser amplifiers. Their parametrization allows the characterization of a gain segment in terms of only the input pulse energy normalized to the saturation energy (as introduced in Chapter 3) and also the unsaturated gain. These rate equations are as follows:

$$P_{out}(\tau) = P_{in}(\tau) \exp[h(\tau)]$$

$$\frac{dh(\tau)}{d\tau} = \frac{P_{in}(\tau)}{E_{sat}}[\exp[h(\tau)] - 1]$$

$$E_{sat} = \frac{h\nu\,A}{\Gamma\,dg/dn}_, \qquad\qquad 4.1.$$

where h is the logarithm of the exponential gain function ( $G(\tau) \equiv \exp[h(\tau)]$ ), $P_{in}$ is the input power, $E_{sat}$ is the saturation energy, $h\nu$ is the photon energy, A the active region cross-sectional area, $\Gamma$ the confinement factor, and dg/dn is the differential gain. $\tau$ is the time measured in the reference frame moving with the optical pulse. Internal waveguide loss is neglected, which is valid if

73

the gain is much higher than this loss. Gain recovery is also neglected in these particular equations, which is valid when the optical pulsewidth is much shorter than the carrier lifetime, which is almost always the case. An analytical solution for the instantaneous gain $G(\tau)$ is [13]:

$$G(\tau) = \frac{G_0}{G_0 - (G_0-1)\exp(-U_{in}(\tau)/E_{sat})}$$

$$U_{in}(\tau) = \int_{-\infty}^{\tau} P_{in}(\tau') \, d\tau'$$

4.2.

where $U_{in}$ is the energy input up to time $\tau$, and $G_0$ is the unsaturated gain. This forms the basis for the elegant logarithmic gain equation approximation used by Helkey et al. [11] to estimate the changes in instantaneous gain for the numerical analysis:

$$U_{in}(\tau) \approx P_{in} \Delta\tau$$

$$\Delta h = \log[G(\tau)] - \log[G_0] = -\log[G_0 - (G_0 - 1)\exp(-U_{in}/E_{sat})]$$

4.3.

which estimates the gain well without having to explicitly compute higher order derivatives.

As such, the model accounts for gain saturation due to carrier depletion from stimulated emission during the amplification process, and gain bandwidth limits, self-phase modulation, group velocity dispersion and other effects are not included. When the model is iterated to obtain a steady-

74

state solution for the pulsewidth, it is important to account for these other temporal and spectral pulse shaping mechanisms.

### 4.3. Modeling of Saturable Absorbers.

This model applies well also to saturable absorbers, with the only modification being a reduction of the satura ion energy parameter by $\sigma$,

$$\sigma = \frac{Esat_{gain}}{Esat_{absorber}}$$

4.4

The saturation energy is typically lower in a saturable absorber segment because it operates at a lower carrier density than in the gain. This causes the differential gain (or loss) in the absorber to be higher due to the sublinearity of the gain vs. carrier density characteristic. It has been shown theoretically that the absorber must saturate at lower energies than in the gain for passive mode-locking to take place [14]. Higher ratios of $\sigma$ also result in enhanced pulse shortening per pass in the absorber [15]. This can be understood intuitively by considering that pulse shor ening in a saturable absorber occurs because the pulse edges (or just the leading edge in the case of a slowly recovering absorber) are attenuated more than the peak of the pulse. Better shortening results when the difference in attenuation between the pulse edges and pulse peak is greater, or equivalently, when the reduction of loss per number of absorbed photons is higher. Of course, this occurs when the differen ial gain is higher in he absorber, which leads to higher values of $\sigma$.

75

## 4.4. Accuracy in Modeling of Flared Amplifiers.

The parametrized rate equations of Agrawal and Olsson may be used to model flared amplifier structures by the use of appropriately scaled saturation energies in each gain segment. The saturation energy, which is proportional to the mode cross sectional area, increases with increasing waveguide width. The unsaturated gain h(0) is left to be the same in the segments, which is reasonable because the initial carrier densities are also assumed to be the same. Linear flares are the subject of analysis in this chapter and are also of the type used in the experiments. However, flares of different shapes may also be analyzed with this model by adjusting the values of saturation energies used in the gain segments.

Especially with large flarings, many gain segments may be required to achieve a sufficiently accurate step-wise approximation to a continuously flared structure. The ultimate determination of whether the segment spacing is fine enough is made by repeating the calculation with more and more segments until the solutions do not change. The most stringent test condition is that of strong gain saturation, where $G_0 E_{in} \gg E_{sat}$.

Figure 4.1. shows the variation vs. the number of segments of the solution for energy gain in an amplifier where the waveguide is flared to be 3 times wider at the output than at the input, which was the case for the flared mode-locked lasers used in the experiments. In this example, the parameters used were $G_0 = 100$, and $E_{in} = 1.0 E_{sat}$, causing strong gain
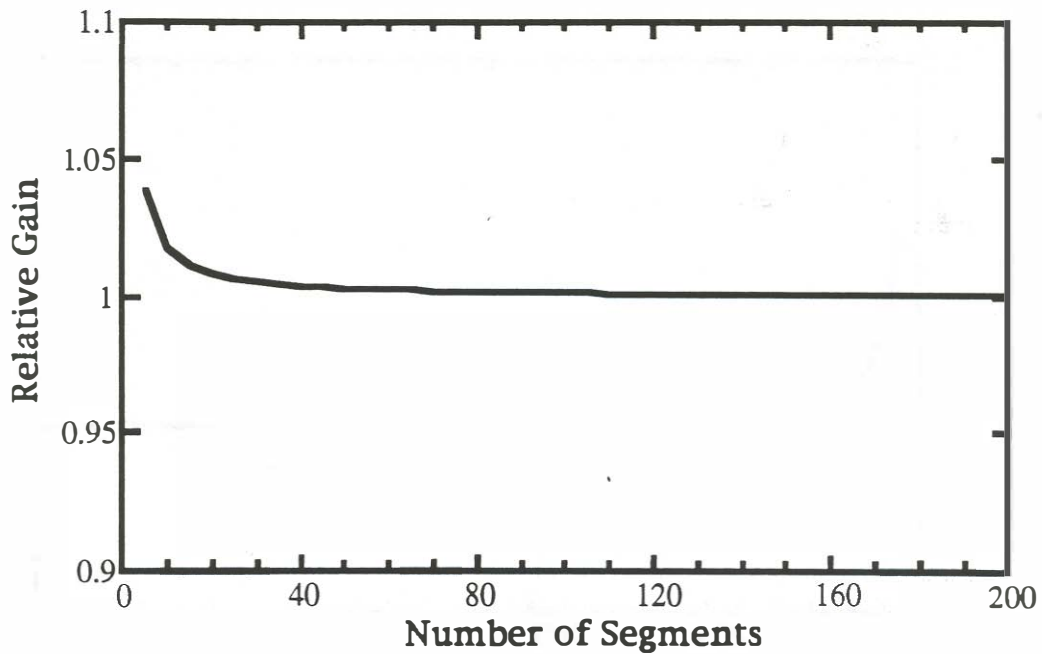
76

Figure 4.1. Solution for flared amplifier saturated gain vs. number of segments used in calculation. Amplifier flare ratio = 3, $G_0$=100, $E_{in}$=1.0$E_{sat}$. The results are normalized to actual gain = 7.6003.

saturation. As can be seen on the plot, 20 segments are required to achieve an accuracy of 1% relative to the ultimate solution of 7.6003. Amplifiers with larger flare ratios will require more gain segments to achieve accurate solutions. A flare ratio of 32 was used for the broad-area amplifier tested in the experiments. Figure 4.2. shows the results for simulating such an amplifier, with the same values of $G_0$ and $E_{in}$ as before. In this case, 100 segments are necessary to achieve an accuracy of ~1%. The actual energy gain was 11.836, still well in the regime of strong saturation compared to $G_0$

77
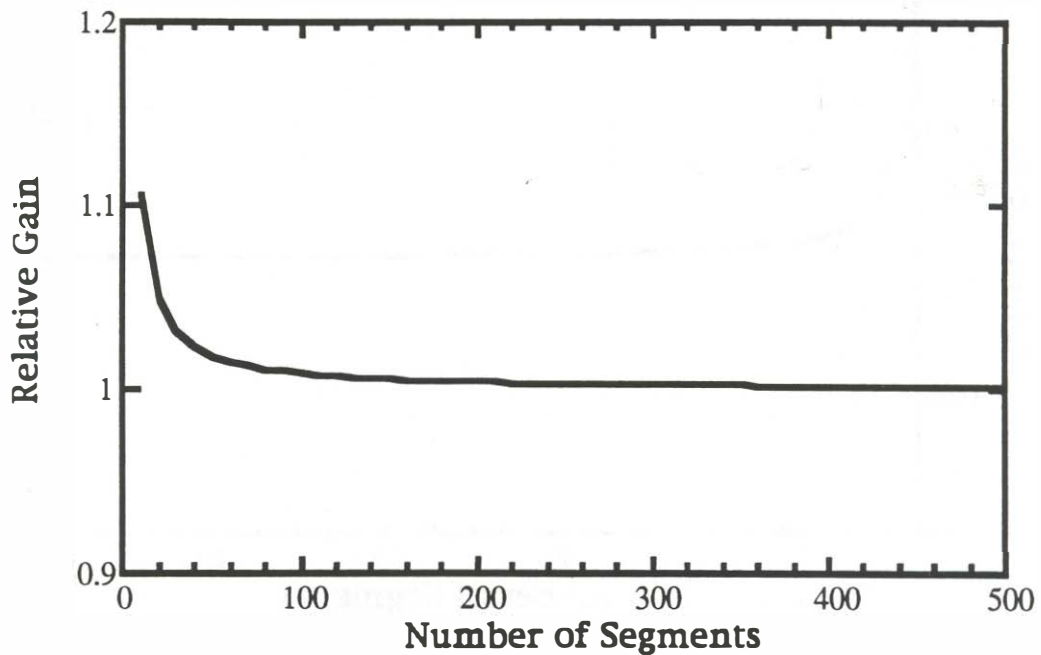
Figure 4.2. Solution for flared amplifier saturated gain vs. number of segments used in calculation. Amplifier flare ratio = 32, $G_0$=100, $E_{in}$=1.0$E_{sat}$. The results are normalized to actual gain = 11.830.

although the final saturated gain (and pulse energy) is higher than in the previous example.

## 4.5. Modeled Pulse Shaping in Flared and Uniform Mode-Locked Lasers.

To gain intuition into the pulse formation process in a mode-locked laser, it is helpful to first consider the case of unidirectional pulse propagation through a laser gain and absorber segment. At higher pulse energies gain

78

saturation causes pulse broadening in the amplifier resulting from the pulse edges being amplified more than the peak. This process eventually overwhelms the pulse sharpening that occurs from the saturable absorber segment, preventing mode-locking at higher pulse energies. In addition, the net energy gain through the entire device must be sufficient to overcome the other losses in coupling to an external cavity. Figure 4.3. shows the result
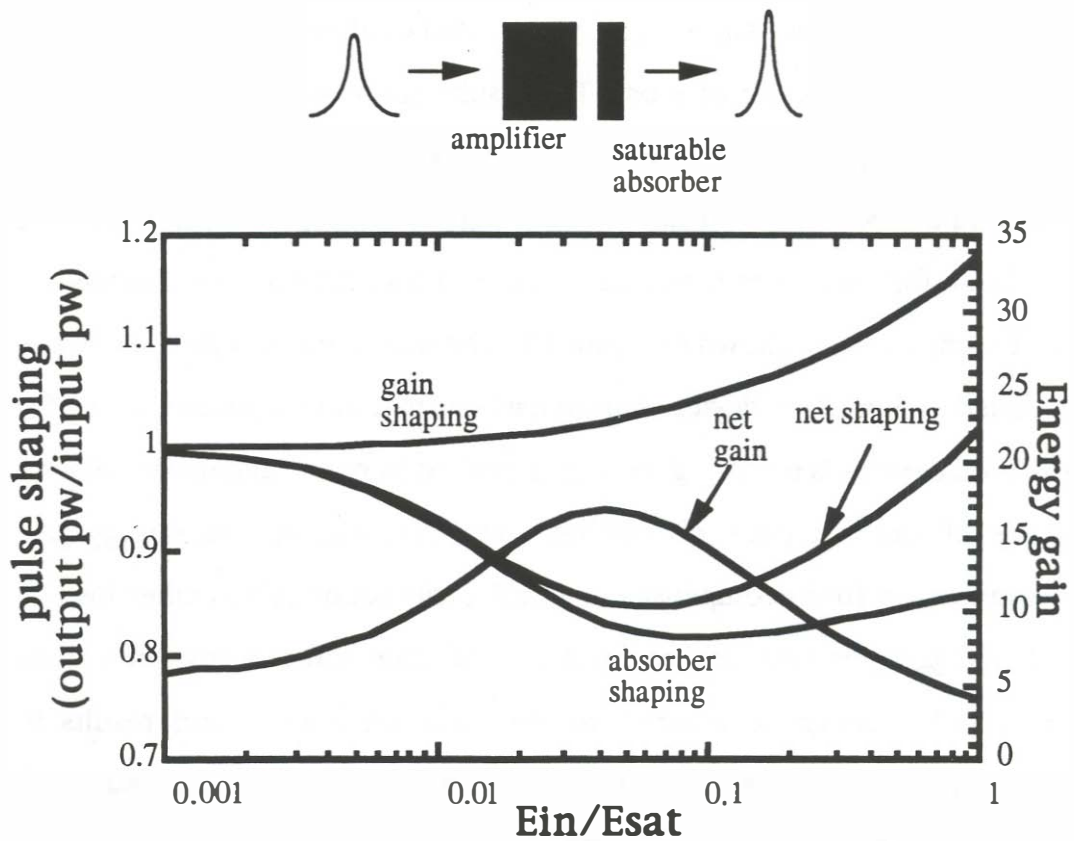


Figure 4.3. Calculated unidirectional propagation through a uniform laser gain and absorber segment for varied input pulse energy normalized to $E_{sat}$ the gain segment input. $G_0 = 130$, $G_{abs} = 0.04$, and $\sigma = 3$.

79

for propagation through a uniform amplifier plotted vs. $E_{in}/E_{sat}$ the amplifier input. The parameters used are $G_0$ = 130, an unsaturated absorber transmission of 0.04, a $\sigma$ of 3, and an input pulsewidth of 3 ps. At $E_{in} \sim E_{sat}$, the net pulse shaping leads to overall pulse broadening through the device.

To study pulse shaping in flared amplifier-absorber structures it is necessary to consider roundtrip propagation because the effect of the flare on gain saturation is very different in the forward and reverse directions. Figure 4.4. shows the case of roundtrip pulse propagation through a gain-absorber cascade with $G_0$ = 17, an unsaturated transmission of 0.2, a $\sigma$ of 3, and an input pulsewidth of 3 ps. The results are qualitatively similar to the previous example, as the device parameters have been adjusted to give similar values of effective roundtrip unsaturated absorption and gain. The calculation for a structure with a flare ratio of 3 with the same parameters for direct comparison is shown in Figure 4.5. The important difference between the flared and uniform device characteristics is that the net saturated gain for the flared devices is much higher, and is peaked in better alignment with the regime of optimal pulse shortening. For example, for an energy gain requirement of 10 (to compensate external cavity coupling and other losses), the flared gain structure reaches this degree of saturation at nearly three times higher pulse energy compared to the uniform device, and results in enhanced values of maximum net pulse shaping due to reduced pulse broadening contribution from the gain.

The flare in the amplifier could also be formed in the reverse direction, such that the waveguide is wider towards the absorber. The mode
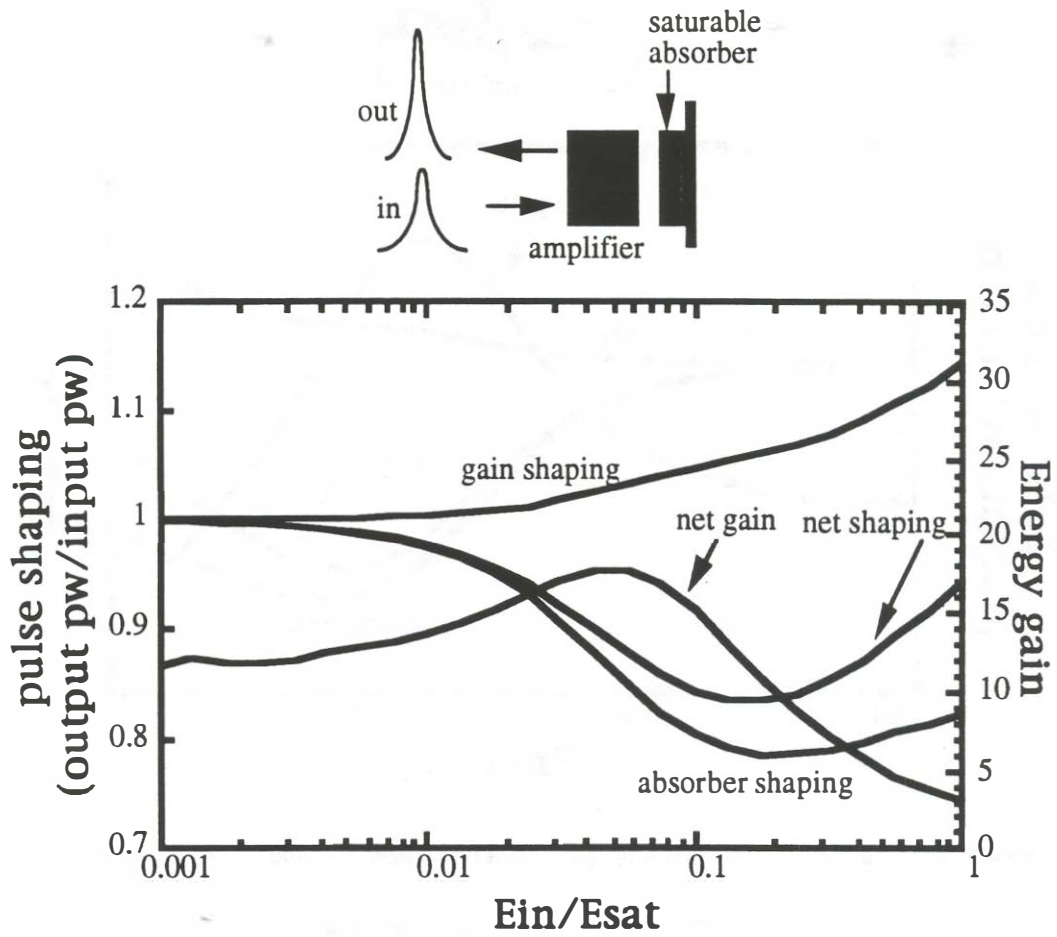
Figure 4.4. Calculated round trip pulse propagation in a uniform laser gain and absorber segment for varied input pulse energy normalized to $E_{sat}$ the gain segment input. $G_0 = 17$, $G_{abs} = 0.02$, and $\sigma = 3$.

81

Figure 4.5. Calculated round trip pulse propagation in a flared laser gain and absorber segment for varied input pulse energy normalized to $E_{sat}$ in the single mode part of the gain. $G_0 = 17$, $G_{abs} = 0.02$, and $\sigma = 3$, with a flare ratio of 3.

increase, resulting in a degradation of $\sigma$ by the flare factor. Figure 4.6. shows the calculated characteristics of this configuration for a flare ratio of 3, with the same parameters as in the previous example but with $\sigma = 1$. The saturation
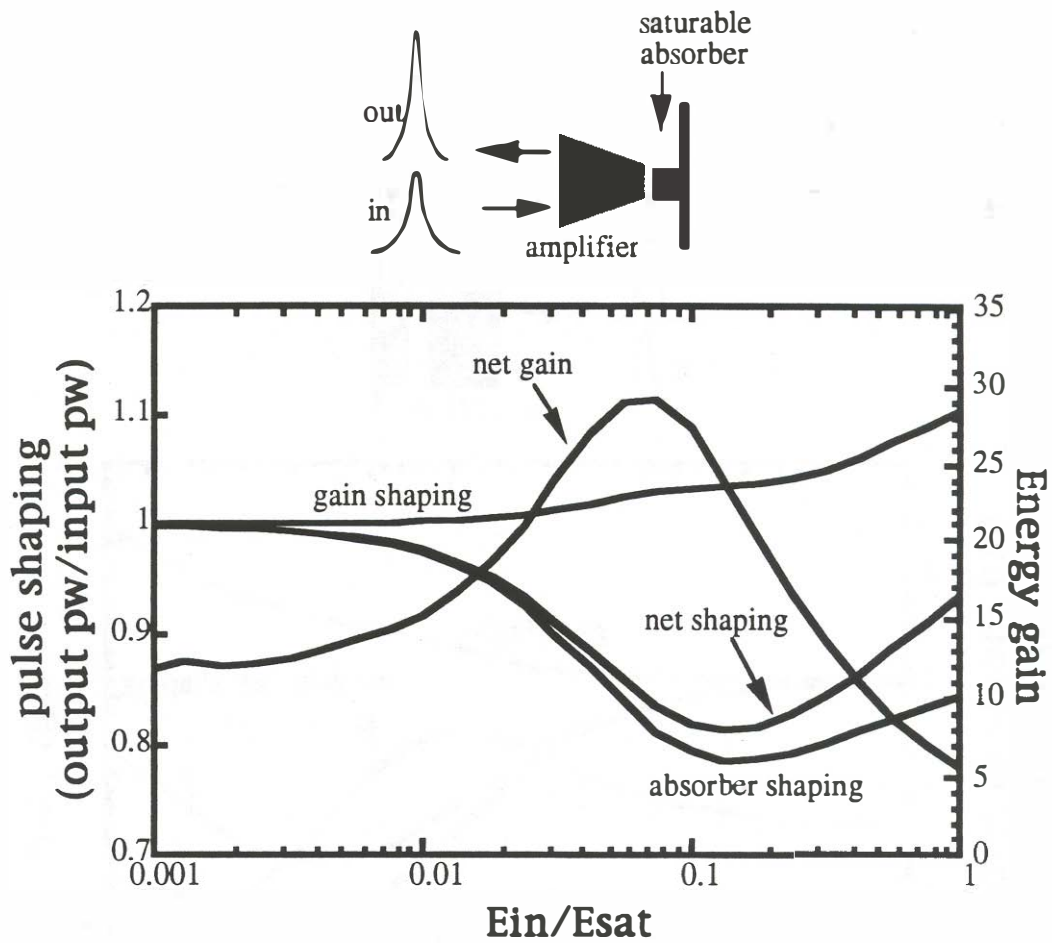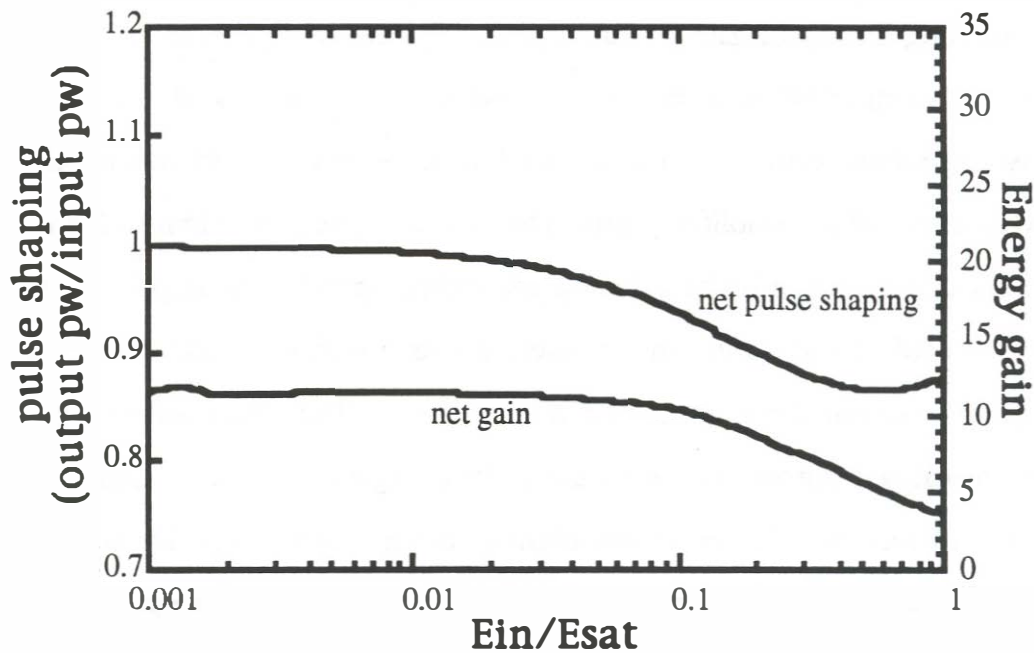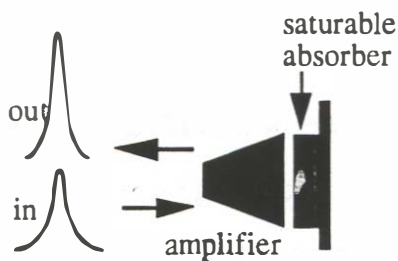
Figure 4.6. Calculated round trip pulse propagation in a flared laser gain and absorber segment for varied input pulse energy normalized to $E_{sat}$ in the single mode part of the gain. $G_0 = 17$, $G_{abs} = 0.02$, and $\sigma = 1$, with a flare ratio of 3.

in the gain segment is much more severe with this flare geometry, and there is a degradation in net pulse shortening due to reduced $\sigma$. This is the opposite of the situation in the devices with the flare towards the gain segment, where the effect of the flare is exploited to enhance $\sigma$, resulting in

improved mode-locking characteristics.

## 4.6. Modeled Pulse Amplification in Highly Saturated Single Pass Amplifiers.

The power amplification stage in a MOPA may be operated in a much more highly saturated regime than in the mode-locked laser. The pulse broadening effects of gain saturation are much less of a problem in a single-pass post-amplification stage, as opposed to the mode-locked laser, where pulse evolution occurs over many round trips. A flared broad-area amplifier is very effective for amplifying pulses to very high energies. Figure 4.7. shows the calculations of pulse broadening and energy gain for an amplifier with a flare ratio of 32 and a uniform amplifier, this time with $G_0 = 1000$. This is the value of unsaturated gain measured in Reference 6. The results are plotted vs. the normalized output energy so the pulse energies being generated can be readily observed. The pulse broadening in the flared amplifier is ~1.1 at levels of high saturation, which will not generally be a problem for most applications.

## 4.7. Flared Waveguide Mode-Locked Lasers With Increased Pulse Energy.

Experiments were performed on devices with both flared towards gain and flared towards absorber configurations in comparison to uniform waveguide devices. The lasers were prepared using the impurity-induced disordering process [16], which allows the definition of non-uniform
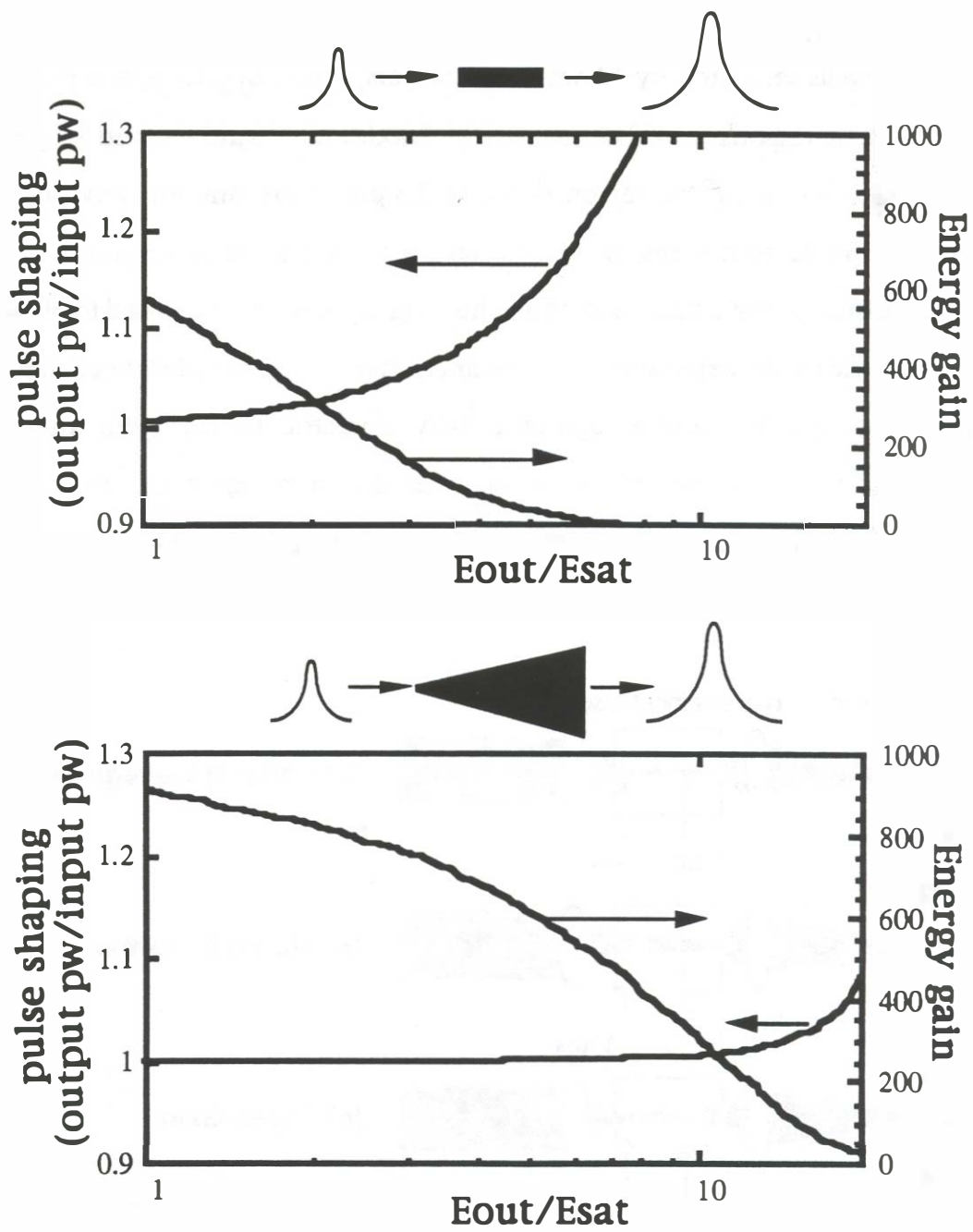
84

Figure 4.7. Calculated pulse shaping and energy gain in uniform and flared (flare ratio = 32) single pass highly saturated amplifiers, plotted vs. output energy to emphasize the output pulse energies being generated.

waveguide shapes. The active region consisted of three 8 nm $In_{0.2}Ga_{0.8}As$ quantum wells separated by 10 nm GaAs barriers, with $Al_{0.2}Ga_{0.8}As$ separate confinement regions on a GaAs substrate. Diodes of 500 $\mu$m cleaved lengths were used, with an active region width of 2.5 $\mu$m in the uniform waveguide device. The flared devices have linear tapers from 2.5 $\mu$m to 7.5 $\mu$m over a 150 $\mu$m distance, for a flare ratio of 3. The long taper region was used to allow for adiabatic mode expansion. Two-segment lasers were coupled to external cavities using a lens and a high-reflectivity dielectric mirror, with an AR coating on the facet coupled to the cavity as shown in Figure 4.8. Passively mode-locked operation was initiated by reverse-biasing the short ($\sim$70$\mu$m)

Figure 4.8. External cavity passively mode-locked multisection diode lasers with (a) uniform, (b) flared absorber, and (c) flared gain waveguides.

absorber section while biasing the gain section above threshold. The pulses are here again characterized by second harmonic autocorrelation.

The autocorrelation measurements of the pulses obtained are shown in Figure 4.9. Pulses of 3.5 ps duration and 1.8 pJ pulse energy were measured from the uniform waveguide laser. The flared towards absorber devices yielded higher pulse energies (4.1 pJ), but with a degradation in pulsewidth (4.2 ps) performance. The increase in pulse energy from the flared towards, absorber laser compared to the uniform case is probably due to the shift of



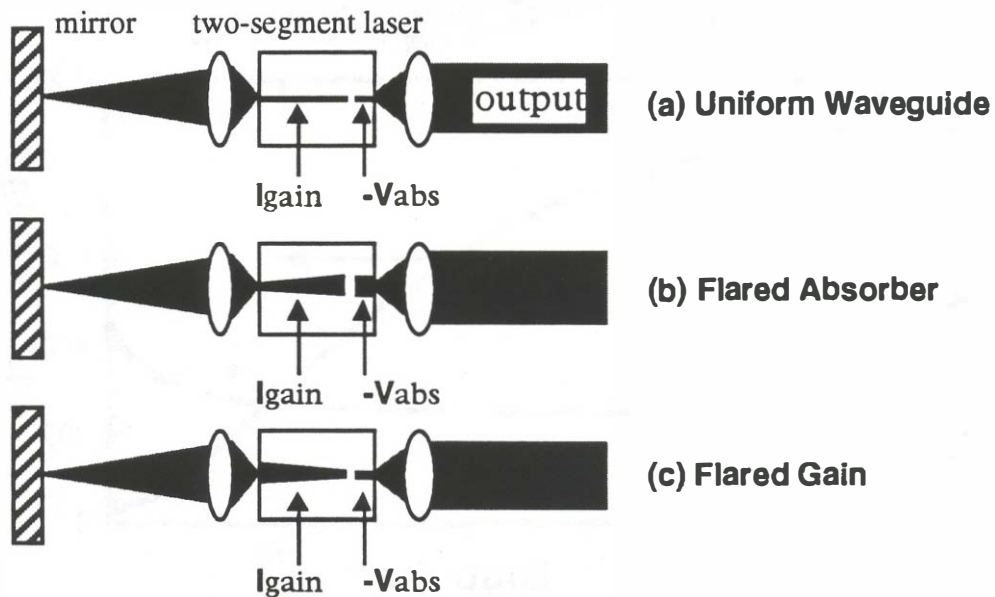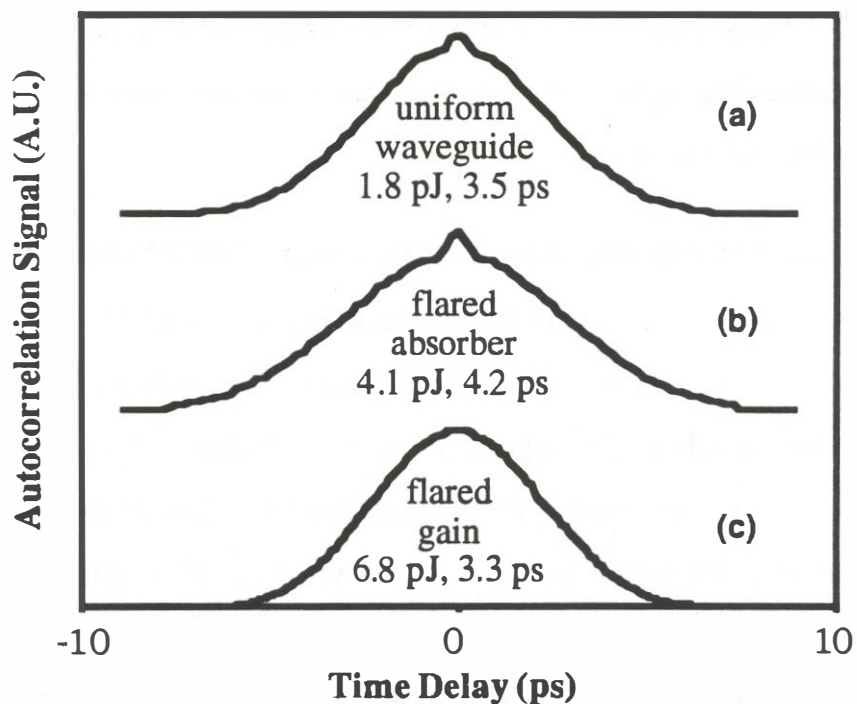Figure 4.9. Autocorrelations, pulse energies, and pulsewidths obtained from passively mode-locked multisection lasers with (a) uniform, (b) flared absorber, and (c) flared gain waveguides.

the pulse shortening curve towards higher energy, as can be seen in Figure 4.6. The broader pulsewidths are also consistent with the overall degradation in pulse shaping found in the calculation. As expected, the best performance was achieved using the flared towards gain type devices, generating pulse energies of 6.8 pJ and over 2 W peak power with a slight improvement in pulsewidth (3.3 ps). This represents an improvement in pulse energy of 3.8 times, in rough agreement with the estimate resulting from the preceding calculations based on this geometry. Accounting for the output coupling losses of about 3.5, this represents approximately 24 pJ internal pulse energy within in the laser itself, or about 6 times $E_{sat}$ in a single-mode amplifier waveguide. These results demonstrate the effectiveness of flared amplifier lasers in achieving higher powers and pulse energies without degrading pulsewidth performance.

## 4.8. Generation of Very High Energy Pulses Using the MOPA Configuration.

The output of the flared waveguide mode-locked laser described above is well-suited for use as an injection source for saturating a flared broad-area amplifier. A schematic diagram of the mode-locked MOPA is shown in Figure 4.10. An external cavity two-section flared waveguide laser emitting at 940 nm is used as the master oscillator. The overall device length was 650 μm, with an absorber section length of 70 μm and the balance of the device used for gain. The use of a 6 cm length external cavity results in a mode-locked pulse repetition rate of 2.5 GHz. The amplifier employs a strained InGaAs single quantum well active region, and has a 4 μm wide single-mode input
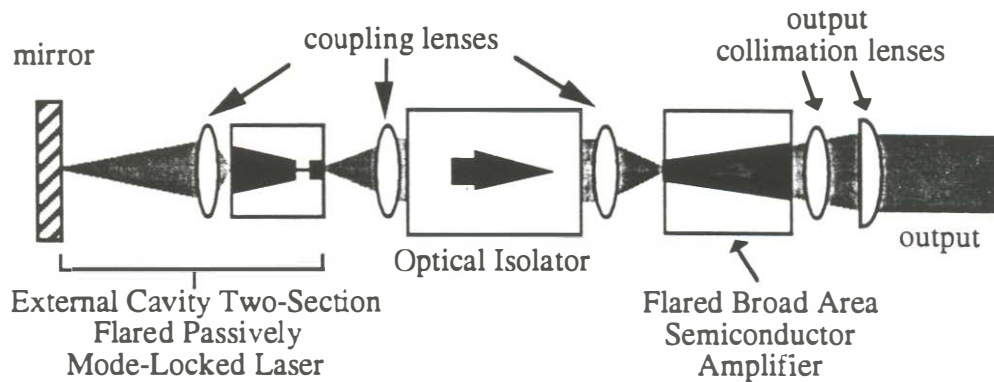
Figure 4.10. Diagram of the flared waveguide mode-locked MOPA laser.

waveguide which expands within the device to 130 μm width at the output facet, for a flare ratio of 32 as used in the simulations. The amplifier is mounted p-side down on a copper heatsink for CW operation, and both the input and output facets of the amplifier are AR-coated. Two AR-coated lenses are used to image the output of the master oscillator onto the input aperture of the tapered amplifier, and an optical Faraday isolator is inserted between the lenses to prevent back-emitted ASE from the amplifier from being injected into the master oscillator. This isolator includes a half-wave plate at the output for polarization matching to the amplifier. A GRINROD lens and cylindrical lens are used to collimate the output of the amplifier with an estimated collection efficiency of approximately 70%. The cylindrical lens compensates for astigmatism in the amplifier output that results because the optical mode inside the amplifier expands laterally towards the output end via diffraction, while the mode is guided in the transverse direction. An aperture

89

is used to select out the main lobe of the amplifier emission pattern. The pulses are characterized both by using a high-speed photodiode and sampling oscilloscope, and by second harmonic autocorrelation.

Amplifier Gain Characteristics

The output power out of the amplifier as a function of input power from the master oscillator is shown in Figure 4.11. The output power from the amplifier is measured after the output collimating lenses and aperture and the master oscillator power is measured between the two coupling lenses. By operating the master oscillator CW and varying the input current, the
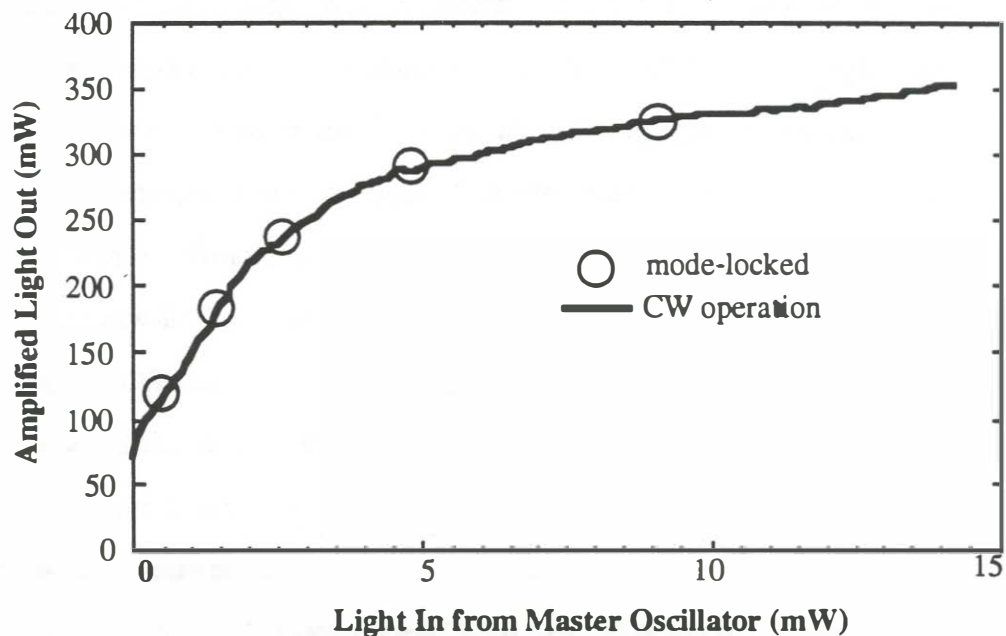


Figure 4.11. Amplifier output power vs. input level, CW and mode-locked.

amplifier power gain is measured as a function of injected power. The amplifier was biased at a current of 2.0 A throughout all the measurements. A clearly saturating output power characteristic above about 0.25 W output is observed. The maximum CW power obtained was 353 mW, corresponding to total output power of over 0.5 W before the losses in the output collimation optics. To properly calculate gain, peak power, and pulse energy, it is necessary to account for the contribution of ASE in the measured output power. At low injected signal levels, quenching of the ASE is minimal and it is appropriate therefore to subtract the full value of ASE power measured with no input signal (73 mW). At higher signal levels, quenching of the ASE is estimated by scaling the zero-input ASE power by the fractional reduction in optical gain. This assumes approximately linear relationships between gain, carrier density, and ASE power. The optical gain (including the lens coupling losses), is approximately 82 at low injection levels, decreasing to 23 at the maximum output power obtained, as shown in Figure 4.12. The scaled value of ASE noise power is subtracted from the total output power in calculating the amplified output powers.

Measurements of the average power gain were also taken under mode-locked operation of the master oscillator. Such operation caused no discernible effect on the output beam divergence. By inserting a variable attenuator at the input of the amplifier, measurements at different injection levels were made. These are the circled data points in Figure 4.8. The close match between the mode-locked and CW power gain indicates that the gain recovery is sufficiently fast to recover between pulses, which in this case

91
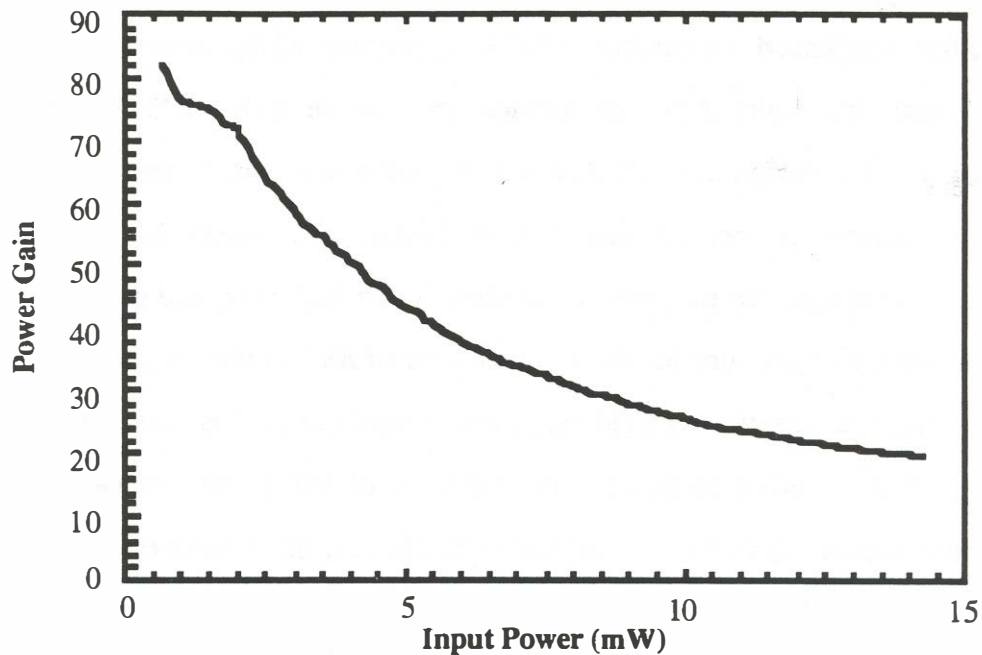
Figure 4.12. CW power gain from the broad-area flared amplifier vs. injected power.

were spaced by 0.4 nS (2.5 GHz repetition rate).

## Mode-Locking Characteristics

Passive mode-locked operation of the master oscillator was achieved by terminating the short absorbing section of the laser into a resistance of 30 $\Omega$ and forward-biasing the gain section of the device with a DC current of 90 mA. This termination of the absorber is optimized for sufficiently fast recovery of the absorption between pulses to insure stable mode-locking, with lower values of impedance or operation under reverse bias resulting in

92

diminished output power due to excess unsaturated absorption. These conditions resulted in an average mode-locked output power of 9.1 mW. The autocorrelation measurement of these mode-locked pulses before amplification is shown in Figure 4.13. The pulses have an autocorrelation FWHM of 5.6 ps, corresponding to a pulsewidth of 3.7 ps, assuming a sech$^2$ pulse shape. Measurements of the optical spectra show that these pulses have a bandwidth of 5.8 nm. The resulting time-bandwidth product of 7.4 is 24 times the transform limit, indicating that these pulses are highly chirped.

Mode-locking of the master oscillator ceased when the back-emitted ASE from the amplifier was injected into the laser. The injection of ASE from
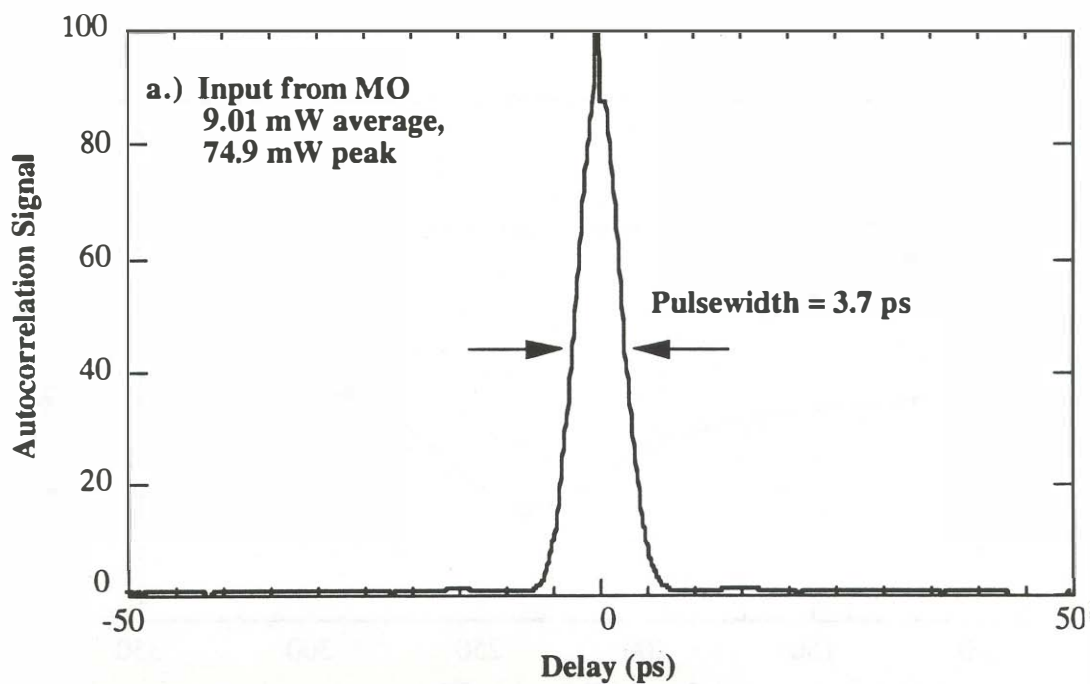


Figure 4.13. Autocorrelation of pulses injected into flared broad-area MOPA amplifier.

the amplifier into the saturable absorption segment of the laser interferes with the recovery of the absorption between pulses. This necessitates the use of an isolator between the master oscillator and the amplifier. An important implication of this phenomenon is that it may not be possible to monolithically integrate a mode-locked master oscillator with the amplifier unless an integrated isolator can be fabricated as well. The pulse characteristics after amplification were measured at various power levels by inserting a variable attenuator at the input of the amplifier. The amplified pulsewidths and optical spectral widths are plotted vs. output power in Figure 4.14. The tendency towards longer pulses and increased spectral width at the higher powers is due to the increased effects of self-phase modulation
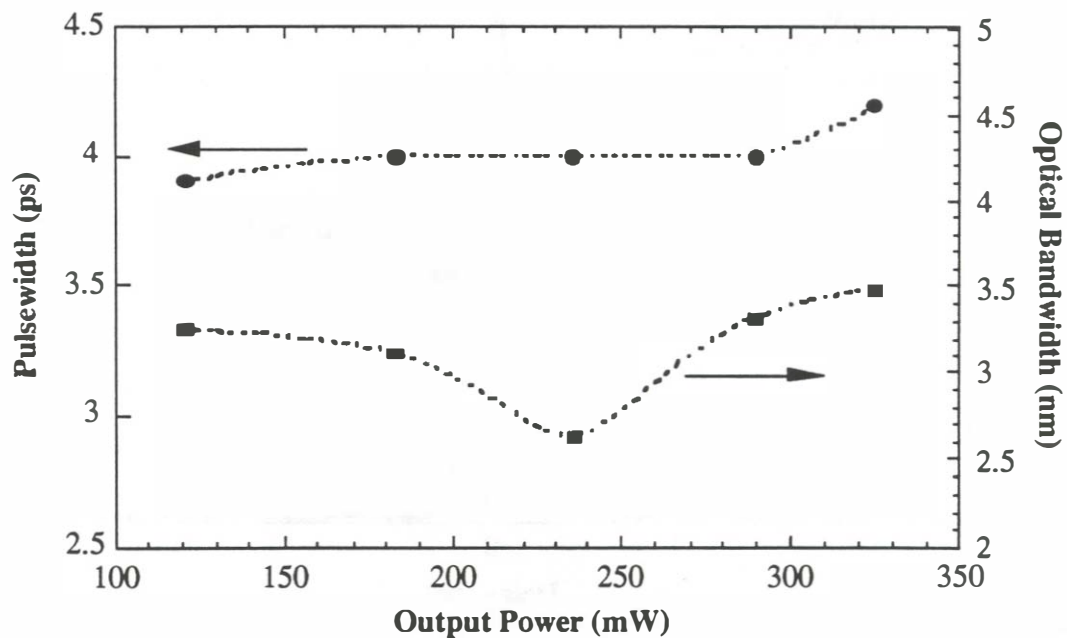


Figure 4.14. Amplified pulsewidths and bandwidths for varied output powers.

94

in the amplifier at higher pulse energies. At low energy, the spectral width also increases because of the relatively large ASE contribution. The amplified spectral widths obtained are narrower than that of the input due to spectral peaks in the gain, which were also observed in the ASE spectrum from the amplifier. This may have been due to an external reflection causing feedback into the amplifier. Figure 4.15 shows the amplified pulse energy for varied input power. The highest pulse energy measured was 118 pJ, corresponding to an internal pulse energy in the amplifier of approximately 170 pJ. $E_{sat}$ the output end of the amplifier, where the gain cross section area is the largest, is approximately 120 pJ. This shows that it is feasible to generate pulses with
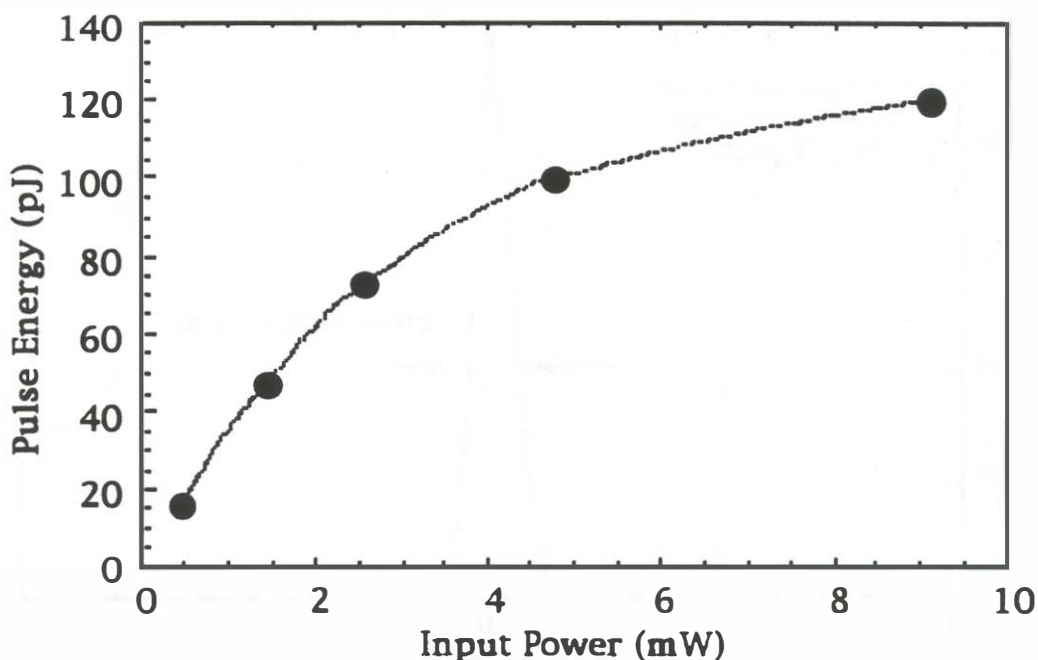
Figure 4.15. Amplified pulse energy for varied input power to the broad area flared MOPA amplifier.

95

energies higher than $E_{sat}$ in a single-pass post-amplification stage, operating at higher levels of saturation than is normally practicable in the mode-locked laser itself because of the pulse broadening at such high pulse energies. The autocorrelation of the highest energy pulses obtained is shown in Figure 4.16. The total average power in this case was 325 mW. Subtracting the estimated ASE contribution of 29 mW, this corresponds to a peak power of 28.1 W. The amount of pulse broadening after amplification (~1.14) is within the range of values found from the calculations for this structure in Section 4.3.

Finally, it is worthwhile to note that although the amplified pulsed output comprises 91% of the total output power (the rest being ASE noise),
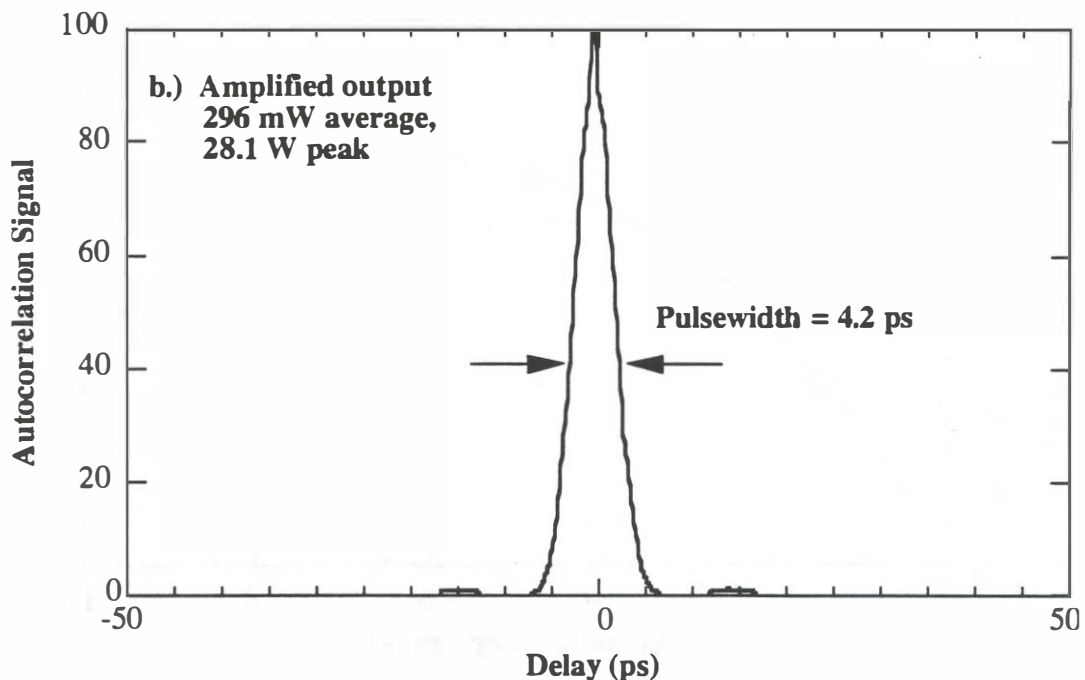


Figure 4.16. Autocorrelation of highest power amplified pulses.

96

the modulation depth is 99.9% due to the very low duty cycle of the pulsed output. The high powers obtainable from the mode-locked MOPA make it a viable, all-semiconductor option for use as a replacement for much larger and more costly mode-locked laser systems.

## 4.9. Summary.

The computationally efficient partial integration model developed by Helkey [11] to analyze pulse propagation in lasers has been adapted using the parametrized rate equations of Agrawal and Olsson [13] for application to flared amplifier and laser structures. The calculations show that two-section passively mode-locked lasers with amplifier flaring towards the gain section operate with higher pulse energies and enhanced pulse shaping compared to uniform waveguide laser structures. The modeling of unidirectional propagation in highly saturated amplifiers shows that a flared broad-area amplifier is very effective for amplifying pulses to very high energies with acceptable levels of single-pass pulse broadening.

Experiments were performed comparing uniform and flared mode-locked laser waveguide geometries. The results verify the conclusions drawn from the model, with a 3.8 times enhancement in pulse energy and peak power from the flared towards gain type device over the uniform waveguide device, simultaneously with an improvement in pulsewidth performance. Peak powers of over 2 W are generated from the flared amplifier mode-locked laser, which currently is the highest peak power that has been

obtained directly from single-stripe diode lasers. The flared mode-locked laser was used as an injection source for a flared broad-area amplifier, resulting in the first demonstration of a flared amplifier MOPA under mode-locked operation. Record average and peak mode-locked output powers without pulse compression were achieved, with pulse energies of 118 pJ and peak output powers of 28.1 W. This is about two orders of magnitude improvement over conventional mode-locked diode lasers.

# References

1. L J. Mawst, D. Botez, C. Zmudzinski, M. Jansen, C. Tu, T. J. Roth, and J. Yun, "Resonant Self-aligned-stripe Antiguided Diode Laser Array," Appl. Phys. Lett. 60 (6), 10 February 1992.

2. J. S. Major, D. F. Welch, D. R. Scifres, "High power high efficiency antiguide laser arrays," Appl. Phys Lett., vol. 59, pp. 2210-2212, 1991.

3. M. L. Tilton, G. C. Dente, A. H. Paxton, J. Cser, R. K. DeFreez, C. E. Moeller, D. Depatie, "High power, nearly diffraction-limited output from a semiconductor laser with an unstable resonator," IEEE J. Quantum Electron., vol. 27, pp. 2098, 1991.

4. E. S. Kintzer, J. N. Walpole, S. R. Chinn, C. A. Wang, L. J. Missaggia, "High-Power, Strained-Layer Amplifiers and Lasers with Tapered Gain Regions," IEEE Photonics Technology Letters, Vol. 5, No. 6, pp. 605, June 1993.

5. L. Goldberg, D. Mehuys, M. R. Surette, D. C. Hall, "High-Power Near-Diffraction-Limited Large-Area Traveling-Wave Semiconductor Amplifiers," IEEE J. Quantum Electron., vol. 29, pp. 2028, 1993.

6. J. N. Walpole, E. S. Kintzer, S. R. Chinn, C. A. Wang, and L. J. Missagia, "High-Power Strained-Layer In GaAs/AlGaAs Tapered Traveling-Wave Amplifier," Applied Physics Letters, 61, 740-742, 1992.

99

# References

1.  L. J. Mawst, D. Botez, C. Zmudzinski, M. Jansen, C. Tu, T. J. Roth, and J. Yun, "Resonant Self-aligned-stripe Antiguided Diode Laser Array," Appl. Phys. Lett. 60 (6), 10 February 1992.

2.  J. S. Major, D. F. Welch, D. R. Scifres, "High power high efficiency antiguide laser arrays," Appl. Phys Lett., vol. 59, pp. 2210-2212, 1991.

3.  M. L. Tilton, G. C. Dente, A. H. Paxton, J. Cser, R. K. DeFreez, C. E. Moeller, D. Depatie, "High power, nearly diffraction-limited output from a semiconductor laser with an unstable resonator," IEEE J. Quantum Electron., vol. 27, pp. 2098, 1991.

4.  E. S. Kintzer, J. N. Walpole, S. R. Chinn, C. A. Wang, L. J. Missaggia, "High-Power, Strained-Layer Amplifiers and Lasers with Tapered Gain Regions," IEEE Photonics Technology Letters, Vol. 5, No. 6, pp. 605, June 1993.

5.  L. Goldberg, D. Mehuys, M. R. Surette, D. C. Hall, "High-Power Near-Diffraction-Limited Large-Area Traveling-Wave Semiconductor Amplifiers," IEEE J. Quantum Electron., vol. 29, pp. 2028, 1993.

6.  J. N. Walpole, E. S. Kintzer, S. R. Chinn, C. A. Wang, and L. J. Missagia, "High-Power Strained-Layer In GaAs/AlGaAs Tapered Traveling-Wave Amplifier," Applied Physics Letters, 61, 740-742, 1992.

7. D. Mehuys, L. Goldberg, D. F. Welch, "5.25 W CW Near-Diffraction-Limited Tapered-Stripe Semiconductor Optical Amplifier", IEEE Photonics Technology Letters, vol. 5, 10, 1179, Oct. 1993.

8. R. J. Lang, A. Hardy, R. Parke, D. Mehuys, S. O'Brien, J. S. Major, D. F. Welch, "Numerical Analysis of Flared Semiconductor Laser Amplifiers," IEEE J. Quantum Electron., vol. 29, pp. 2044, 1993.

9. D. Mehuys, D. F. Welch and L. Goldberg, "2.0 W CW Diffraction-Limited Tapered Amplifier With Diode Injection", Electron. Lett., vol. 28, 21, 1944, Oct. 1992.

10. S. O'Brien, D. F. Welch, R. A. Parke, D. Mehuys, K. Dzurko, R. J. Lang, R. Waarts, D. Scifres, "Operating Characteristics of a High-Power Monolithically Integrated Flared Amplifier Master Oscillator Power Amplifier," IEEE Journal of Quantum Electronics., 29(6), 1426-1439, June 1993.

11. R. J. Helkey, P.A. Morton, and J. E. Bowers, "A New Partial Integration Method for Analysis of Mode Locked Semiconductor Lasers", Optics , 1 5, 112 (1990).

12. J. E. Bowers, P.A. Morton, S. Corzine and A. Mar, "Actively Mode Locked Semiconductor Lasers," IEEE Journal of Quantum Electronics., 25(6), 1426-1439, June 1989.

13. G. P. Agrawal and N. A. Olsson, "Self-phase modulation and spectral broadening of optical pulses in semiconductor laser amplifiers," IEEE J. Quantum Electronics, vol. QE-25, pp. 2297-2306, 1989.

14. H. A. Haus, "Parameter ranges for CW passive mode-locking", IEEE Journal of Quantum Electronics., QE-12, pp. 169-176, 1976.

15. D. J. Derickson, R. J. Helkey, A. Mar, J. R. Karin, J. G. Wasserbauer, J. E. Bowers, "Short Pulse Generation Using Multi-Segment Mode-Locked Semiconductor Lasers", IEEE J. of Quant. Electron., **28**, p. 2186, Oct. 1992.

16. R. J. Helkey, W. X. Zou, A. Mar, D. B. Young, J. E. Bowers, "Curved and tapered waveguide modelocked InGaAs/AlGaAs semiconductor lasers fabricated by impurity induced disordering", Device Research Conference,Santa Barbara CA,vol. 1861, (1993).

# Chapter 5

# Epilogue

## 5.1. Summary of Results.

Two major areas of deficiency regarding conventional mode-locked semiconductor lasers have been addressed in this dissertation. The first is the tendency for external cavity lasers to emit multiple pulse bursts per repetition cycle. For most applications, the effective system impulse response from such an output is not the response to the stimulus of a single pulse, but rather to the long decay envelope of the multiple trailing pulses. The second general issue investigated forms the greater part of the dissertation, namely that of improving on the relatively low power levels generated from diode lasers under mode-locked operation.

This multiple pulse phenomenon originates from the finite residual reflection from the antireflection coating that is used to couple the laser diode to the external cavity. The multiple pulse phenomenon exists for even very low values of reflectivity from this coating, and it is not a practical approach to attempt to eliminate multiple pulsing by further reductions in the coating reflectivity. It is demonstrated that this effect is very effectively suppressed in actively mode-locked lasers by designing the laser so that the time delay between such reflected pulses is made longer than the drive pulse fall time. This is done through the use of longer cleaved device lengths, fast electrical drive pulses, and multi-segmented laser designs with reverse biased

102

modulators. By implementing these techniques, nearly transform-limited, single pulses of 1.4 ps duration were generated from an actively mode-locked external cavity laser. At the time the work was published, these were the shortest single pulses generated from an actively mode-locked external cavity laser. An external cavity laser suitable for use as a soliton source was also demonstrated, employing a reflection grating in the external cavity to generate clean hyperbolic secant squared pulses with time-bandwidth products of 0.30.

Arrayed lasers were used to construct high power mode-locked lasers. Anti-guide array structure devices are used because of their excellent far-field characteristics, and it is demonstrated that such devices couple well to external cavities with careful optical design, with coupling efficiencies comparable to those obtained using conventional single-element lasers. Comparison was made between active, passive and hybrid mode-locking of array lasers using multisegmented devices. Active mode-locking of such lasers resulted in >50 pJ pulse energies that are not limited by the gain saturation energy, but were relatively long in duration (22 ps) because high-speed gain modulation was not feasible. By utilizing multi-segment devices with a short saturable absorber segment, passively mode-locked pulses as short as 5.6 ps were generated without multiple pulsations. The maximum passively mode-locked pulse energy was 21.9 pJ with peak powers of over 3 W. This is about the value of pulse energy one would expect based on a scaling of the saturation energy by the number of array elements, demonstrating that ROW arrays are effective for increasing the output powers

103

from mode-locked semiconductor lasers with intra-waveguide saturable absorbers. Hybrid mode-locking resulted in pulse characteristics similar to that of the passively mode-locked case, with the additional advantage of having output synchronized to the external drive signal with very low timing jitter. The hybrid mode-locked configuration therefore is preferred for most applications, offering both the short pulse performance from saturable absorption pulse shaping and synchronized, low jitter output. The characteristics of mode-locked ROW array lasers indicate a strong potential for use in applications requiring high output powers.

Flared waveguide lasers and amplifiers were also investigated for generation of high power pulses. Numerical and experimental comparisons are made between uniform waveguide devices and devices with waveguide flaring both in the absorber and in the gain segments. By flaring the waveguide to be wider in the gain segment of the laser than in the absorber region, improvements in both pulse energy and pulsewidth are obtained compared to the uniform waveguide device and the device with the flared absorber. Such a device was used as the injection source for a flared broad-area amplifier in the so-called master oscillator power amplifier (MOPA) configuration. This allows independent optimization of the mode-locked laser oscillator from the power amplification stage. The power amplifier is of a flared waveguide design, with a large saturation energy at the output end. Because the external power amplification occurs in a single pass, the amplifier may be operated in a more heavily saturated regime than in a mode-locked laser, where pulse evolution occurs over many round trips. Using the

104

MOPA approach, record average and peak powers and pulse energies have been achieved, with pulses being generated of energies exceeding 100 pJ and peak powers of nearly 30 W.

## 5.2. Conclusions and Future Development.

With proper design, external cavity mode-locked lasers are capable of generating clean single-pulse outputs. External cavities also provide the designer great flexibility for the selection of repetition rates and insertion of intra-cavity tuning and filtering elements. The insertion of intra-cavity dispersive elements may serve to counteract the effects of SPM and GVD in the laser diode, so that gain bandwidth limited (~5 THz) output pulsewidths (~100 fs) can be achieved directly from the laser cavity. Such dispersion compensation has been used outside the cavity to achieve pulsewidths of 200 fs [1]. As fabrication technologies improve, monolithically integrated mode-locked laser structures will be preferred for most applications over external cavity lasers. However, the external cavity laser is likely to remain an important vehicle, particularly for research, and its understanding and continued evolution will serve to aid in the understanding and design of monolithic structures.

The directions pursued for high-power mode-locked lasers mirror the approaches that have been pursued in the development of high-power diffraction-limited CW sources. The arrayed laser approach has been successful in increasing the pulse saturation energy in a lateral array mode

with large cross sectional area. Flared waveguide lasers also expand the mode area and saturation energy in the widened section of the devices, and this type of laser also has the important advantage of increased gain-to-absorber saturation energy ratio when the absorber is integrated in the single-mode region of the device. For this reason, and also because of the relative difficulty in fabricating diffraction-limited laser arrays, the flared waveguide laser approach at the present appears to be the more promising of the two techniques. Such a laser is also well-suited to inject high-gain flared broad area amplifiers, providing an additional order of magnitude increase in pulse energy. This finally puts the mode-locked diode laser in the realm of large benchtop laser systems such as dye lasers and solid-state lasers in terms of average power and pulse energy. An important next step is to develop an integrated mode-locked MOPA laser, with the most formidable challenge perhaps being the need for optical isolation between the oscillator and amplifier sections of the device.

There are many important potential new applications for high power mode-locked diode lasers. The high peak power pulses generated from the mode-locked MOPA laser are suitable for high-efficiency harmonic generation. Recently, a mode-locked flared broad area laser was used to generate frequency doubled blue light with nearly 10% efficiency [2]. A mode-locked MOPA laser, using either a pulse compressor or a femtosecond pulsewidth master oscillator, would generate pulses with 100's of Watts peak power, and might be used to pump an optical parametric amplifier or oscillator. High power mode-locked semiconductor lasers may also serve as

convenient, relatively low-cost and reliable sources for measurement techniques such as electro-optic sampling [3], whose proliferation thus far has been limited due to the requirement of a large and expensive mode-locked laser system for the optical pulse stream. General'y speaking, the possibility of using high-power mode-locked semiconductor laser sources (especially an integrated mode-locked multi-Watt MOPA laser) to replace large benchtop lasers such as dye and solid-state lasers is an extremely attractive and exciting prospect.

# References

1. P. J. Delfyett, L. T. Florez, N. Stoffel, T. Gmitter, N. C. Andreadakis, Y. Silberberg, J. P. Heritage, G. Alphonse, "High-Power Ultrafast Laser Diodes," Journal of Quantum Electronics, 28, 10, 2203-2219, Oct. 1992.

2. L. Goldberg, D. Mehuys, "Efficient blue light generation with a modelocked tapered stripe semiconductor laser", Conference on Lasers and Electrooptics, Anaheim CA, postdeadline paper CPD17-3/39, 1994.

3. J. M. Weisenfeld, " Electrooptic sampling of high speed devices and integrated circuits," IBM Journal of Research and Development, 34, pp. 141-161, 1990.

# Reactively Sputtered Silicon Oxynitride For Anti-Reflection Optical Coatings

Anti-reflection (AR) optical coatings have many important applications for optoelectronic devices. A semiconductor laser is used as an optical amplifier by suppression of both facet reflectivities to prevent lasing oscillation. Single-facet AR coatings are used to make high-power superluminescent LED's. Mode-locking of semiconductor lasers to generate picosecond optical pulses is achieved by AR-coating a single facet and coupling into an external cavity. Such external cavity lasers are also used to obtain narrow optical linewidths and can be made wavelength-tunable. Another important application is the AR-coating of photodetectors to increase responsivity.

For good performance of external cavity lasers it is important that the AR-coated facet reflectivity be reduced to below 0.5%. The requirements for optical amplifiers are more stringent, requiring reflectivities of less than 0.1% to achieve a large, spectrally flat gain without lasing. Achieving such low reflectivities requires precise adjustment of the optical refractive index and film thickness. In addition, to preserve device performance, it is vital that the deposition occurs at low temperature ($<100°$ C).

Sputtered deposition offers the advantage of low temperature compared to evaporation techniques. Therefore, reactive DC sputtering of a
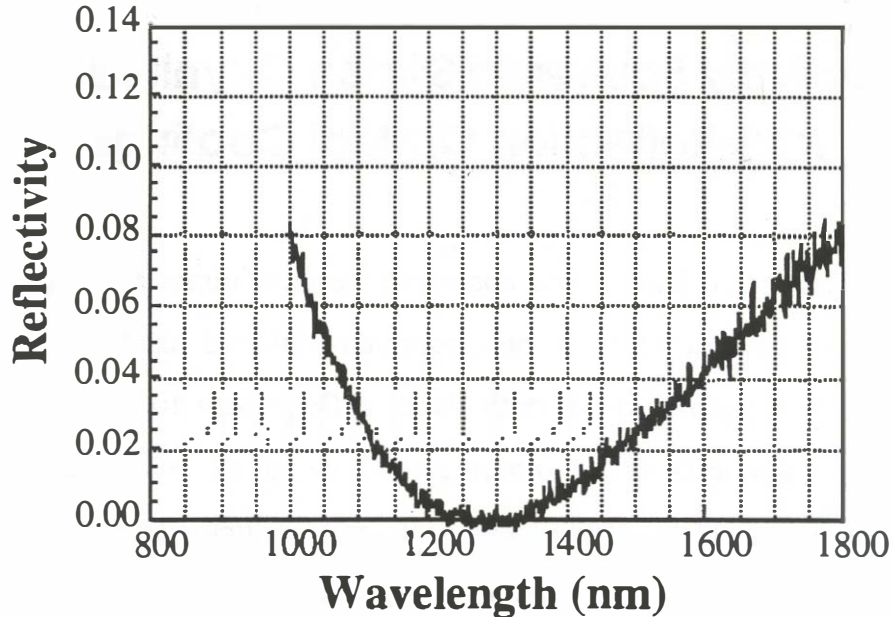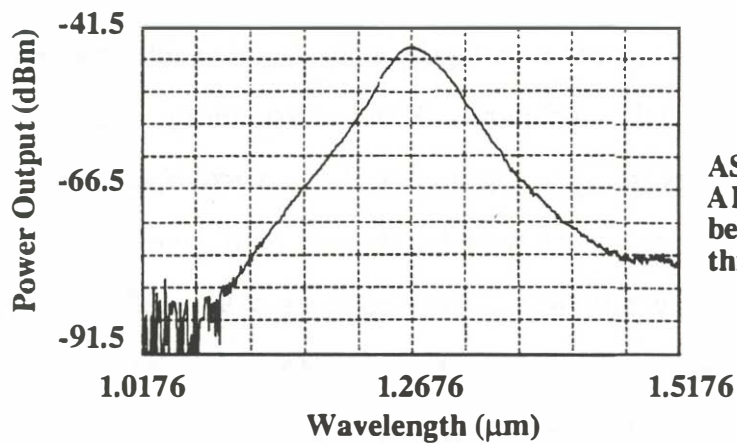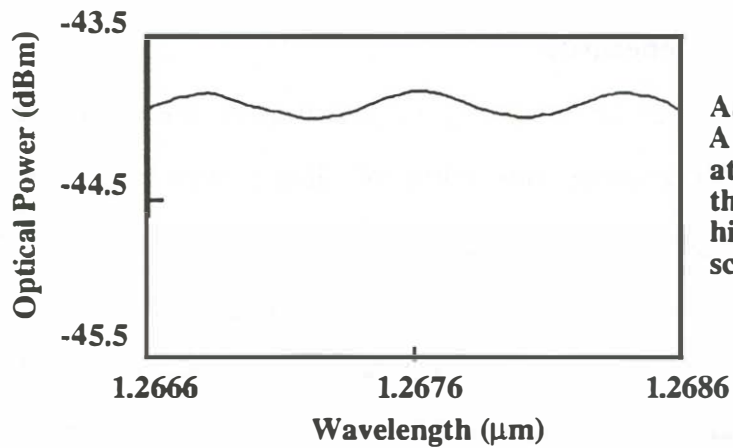
Figure A.1.  Reflectivity of single-layer AR coating on Si, with center wavelength = 1300 nm.

silicon target in a mixture of argon, nitrogen, and oxygen is used to reproducibly form high-quality silicon oxynitride AR films. The particular technique chosen allows the achievement of the optimal film index for single-layer AR films (1.78-1.87),but also is robust against process variability. The coating reflectivities on silicon are measured to be <0.3% by use of a spectrophotometer, as shown in Figure A.1. This measurement is limited by the noise floor of the instrument. A more sensitive method is the determination of the AR-coated facet reflectivities of a laser by measuring the spectral modulation of its amplified spontaneous emission [Hakki and Paoli, J.

110

Figure A.2. Determination of AR-coated facet reflectivity from ASE spectrum.

The first plot: y-axis "Power Output (dBm)" with values -41.5, -66.5, -91.5; x-axis "Wavelength (μm)" with values 1.0176, 1.2676, 1.5176. Label: "ASE spectrum after AR coating, biased at before-coating threshold"

The second plot: y-axis "Optical Power (dBm)" with values -43.5, -44.5, -45.5; x-axis "Wavelength (μm)" with values 1.2666, 1.2676, 1.2686. Label: "ASE spectrum after AR coating, biased at before-coating threshold, high sensitivity scale"

$$m = \text{modulation index} = \frac{P_{max} - P_{min}}{P_{max} + P_{min}}$$

$$= \frac{2a}{1 + a^2} \quad \text{(m measured at before-coating threshold current)}$$

$$R = \frac{a R'}{R_2}$$

$$= 4.1 \cdot 10^{-5}$$

@ 0.2 dB modulation depth

$a$ = "amplification factor"

$R'$ = reflectivity before coating

$R_2$ = 2nd facet reflectivity = 0.3 = $R'$

of Appl. Phys., 44, 1973], as shown in Figure A.2. Coating reflectivities of <0.02% are measured using this technique. Reactive sputtering also allows a wide variation of film index through adjustment of the reactive gas flowrates, making possible the fabrication of wide-bandwidth multi-layer or graded-index AR coatings. Multi-layer high-reflectivity coatings of 98% reflectivity for both surface-emitting and in-plane lasers have also been demonstrated. Sensitive control of film thicknesses is accomplished through *in situ* monitoring of the coating reflectivity.

Alternative techniques for achieving AR coatings of the appropriate index involve either decreasing the index of silicon nitride ($\approx$2.0) by introducing excess nitrogen, or increasing the index of silicon dioxide ($\approx$1.45) by decreasing the amount of oxygen present. Such approaches generally produced less than satisfactory films, or suffered from process variability. For example, silicon nitride targets can be RF sputtered in argon to produce nitride films; the addition of excess nitrogen into the chamber will increase the nitrogen content of the film and decrease the index. In practice however, non-uniformities of the silicon nitride target causes reproducibility problems with this technique. We have deposited nitrogen-rich silicon nitride by DC sputtering a silicon target in argon with excess nitrogen, but poor film quality results from this method because the excess nitrogen causes nitride to form on the target itself, causing plasma arcing and particle generation into the film. Silicon dioxide can be deposited by sputtering silicon with argon and oxygen; reducing the oxygen discharge results in silicon-rich (oxygen
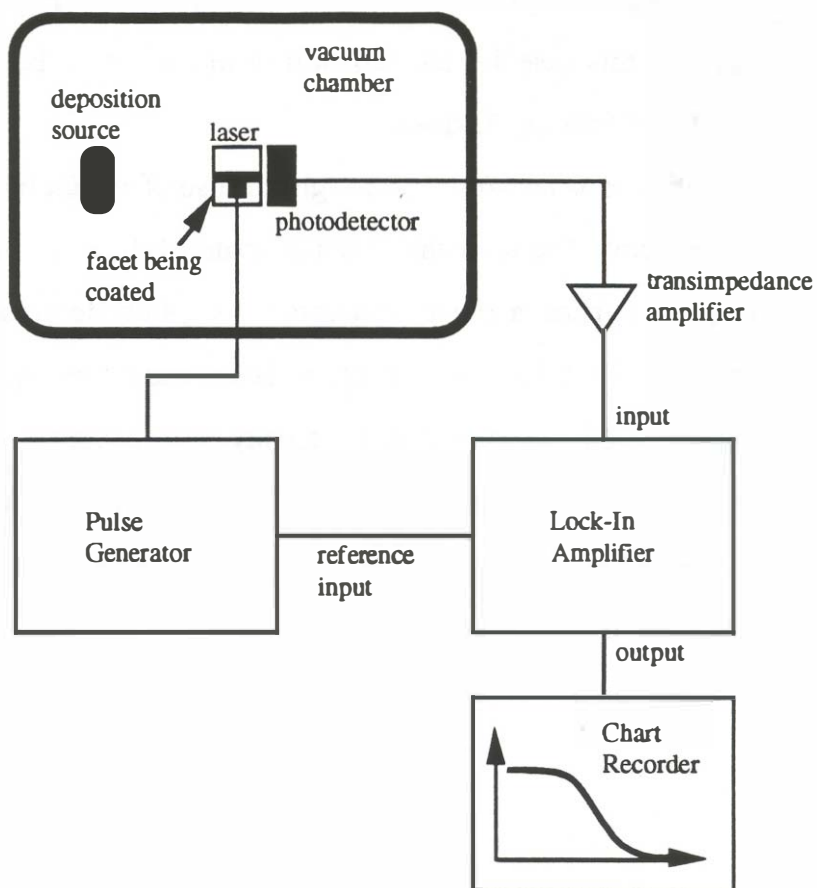
112

Figure A.3. Apparatus for in-situ monitoring of laser facet coating thickness.

deficient) coatings of higher index. We have found, however, that the resulting index is too sensitive to small variations in oxygen flow and background gases to be reproducible. This is due to the large index variation between silicon dioxide and silicon ($\approx 3.5$). Our present technique uses flowrates similar to those employed to obtain stoichiometric silicon nitride, but with oxygen introduced to lower the index to the optimum value. This

technique overcomes the problem of sensitivity to oxygen flowrate fluctuation because in this case the full variation of index is only between 2.0 (silicon nitride) and 1.45 (silicon dioxide).

The film thickness is controlled through the use of *in situ* monitoring of the coating reflectivity. The laser that is being coated is biased *in-situ* using low duty cycle pulses from a pulse generator. A photodetector in the chamber monitors the back facet output of the laser, and a preamplifier and lock-in amplifier are used to monitor the intensity during deposition. The coating is of optimally correct thickness when the back facet emission beam intensity reaches a null for a given bias level, indicating maximized increase of lasing threshold and highest facet loss.

# High-Speed, Low-Threshold InGaAsP Semi-Insulating Buried Crescent Lasers

The development of reliable laser structures for high speed operation at 1.3 μm wavelength continues to be of great interest for applications involving fiber optic transmission operating at multigigabit data rates. To the date of this work, the highest modulation bandwidths for InGaAsP lasers have been demonstrated using a mesa structure [1]. Concerns over the reliability of such a structure have motivated the development of high speed laser structures with greater reliability. The semi-insulating buried crescent (SIBC) laser structure has been demonstrated to be capable of reliable high-power operation over wide temperature ranges [2]. This appendix describes the refinement of this laser structure for high speed operation and record bandwidths for a planar structure at the time this work was done.

Fe-doped semi-insulating layers are used in the SIBC lasers, resulting in low parasitic capacitance and high resistivity current-confinement which is essential for minimizing the rf and dc leakage currents bypassing the active region. SIBC lasers employing such layers have been shown to be capable of operation up to 100°C with 9 mW CW output power. The bandwidth of these lasers was limited by heating, which limits the maximum output power and lowers the differential gain at high bias levels.

To achieve bandwidths in excess of 20 GHz, it is necessary to increase

Metal
Polyimide
SiNx
p-InGaAs
p-InP
InGaAsP
n-InP
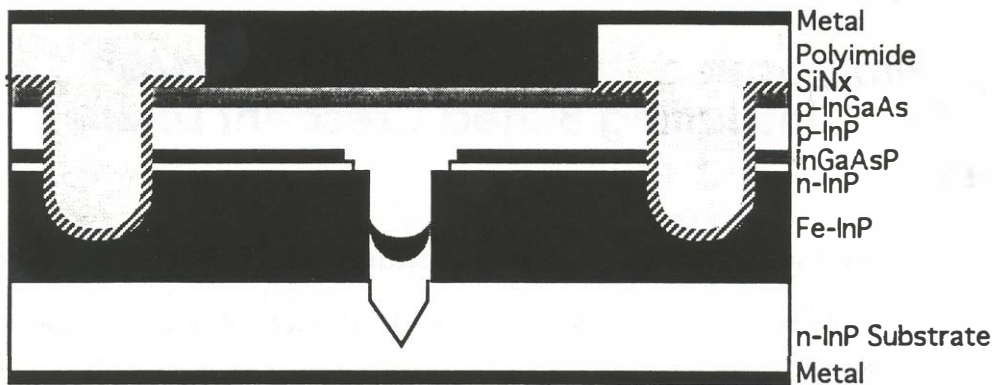Fe-InP

n-InP Substrate
Metal

Figure B.1. Schematic of the SIBC laser structure.

the slope of resonance frequency vs. output power so that higher bandwidths are achieved at lower bias currents. This is accomplished by reducing the active channel width to 1 $\mu$m, by p-doping the active layer, and by cleaving cavity lengths as short as 100 $\mu$m. In addition, the parasitic capacitance is further reduced by limiting the p-contact width to 12 $\mu$m, and by the use of a thick polyimide layer under the bond pad metal, as shown in Figure B.1.

Lasers fabricated in this manner exhibited thresholds as low as 6 mA, with maximum output powers of 15 mW per facet at 100 mA bias current. The total differential quantum efficiency was typically 45-55%. The parasitic capacitance of these lasers at zero bias was measured to be 1.1-1.3 pF using a vector network analyzer. The series resistance was 6-9 $\Omega$, resulting in RC rolloff frequencies of up to 20 GHz.

The small-signal modulation response was measured using a high-speed InGaAs photodetector and vector network analyzer. The lasers were
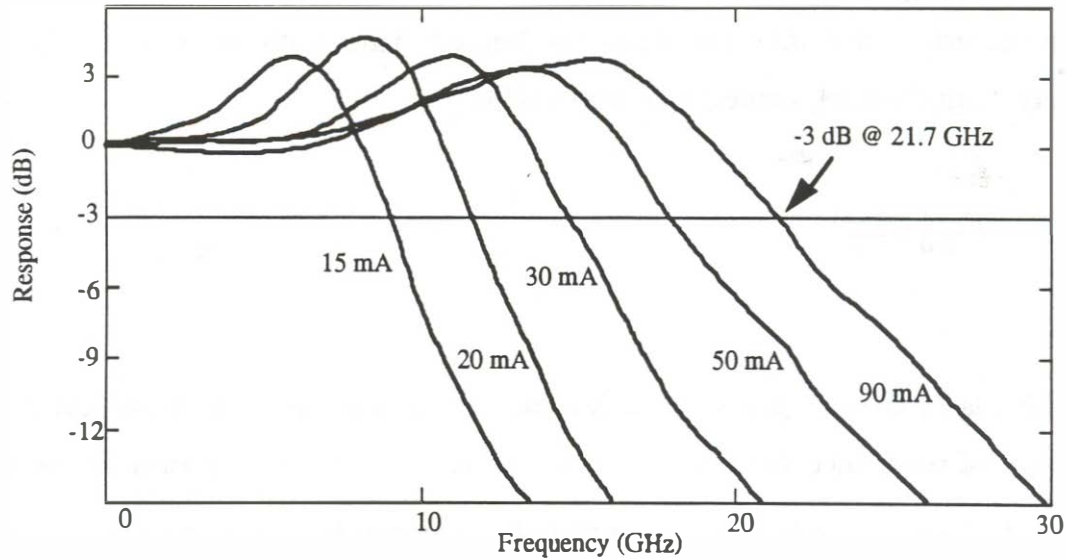
116

Figure B.2. Modulation response at several different bias currents.

mounted p-side up on a copper heatsink and bonded to a 50 Ω microstrip line using low-inductance Au ribbon wire. A Wiltron K-connector is used to launch into the transmission line. The modulation response at several bias currents is shown in Figure B.2. A maximum 3-dB bandwidth of 21.7 GHz (without correction for detector rolloff) is achieved at a CW bias current of 90 mA. All the lasers with threshold currents less than 8 mA had bandwidths in excess of 18 GHz. At the time this work was done, this was the highest bandwidth demonstrated for InGaAsP lasers using a planar structure.

Measurements of the relative intensity noise in these devices were made to determine the inherent bandwidth. The K value, extracted as the slope of the dependence of damping rate on the square of resonance

117

frequency, varies from 0.21 to 0.26 ns at higher output powers. The K factor characterizes the inherent damping limited bandwidth of a laser. This maximum damping limited bandwidth is [3]:

$$f_{-3dB}^{max} = \frac{2\pi\sqrt{2}}{K}$$

(B.1)

which is 34 GHz for the value of K measured in these devices. Based on the slope of resonance frequency vs. the square root of output power in these lasers of 5.6 GHz/mW$^{1/2}$, this bandwidth corresponds to an output power of 37 mW. This is far greater than the actual maximum output power for these lasers (~15 mW). Most lasers employing a bulk active region have a modulation bandwidth lower than the bandwidth projected from measurements of K. Typically, the maximum power output limit is reached before the bandwidths become limited by damping effects.

The resonance frequency of a laser is often expressed as [5]

$$\omega_0 = \sqrt{\frac{gS}{\tau_p}}$$

(B.2)

where g is the differential gain, S is the photon density and $\tau_p$ is the photon lifetime. In InGaAsP lasers, the maximum resonance frequency obtained is not typically limited by damage induced at high photon densities, but rather by the maximum level of input current. The heating and leakage that occurs at high injection levels reduces the differential gain and limits the maximum

118

output power of the laser. In light of these limitations, it is more appropriate to write Equation B.2 in terms of the current [4]:

$$\omega_0 = \left[ \frac{g \, \Gamma \, \eta_i}{e \, V} \left( I - I_{th} \right) \right]^{\frac{1}{2}}$$

(B.3)

where where V is the active region volume, G the confinement factor, hi the internal differential quantum efficiency, I the input current, and $I_{th}$ the threshold current. It has been shown that the maximum relaxation oscillation frequency of a laser can be increased through the use of high reflectivity mirrors [5]. Note that $I_{th}$ is the only term in Equation B.3 that is dependent on facet reflectivity. The decrease in threshold current caused by higher facet reflectivities results in higher obtainable values of $(I-I_{th})$ and therefore results in increased resonance frequencies. The use of reduced facet reflectivity increases the threshold current of the laser and will reduce the maximum resonance frequency, despite the reduction in the photon lifetime. Note that this is not necessarily the case for GaAs lasers where optically-induced facet damage is a limit. Lowering facet reflectivities reduces the internal photon densities, thereby possibly increasing the obtainable values of $(I-I_{th})$ for such GaAs lasers.

Because the increase in resonance frequency for higher facet reflectivities occurs through reduction of $I_{th}$, a subtractive term, the most significant bandwidth improvements are expected for values of input current comparable to threshold. The relative improvements in $(I-I_{th})$ become

119

smaller at higher current levels. Therefore, large increases in the ultimate maximum bandwidth are not to be expected in lasers that are current limited only at levels that are many times the threshold current.

The modulation responses of several lasers with high reflectivity facet coatings were measured. Figure B.3 shows the dependence of the square of resonance frequency vs. input current for a device with (a) no coatings, (b) one facet uncoated, the other coated for 65% reflectivity, and (c) one facet 65% reflectivity, the other 85%. The threshold currents were 9.3, 8.6, and 6.2 mA, respectively. The sublinearity of the curves at higher biases is due to heating and current leakage which cause sublinearity of the L-I curves at
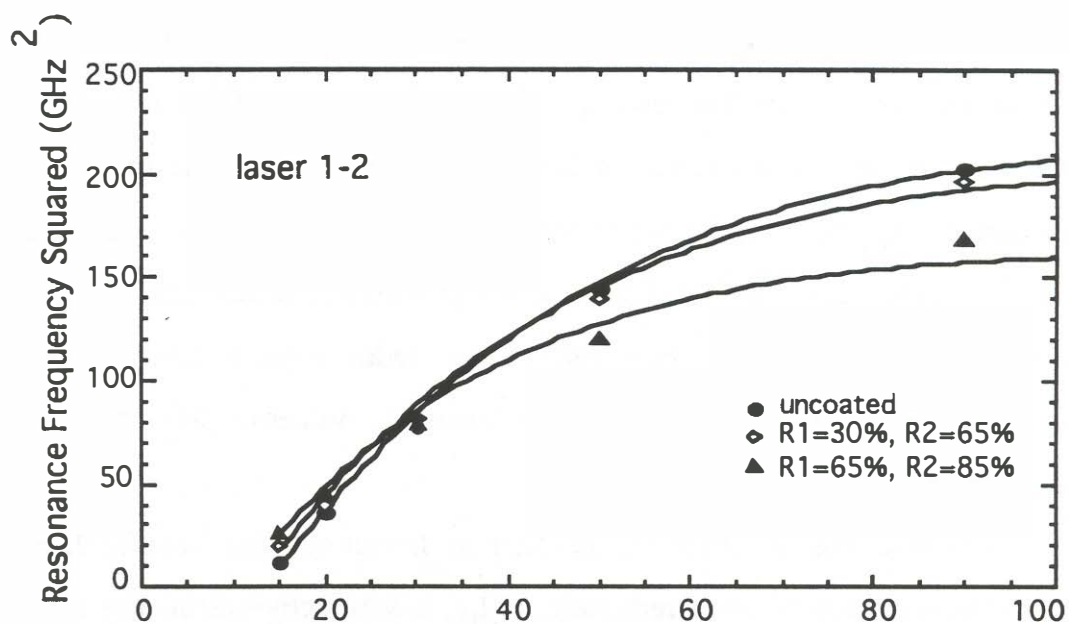


Figure B.3. Measured and calculated dependence of the square of resonance frequency on input current for different facet reflectivities. The curves were obtained using Equation B.5.

120

higher current levels.

Higher resonance frequencies at bias levels below 30 mA are obtained for the lasers with high reflectivity coatings. The 3-dB bandwidth at 15 m A bias current increased from 6 GHz for the uncoated laser to 7.5 GHz for the laser with both facets high reflectivity coated. At higher bias levels, slightly lowered resonance frequencies are obtained for the higher facet reflectivities. This is due to damping which causes a lowering of the peak frequency from the undamped resonance frequency.

Equation B.1 is readily modified to reflect the lowering of peak frequency due to damping by the substitution of g with a nonlinear gain, $g/(1+\epsilon S)$ [6], where $\epsilon$ is the nonlinear gain parameter. Thermal and leakage effects can be explicitly represented by substituting temperature and voltage dependent expressions for the differential gain and threshold current. Again rewriting in terms of input current, we obtain

$$\omega_0 = \left[ \frac{g \Gamma \eta_i (I - I_{th})}{e V \left[ 1 + \frac{\epsilon \Gamma \eta_i \tau_p}{eV} (I - I_{th}) \right]} \right]^{\frac{1}{2}}$$

$$I_{th} = I_o e^{(I V_t R_{th} + T_a)/T_o}$$

$$g = g_o(1 - A I V_t R_{th})$$

121

$$I = I_{Total} - I_{Leakage} = I_{Total} - I_{Total}\left(1 - e^{-V/V_L}\right)$$

$$(B.5)$$

where $T_a$ is the ambient temperature, $V_t$ the threshold voltage, $R_{th}$ thermal resistance, A the fractional reduction of differential gain vs. temperature, To the characteristic temperature of the threshold current, V the applied voltage to the laser, and $V_L$ (~2.7V) is the characteristic turn-on voltage of the leakage current. The dependence of resonance frequency obtained from Equation B.5 is shown in Figure B.3, where good agreement with the data is observed using $\varepsilon = 2.4 \times 10^{-23}$ m$^3$. This expression can be used to optimize the facet reflectivity to maximize the bandwidth at a given operating current.

# References

1. Meland, E., Holmstrom, R., Schlafer, J., Lauer, R. B., Powazinik, W., "Extremely High-Frequency (24 GHz) InGaAsP Diode Lasers With Excellent Modulation Efficiency", Electronics Letters vol. 26, pp. 1827-1829, 1990.

2. Cheng, W-H., Buehring, K., Appelbaum, A., Renner, D., Shin, S., Su, C. B., Mar, A., Bowers, J.E., "High-Speed and Low-Relative-Intensity Noise 1.3 μm InGaAsP Semi-Insulating Buried Crescent Lasers", IEEE J. Quantum Electronics, QE-27, pp. 1642-1647, 1991.

3. Olshansky, R., Hill, P., Lanzisera, V., Powazinik, W., "Frequency Response of 1.3 μm InGaAsP High Speed Semiconductor Lasers", Journal of Quantum Electronics, QE-23, No. 9, 1410, 1987.

4. Ikegami, T., and Suematsu, Y., "Direct Modulation of Semiconductor Lasers", Electron. Commun. Japan, vol. B51, 51-58, 1968

5. Lau, K. Y., and Yariv, A., "Ultra-High Speed Semiconductor Lasers," IEEE Journal of Quantum Electronics, vol. QE-21, No. 2, Feb. 1985.

6. Mar, A., Morton, P. A., Bowers, J. E., "Optimum Facet Reflectivities for High Speed Lasers", Electronics Letters, vol. 26, 1384, 1990.

7. Bowers, J. E., "High Speed Semiconductor Laser Design and Performance," Solid-State Electronics, vol. 30, No. 1, 1987.